A PWM BASED SERIES COMPENSATOR FOR POWER SYSTEM STABILITY ENHANCEMENT

BY

ROMMAN AHMED MOSTAFA KAMAL

A Thesis Presented to the
DEANSHIP OF GRADUATE STUDIES

KING FAHD UNIVERSITY OF PETROLEUM & MINERALS

DHAHRAN, SAUDI ARABIA

In Partial Fulfillment of the
Requirements for the Degree of

MASTER OF SCIENCE

In

ELECTRICAL ENGINEERING

MAY 2014

KING FAHD UNIVERSITY OF PETROLEUM & MINERALS
DHAHRAN- 31261, SAUDI ARABIA
DEANSHIP OF GRADUATE STUDIES

This thesis, written by **ROMMAN AHMED MOSTAFA KAMAL** under the direction his thesis advisor and approved by his thesis committee, has been presented and accepted by the Dean of Graduate Studies, in partial fulfillment of the requirements for the degree of **MASTER OF SCIENCE IN ELECTRICAL ENGINEERING**

A. H. Rahim

Dr. Abu Hamed M. Abdur Rahim
(Advisor)

Dr. Ali Ahmad Al-Shaikhi
Department Chairman

Dr. Mohammad Ali Abido
(Member)

Dr. Salam A. Zummo
Dean of Graduate Studies

Dr. Ibrahim Omar Habiballah
(Member)

17/8/14

Date

عمادة الدراسات العليا
DEANSHIP OF GRADUATE STUDIES

Dedicated

to

My Parents, wife & son

ACKNOWLEDGMENTS

All praise be to Allah, *subhanahu-wa-ta'ala*, the Almighty who gave me the opportunity to accomplish my MS degree at King Fahd University of Petroleum and Minerals, and may the peace and blessings of Allah be upon his prophet, Muhammad (S.A.W).

With deep and indebted sense of gratitude, I would like to express my sincere thanks to my thesis advisor, Dr. Abu Hamed M. Abdur Rahim for his invaluable support, guidance, continuous encouragement and all possible cooperation throughout the period of my research and preparation of thesis documentation. Working with him was a wonderful and learning experience, which I thoroughly enjoyed.

My sincere thanks and appreciation is due to the thesis committee members Dr. Mohammad Ali Abido and Dr. Ibrahim Omar Habiballah for investing their time and their support, critical reviews and suggestions to improve this work.

Acknowledgement is due to the King Fahd University of Petroleum and Minerals for providing the financial support and world class facilities which made my life smoother and easier to devote myself fully in academic and research works. Especially, I am grateful to all the faculty and staffs of the Electrical Engineering department at KFUPM.

I owe a deep sense of gratefulness to my numerous friends and colleagues whose presence and moral support made my entire stay at KFUPM enjoyable and fruitful.

Finally, I would like to express my profound gratitude to my parents, my siblings, my wife and my son for their sacrifice, incessant prayers, love and support that motivated me to complete this work.

TABLE OF CONTENTS

LIST OF TABLES

LIST OF FIGURES

LIST OF ABBREVIATIONS

PWM	: Pulse width modulation
PWMSC	: Pulse width modulated series compensator
AC	: Alternating current
DC	: Direct current
FACTS	: Flexible AC transmission system
SVC	: Static var compenstor
TCSC	: Thyristor controlled series capacitor
STATCOM	: Static synchronous compensator
SSSC	: Static synchronous series compensator
UPFC	: Unified power flow controller
PID	: Proportional-integral-derivative
PSS	: Power system stabilizer
GTO	: Gate turn-off thyristor
VSC	: Voltage-sourced converter
SMIB	: Single machine infinite bus
RCGA	: Real-coded genetic algorithm

ABSTRACT

Full Name : ROMMAN AHMED MOSTAFA KAMAL
Thesis Title : A PWM BASED SERIES COMPENSATOR FOR POWER SYSTEM STABILITY ENHANCEMENT
Major Field : ELECTRICAL ENGINEERING
Date of Degree : May, 2014

Maintenance of stability is one of the most important conditions for reliable and efficient operation of a power system. Many methods have been reported till to date to enhance the stability of a power system. In this thesis, the enhancement of power system stability through a relatively new FACTS device named pulse width modulated series compensator (PWMSC) in the transmission line has been investigated. The three-phase PWMSC is realized with a simple pulse width modulated (PWM) AC link converter consisting of four force-commutated switches and a three-phase diode bridge. The PWMSC is modeled as a continuously controllable series capacitive reactance in the transmission line of a power system. Nonlinear model of single machine infinite bus (SMIB) & multi-machine power system with PWMSC installed are derived and tested for various disturbances including three phase faults in the system. Proportional-integral (PI) and proportional-integral-derivative (PID) controllers are incorporated to control the duty ratio of the switches of the PWMSC, thus controlling the equivalent injected line reactance. Effectiveness of different stabilizing input signals for these supplementary PI, PID controllers has been investigated. A genetic algorithm based optimization procedure has been employed to optimize the controller parameters. Different objective functions have been used in the optimization algorithm to examine their efficiency in enhancing power system stability. The effect of PWMSC placement in the multi-machine system in

power system stability is also explored. The nonlinear system model is simulated in MATLAB and from a number of simulation studies on a single machine infinite bus power system and also the multi-machine system, it was observed that the proposed PWMSC controller provides excellent damping of electromechanical mode oscillations.

ABSTRACT (ARABIC)

ملخص الرسالة

الاسم الكامل : رومان أحمد مصطفى كمال

عنوان الرسالة : تحسين استقرارية تظام القدرة الكهربائي باستخدام المعوضات المتوالية المبنية على تضمين عرض النبضة

التخصص : الهندسة الكهربائية

تاريخ الدرجة العلمية : مايو- 2014

يعتبر شرط الحفاظ على الاستقرار واحدا من أهم الشروط لتشغيل نظام طاقة يعتمد عليه وفعال. حتى وقتنا الحالى، قدمت العديد من الأساليب لتعزيز الاستقرار في نظام الطاقة.

هذا البحث يقدم دراسة وتحليل للأداء في تعزيز استقرار نظام الطاقة عن طريق استخدام جهاز FACTS الجديدة نسبيا والمسمى بمعادل متسلسلة التضمين بعرض النبضة (PWMSC) في خط النقل. تم الحصول على متحكم بعرض النبضة ثلاثي الأطوار PWMSC عن طريق محول تيار متردد الذي يعتمد على متحكم بسيط بعرض النبضة (PWM), ومحول التيار المتردد يكون من أربعة مفاتيح الكهربائية توحيد وقنطرة توحيد تيار ثلاثى الأطوار. في هذا العمل، تم تمثيل جهاز PWMSC في خط النقل من نظام الطاقة بمفاعلة سعوية ذات التحكم المتصل المتسلسل. تم نمذجة واختبار نماذج غير خطية لالة واحدة مربوطة مع ناقل لانهائى (SMIB) وكذلك لنظام الطاقة المتكون من الآت متعددة مثبتة مع جهاز PWMSC لمختلف الاضطرابات والتي منها تيارات القصر ثلاثية الأطوار. تم استخدام المتحكم النسبي والتكاملي (PI) والمتحكم التناسبي التكاملي التفاضلي (PID) للتحكم في فترات العمل للمفاتيح الكهربائية المستخدمة في PWMSC ، وبالتالي التحكم بقيمة المحاثة المكافئة المربوطة في نظام النقل. تم فحص مدى فعالية نوع الاشارة الداخلة للمتحكمات مثل PI و PID في استقرارية النظام الكهربائي. تم استخدام الخوارزمية الجينية لإيجاد القيم المثلى للمتحكمات. تم استخدام مجموعة متعددة من الدالات الموضوعية في خوارزمية الجينات لفحص مدى فعاليتها في استقرارية نظام القدرة الكهربائي. تم أيضا استكشاف مدى تأثير PWMSC عند تركيبها في اماكن مختلفة من أنظمة متعددة الالات على استقرارية نظام القدرة الكهربائي. تم

تحليل الأنظمة غير الخطية باستخدام الماتلاب حيث أظهرت الدراسات التحليلية لنظام أحادي الآلة ومتعدد الآلة على فعالية PWMSC في اخماد التذبذبات الكهرومكانيكية.

CHAPTER 1

INTRODUCTION

1.1 Power System Stability

Stability is one of the very important aspects of reliable and efficient operation of power systems. In early days, power systems were isolated from each other. In order to increase the reliability & efficiency of the power system and also to make it more economic, isolated power systems began to interconnect. Eventually the power system has become a complex network of large generating units, transmission & distribution lines and loads. Though this interconnection has enhanced the reliability of power system, it has also complicated the stability problem and made the system more vulnerable to disturbance. When large power systems are interconnected with long transmission lines, the power system may experience low frequency oscillations. If these oscillations are not adequately damped it may sustain, grow and even lead to separation of the systems [1],[2]. Moreover, in an interconnected system the disturbances may propagate through the interconnections to the whole system depending on the scale of the disturbance. Following a large disturbance like three phase line faults, major line or load switching, the system may go unstable or it may also lead to widespread blackout if proper damping is not provided [3],[4]. So, a good power system should be able to regain its normal operating condition or at least to an acceptable operating equilibrium following a disturbance. A reliable power system should supply uninterrupted power to its load. And

this capability of power system to remain in synchronism following a disturbance is termed stability [5].

Many methods have been employed to damp the oscillations which lead to system instability. The most commonly used method is supplementary excitation system which is also referred to as power system stabilizer (PSS). PSS is both efficient and economic. But it causes great variations in the voltage profile which may be followed by leading power factor operation and loss of system stability under severe disturbances [6]. Supplementary governor control system is also studied by researchers and yielded very attractive results but is not practiced due to physical limitations of large valves switching [7]. Braking resistors are also used to damp the first swing by absorbing the unbalanced real power which accelerates the synchronous machine [8],[9]. [10] presents a fuzzy logic switching of the thyristor controlled braking resistor to augment the transient stability in a multi-machine power system and [11] analyzes the effect of the temperature rise of the fuzzy logic-controlled braking resistor on the transient stability in a multi-machine power system. Generator tripping and load shedding are also considered as a method to avoid system instability when all other measures fail [12],[13]. Another method to damp out oscillations is control of reactance of the transmission lines. Mainly by injecting series, shunt capacitances to the lines or by using phase shifters [14],[15]. This injection of reactance not only damps the electromechanical oscillations but also increases the transmission line loading capacity by increasing the steady state stability limit and controlling the steady state power flow. In the present days many of the transmission lines carry currents much below their thermal limits because of stability limit of that line. Building new transmission lines has become more & more difficult because of high costs,

environmental restrictions, right of way difficulties and other social problems. It is a concern for the utilities to use their power system resources at their full capability. But as these are based on mechanical switching they can't give adequate fast response needed to damp out oscillations following a major disturbance. With the advancement of power electronics in late 1980's Electric Power Research Institute (EPRI) has introduced new power electronics based controllers commonly called flexible AC transmission systems (FACTS) devices that have very fast switching capability. These are widely used in modern power system to mitigate the oscillations fast and effectively[16].

1.2 FACTS Devices

Flexible AC transmission systems (FACTS) devices regulate the power flow and transmission voltage through rapid control action. FACTS devices have opened a new horizon for controlling transmission line parameters such as series impedance, shunt impedance, current, voltage, and phase angle fast enough to maintain the system stability in steady state, transient conditions or even in contingency where the previously used mechanically controlled systems failed. FACTS devices have increased the line loading without compromising reliability. Although the primary objectives of FACTS are to increase the usable transmission line capacity near their thermal limits by controlling power flow over designed routes, it can also be used to mitigate the oscillations in the system following small disturbances from load changes or even large disturbances occurring from three phase faults or sudden transmission line outage and thus enhancing both power system steady state and transient stability.

Generally, FACTS controllers are divided into four categories:

• Series controllers which inject voltage in series with the line.

• Shunt controllers which inject current into the system at the point of connection.

• Combined series-series controllers which are a combination of separate series controllers.

• Combined series-shunt controllers which are a combination of separate shunt and series controllers

Based on the power electronics technology used FACTS devices are also divided into two generations. First generation FACTS devices used thyristor or SCR based converters which don't have gate turn off capability, or turning off of these converters cannot be controlled. They are also called line commutated converters. Examples of these FACTS devices are SVC, TCSC, and TCPS etc. Second generation FACTS devices are those who uses gate turn off (GTO) based voltage sourced converters which can control both on and off of these converters. These converters are also called forced commutated converters. Examples of these second generation FACTS devices are STATCOM, SSSC and UPFC etc. These voltage source converters require dc links and dc capacitors for their operation [17].

1.3 Pulse Width Modulated Series Compensator

Classical methods of adding fixed series capacitors or phase shifting transformers in the transmission lines through mechanical switchgears have been used for many years in transmission lines for compensating the series line reactance thus increasing power transfer capability and enhancing the transient stability. But due to the slow response of the mechanical switchgears, they were eventually replaced by power electronics based

FACTS controllers. At the beginning of the voyage of FACTS devices in power system applications the thyristor controlled series compensators (TCSC) gained huge popularity & applications in the power system. These first generation series compensators, TCSCs, used power electronic based line commutated thyristors which have very fast switching capability & high voltage, current ratings [18]. As TCSCs are based on line commutated thyristors, they cannot be operated at high frequencies. Thus producing low order harmonics and requiring large filters. Another disadvantage of TCSC is it has a resonance region where it can't vary the equivalent reactance [19]. Many improvements of this TCSC scheme are reported in the literature. Continuous regulation of series compensation is reported in [20] by using force commutated gate turn-off (GTO) based thyristors. But the problem of low order harmonics was not solved until the replacement of the controllers of these line commutated thyristors by pulse width modulation (PWM) based AC controllers which can switch at much higher frequencies than line frequency.

The utilization of PWM AC controllers was made possible when the force commutated (GTO) based thyristors came into picture. It was the second generation of FACTS devices; SSSC (series compensators), STATCOM (shunt compensators), UPFC (series-shunt controllers) emerged into the scenario. These employ voltage sourced converters (VSC) which uses PWM AC controls. These VSCs have overcome the drawbacks of first generation series compensators (TCSCs) but their power structure and control scheme are complicated. Moreover, as they have DC-AC converters, generally 30 to 50 % of the entire converter size and volume is occupied by these DC-link capacitors of the converters [21]. And also these DC capacitors cannot withstand high temperature like AC capacitors.

In order to bridge the gap between the first generation FACTS devices, TCSC and second generation FACTS devices like SSSC, researchers presented a PWM based AC link converter which employs pulse width modulation technique like SSSC. The PWMSC uses self-commutated GTOs to switch at a very high frequency, thus eliminating the need of large filters for filtering low order harmonics which is needed in TCSCs. And PWMSC can also vary the effective injected reactance continuously, doesn't have any restricted region like TCSCs [22]. At the same time, PWMSC employs AC link converters like TCSCs. PWMSC doesn't employ any voltage sourced converters (VSC) which make its circuit structure & control scheme both simpler like TCSCs. The PWMSC is compared with SSSC based on detailed switching models in [23]. It was observed that twice the capacitive energy storage and about 66% additional semiconductor MVA rating is required by DC link converters than AC link converters. PWMSC is also reported to be cheaper than SSSC based on estimated components cost of these two compensators. The vulnerability of SSSCs in high temperature applications compared to PWMSCs because of using DC capacitors has also been presented.

In [24], [25] authors have proposed a PWM structure for AC line conditioning which is also used as PWM based series compensator. The structure uses fewer switch components compared to others which made its gating signals less stringent and more reliable. The three phase PWMSC has been realized in [24], [25] with four standard unilateral self-commutated switches together with six diodes.

1.4 Thesis Objective

The objective of this thesis is to investigate the performance of the PWMSC controllers in damping power system oscillations. This is broken down as:

a) To develop a nonlinear model of a single machine infinite bus (SMIB) system installed with pulse width modulated series compensator (PWMSC).

b) To design a PI controller to control the duty ratio of the PWMSC switches to obtain optimum damping.

c) To optimize the PI or PID controller parameters using different optimization techniques.

d) To test the SMIB system with PWMSC, incorporating PI controller for step disturbance of input power of the generator and three phase fault in the system.

e) To develop a nonlinear model of a multi-machine system installed with PWMSC and a PID controller.

f) To test the multi-machine system stability by subjecting it to various disturbances.

g) To explore the effect of PWMSC locations in the multi-machine system in damping enhancements of the system oscillations.

h) To explore different stabilizing signals keeping in view that generator speed is not available at all locations of the system.

i) To develop methods to synthesize speed from the signals available at all location of the system.

1.5 Thesis Outline:

The chapter wise summary of the work reported is as follows,

Chapter 2 provides a detail picture of the evolution of the series compensator structures, their mathematical models and applications in power systems reported in the literature. This chapter also presents an extensive review of the pertinent literature related to the scope of this thesis.

Chapter 3 introduces the PWMSC structure, model used in this thesis and its operating principles. Design of the PWMSC controllers and their optimization technique, real coded genetic algorithm (RCGA) is also presented in this chapter. In addition, the problem formulation for this RCGA is outlined in this chapter.

Chapter 4 describes the nonlinear models of the single machine infinite bus power system as well as multi-machine power system equipped with PWMSC. Different PWMSC controller configurations are also modeled in this chapter.

Chapter 5 presents the nonlinear simulation results of the SMIB model with PI and PID controllers.

Chapter 6 is devoted to the results of multi-machine system model equipped with different PI and PID controller configurations. Effect of different fault and PWMSC locations in the multi-machine system in terms of damping oscillations are investigated in this chapter.

Conclusions and future works are discussed in chapter 8.

CHAPTER 2

LITERATURE REVIEW

2.1 PWMSC structure & modeling

Pulse width modulation technique is adopted in power system for a long time and for various applications. It has opened a new horizon for the use of force commutated thyristors like GTOs, IGBTs, etc. Forced commutated ac-to-ac converter topology has been studied for more than 25 years [26], [27]. The idea of controlling the injected reactance in the line continuously was realized by force commutated thyristors where the thyristors are fired at zero voltage and switched-off at a variable time in the ac cycle. This type of compensator was proposed in [20] where it has used GTOs in a bidirectional configuration. The circuit they have proposed is the dual of thyristor controlled reactors.

But still, these switches were gated at line frequency, so, creates low order harmonics and it has to be synchronized with line frequency. These problems were overcome by the introduction of PWM controlled switches or converters which can operate at very high frequencies. So, only high order harmonics are generated around line frequency and synchronization with line frequency is also not required.

A PWM controlled series compensator was designed in [28] with a four force commutated thyristors per phase. It has used 12 switches for three-phase compensator.

In [29], a PWM ac link converter is proposed using six bi-lateral switches or 12 standard switches.

A three-phase PWM ac controller, proposed in [30], used only six standard unilateral switches. Three of them conduct during the active mode to commutate the load and other three switches conduct during the freewheeling mode to free wheel the loads. It has also proposed three snubber capacitors to maintain current flow during the dead times when all the switches were off to avoid short circuiting of all switches. They have also verified their important theoretical results on a 10 kVA breadboard experimentally.

An improved version of the structure in [30] is proposed in [24]. In [24], the authors have designed a PWM based ac line conditioner consisting of only four unilateral force commutated switches and a three phase diode bridge.

A series compensator based on AC link converter utilizing pulse width modulation (PWM) is reported in [22]. They have designed the PWMSC controller using six unilateral force commutated switches, but they didn't discuss about the 'dead times' for avoiding conduction of all switches together in their literature.

In [25], the authors have presented a series reactive power compensator utilizing pulse-width modulation. They have designed their PWM AC controller with only four force-commutated switches and a three-phase diode bridge [24]. Their PWMSC is the dual of the PWM switched shunt reactor presented in [31].

[32] presents a PWM-based series compensator (PWMSC) with AC link. Its PWM AC link converter structure is similar to [22].

Direct AC-AC conversion using matrix converters or vector switching converters based on PWM strategy is also reported in the literature to control power flow in the transmission lines [33], [34], [35]. Vector switching converter based AC link UPFC is also proposed in [36], [37] .But these matrix converter topology control scheme is

complex, it needs large amount of switches, costly overvoltage protection and its commutation process is also questionable [34]. Research is going on to overcome these issues.

PWM ac link converter topology used for making static phase shifters in order to control the power flow in transmission line is also reported in the literature [38], [39].

Almost throughout the literature [21]- [24], [28]-[40], the injection of series reactance in the transmission line is controlled by varying of the duty cycle of the gating signal to all switches which is a single asynchronous train of pulses of fixed frequency. In [21], [22], [28], [32], [37], [40] the PWM AC link converter is modeled as a variable reactance in series with the transmission line whose equivalent reactance depends on the leakage reactance of the coupling transformer, turns ratio of this transformer, the capacitance of the capacitor bank and most importantly duty ratio of the gating signal of PWM controlled switches. All of these papers have ended up with the same expression,

$$X_{eq} = -n^2\left(1 - D_p\right)^2 X_c + X_{LT} \tag{2-1}$$

Where, n is the turns ratio of the transformer and X_{LT} is leakage reactance of the transformer, D is the duty cycle of the AC link converter is defined as the ratio of the on-period of switch S_4 with respect to the total switching period and X_c is the capacitive reactance of the capacitor bank. In these papers state-space averaging techniques [41] or average modeling technique is used in deriving the equivalent reactance expression.

As the selection of the modeling technique depends on the purpose of the model, the required accuracy level and complexity level, in some papers the PWM AC link converter is also modeled focusing on voltage injection [24] & harmonic distortion [28].

2.2 PWMSC controller design for damping of power system oscillation

Use of PWM AC link converter for series compensation is addressed in many researches. But the performance of the design is evaluated on the basis of several features. Some salient features are injected voltage in the line [20], [22], injected reactance in the line [25], harmonics of waveforms [25], [28], reactive component requirements [30], ratings of power converters & complexity of control [33], etc.

However, dynamic response of the PWMSC controllers in terms of improving voltage stability, small-signal and large-signal stability, damping of power system oscillations is also explored in [21], [23], [32], [37], [40].

In this work, the PWM based ac link converter is employed to test the performance of this controller in damping the oscillations following a small or large disturbance in the power system. Nonlinear model of system installed with PWMSC is derived and tested with step and pulse change of input power.

2.3 PWMSC in multi-machine system

A very limited work is available in the literature on damping control of power system oscillations in multi-machine system using PWM series compensators.

In [21], the authors have included the PWM based series compensator into the Newton-Raphson power flow formulation. They have used the 3-machine power system to test the PWMSC performance in regulating the power flow following a three phase fault. They

have adopted a simple proportional-integral (PI) control which controls the duty ratio for tracking the active power deviations.

In [40], the authors have employed the PWMSC in a 3-machine power system to test its feasibility in mitigating the transient behavior. They have designed a lead-lag controller to compensate the switches' duty cycle to regulate power flow. The system is tested with a three phase fault in the transmission line.

[36] has included both the pulse width modulated (PWM) ac link unified power flow controller [35] and the PWMSC in a 10 machine system to regulate the active power flow on the corresponding transmission line for different operating conditions.

In this work, the PWMSC controller has been tested for a multi-machine system. Nonlinear model of this multi-machine system is developed with PWMSC and PI controllers. Disturbances were simulated on various machines and for each disturbance the damping performance of the system was observed for different locations of the controller in the system. Simulation studies indicate that PWMSC controllers are promising candidate for stabilization of modern power system.

2.4 Location of PWMSC for damping enhancement

Optimal location for FACTS devices in the power system for damping enhancement has attracted a lot of researchers. Taking advantages of the FACTS devices depends largely on how these devices are placed in the power system, namely, on their location and size. Many different techniques are adopted to find out the optimal number & location of FACTS devices to enhance power system stability. Over the last decades, there has been a growing interest in algorithms inspired by observing natural phenomenon. It has been

shown that these algorithms are good alternatives as tools in solving complex computational problems. Various heuristic approaches have been adopted in research, including genetic algorithm, tabu search [42], simulated annealing [43], particle swarm optimization [44], etc. Cai *et al.* [45] used a genetic algorithm to determine the best location of a given set of FACTS devices in a deregulated electricity market. In [46] and [47], the optimal locations of FACTS devices are obtained for Var planning. Gerbex *et al.* [48] used a genetic algorithm to place different types of FACTS devices in a power system. In their study, the number of devices to install is assigned before optimization. In [49], a methodology is carried out using a genetic algorithm to find the optimal number and location of thyristor-controlled phase shifters in a power system. In [50], optimal allocation of SVCs has been carried out using modal analysis and genetic algorithms. Modal analysis is also used in [51] to find out the optimal location of SVCs. But the optimal location search specifically for PWM based AC link converters for series compensation is not found in the literature. In this work, the PWMSC is placed in different locations in multi-machine system and nonlinear simulation of the system is carried out in order to explore the effect of locations in damping performance of the PWMSCs.

2.5 Selection of best stabilizing input signals for PWMSC controllers

Selecting the proper stabilizing input signals plays an important role in the damping performance of the FACTS devices. A comprehensive review is done in [50] showing how other researches answer the question of which locations and feedback signals could result in the power system stabilizers (PSSs) and the FACTS devices having the

maximum effect on the system damping. A detailed study on the use of an SVC for damping system oscillation is carried out in [52]. Having considered several factors including observability and controllability, it was concluded that the most suitable supplementary input signal for an SVC for damping improvement is the locally measured transmission line-current magnitude. This signal is also used in the study system carried out in [53] and [54]. Other studies, however, select locally measured active power [55],[56] or generator angular speed [57],[58] as a supplementary input signal. Static interaction measures derived from decentralized control theory such as the relative gain array (RGA) and controllability and observability have been applied in determining both the best location and the best input signals for multiple FACTS [59]. Several papers also deal with the combined application of controllability and observability using the singular value analysis [60], [61]. The proposed method by the authors in [62] used the minimum singular values (MSV), the right-half plane zeros (RHP-zeros), the relative gain array (RGA), and the Hankel singular values (HSV) as indicators to find stabilizing signals in single-input single-output (SISO) and multi-input multi-output (MIMO) systems. The work presented in [63] is a modified method of [62] to select the supplementary input signal for STATCOM. In this work, generator angular speed, generator active power output and locally measured active power has been analyzed as stabilizing input signals. The PWMSC controllers are optimized with genetic algorithm and the damping performance of the PWMSC controller is examined for each stabilizing input signal.

CHAPTER 3

PULSE WIDTH MODULATED SERIES COMPENSATOR

3.1 PWMSC structure

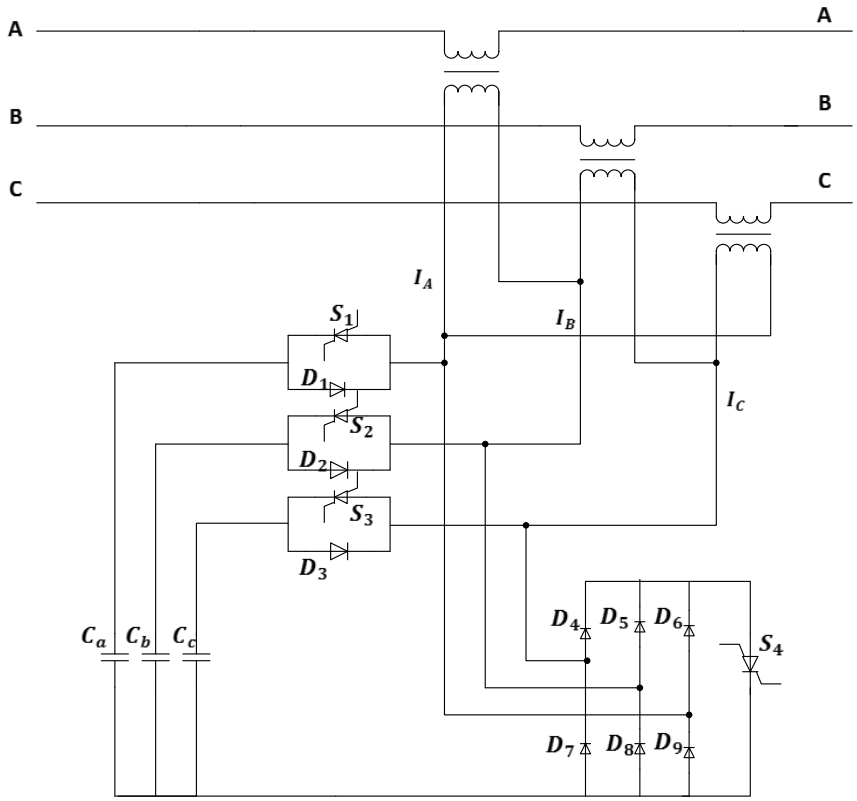

Figure 3-1: PWMSC inserted in series with the transmission line

A typical power circuit structure of the PWMSC is shown in Figure 3-1 [24]. The per-phase representation of this structure is shown in Figure 3-2 where the inserted series capacitor C_a is shown to be in series with switch S_1. The capacitor is connected to the transmission line through a coupling transformer. Another switch S_4 is connected in

parallel to the capacitor & switch S_1 to bypass the capacitor. The switches S_1 & S_4 closes, in compliment, to inject and bypass the capacitor into the transmission line respectively.

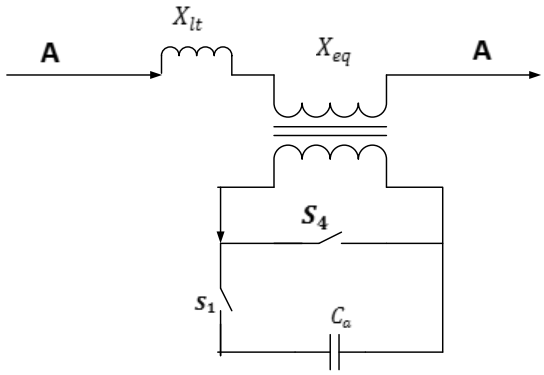

Figure 3-2: Single-phase equivalent model of the PWMSC

In the three-phase configuration of Figure 3-1, unilateral force-commutated switches S_1, S_2 & S_3, with anti-parallel diodes, are gated simultaneously to inject the capacitor bank in the transmission line through the three coupling transformers. The capacitor bank is consisting of capacitors C_a, C_b, C_c connected in Y. The secondary of these transformers are connected in delta Δ which helps to trap the triple-N harmonics. For bypassing the capacitor bank only one unilateral force-commutated switch, S_4 with three phase diode-bridge is sufficient. While the switch S_4 is gated complimentarily to the capacitor side switches S_1, S_2 & S_3. Now, depending on the duty ratio of the main switches S_1, S_2 & S_3 the equivalent reactance will be injected in the transmission line and the variation of this duty ratio or the equivalent reactance, seen from the primary side of the transformer, is done by a pulse width modulated ac controller. This PWM ac controller provides same gating signal to switches S_1, S_2 & S_3 and a complimentary signal with small dead time to switch S_4. This gating signal has a series of pulses whose duty ratio is varied and its frequency is kept fixed. A fault protection scheme could be

used for protection of the compensator from short-circuit faults occurred in the transmission line [27].

3.2 Operating Principles:

There are two modes of operations of this PWMSC controller. Active mode and bypass mode. These are explained below:

Active mode: During this mode, the main three switches S_1, S_2 & S_3 are on and switch S_4 is off. The capacitor bank is active in the circuit during this mode. Currents from the secondary of the transformer flow through one or two switches, the capacitor bank and then return through one or two anti-parallel diodes. If we take a particular case for example, currents I_A & I_B flow from the transformer secondary through switches S_1& S_2 respectively to the capacitor bank & then the returning current I_C flows through anti-parallel diode D_3. Figure 3-3 shows the equivalent circuit representation for this mode.

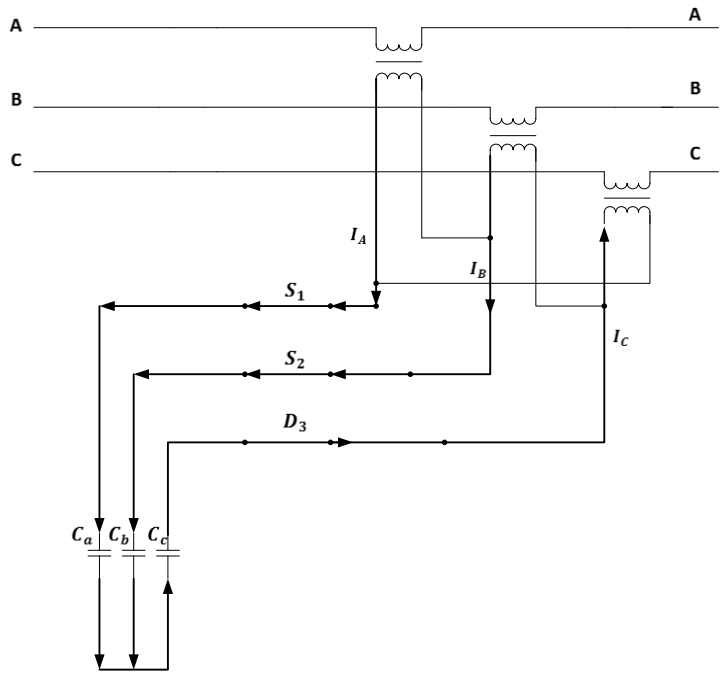

Figure 3-3: Active mode equivalent circuit representation

Bypass mode: during this mode all four switches S_1, S_2, S_3 are off and switch S_4 is on. The capacitors are bypassed and the coupling transformer secondaries are short-circuited. Currents from the secondary of the transformer flow through one or two top diodes of the three phase diode bridge, switch S_4 and return through one or two bottom diodes of the three phase diode bridge. For the particular case stated above, currents I_A and I_B flow from the transformer secondary through diode D_5, D_6 of the three phase diode bridge, the switch S_4 and the returning current I_C flows through diode D_7 of the three phase diode bridge. Figure 3-4 shows the equivalent circuit representation for this mode.

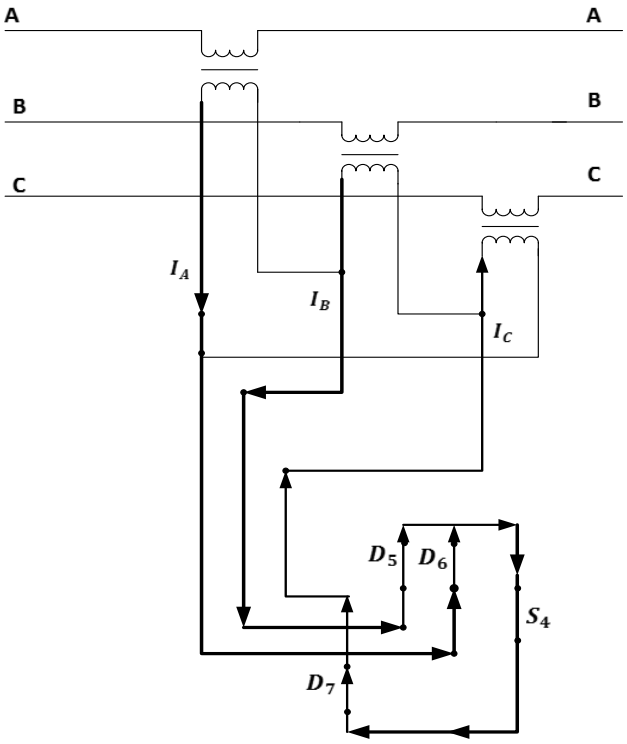

Figure 3-4: Bypass mode equivalent circuit representation

3.3 PWMSC model

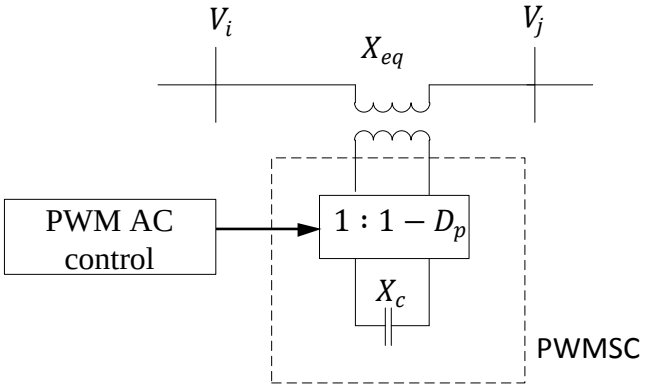

Figure 3-5: PWMSC in the transmission line

In this work PWMSC is modeled as a continuously controllable series capacitive reactance in the transmission line as shown in Figure 3-5. The equivalent reactance seen

from the primary side of the coupling transformer or the equivalent injected series reactance can be derived using state space averaging technique as

$$X_{eq} = -n^2\left(1 - D_p\right)^2 X_c + X_{LT} \tag{3-1}$$

Here, n is the turns ratio of the transformer and X_{LT} is leakage reactance of the transformer, D_p is the duty cycle of the AC link converter is defined as the ratio of the on-period of switch S_4 with respect to the total switching period and X_c is the capacitive reactance of the capacitor bank. This expression was verified in [25] in a laboratory prototype experimental setup.

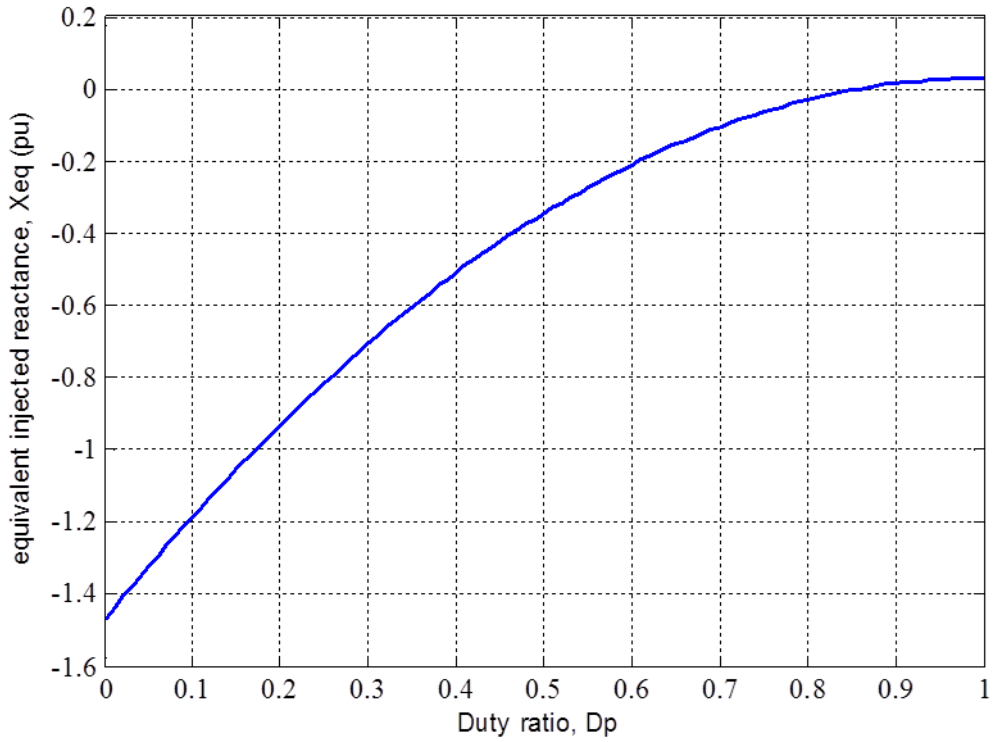

Figure 3-6: Variation of the net injected reactance of the series compensator with the duty ratio

For a typical PWM series compensator with $X_{LT} = 0.03\,pu,\ X_c = 1.5\,pu,\ n = 1$, the variation of the equivalent injected reactance X_{eq} of the series compensator with the duty ratio D_p is shown in Figure 3-6 From (3-1) and Figure 3-6 it is seen that the equivalent injected reactance of the compensator can be varied continuously between two extreme values: the leakage reactance (inductive) of the coupling transformer X_{LT} and almost the rated capacitive reactance of the compensator X_c. One limitation of this PWMSC is that it cannot inject substantial amount of inductive reactance in the transmission line but only the leakage reactance of the coupling transformer. But in simulations of a power system it is observed that, both inductive and capacitive compensation is needed during contingency.

So, in order to have both upwards & downwards swing of the equivalent injected reactance, the PWMSC switches' duty ratio, D_p is kept at 0.5 ($D_p = 0.5$). Thus, the PWMSC can contribute to both inductive and capacitive reactance injection by decreasing & increasing the duty ratio D_p respectively.

3.4 PWMSC controllers

In order to control the equivalent injected series reactance X_{eq} of the PWMSC, or to control the degree of compensation of the PWMSC we have to control the duty ratio, D_p. The duty ratio is controlled by a conventional PID controller as shown in Figure 3-7.

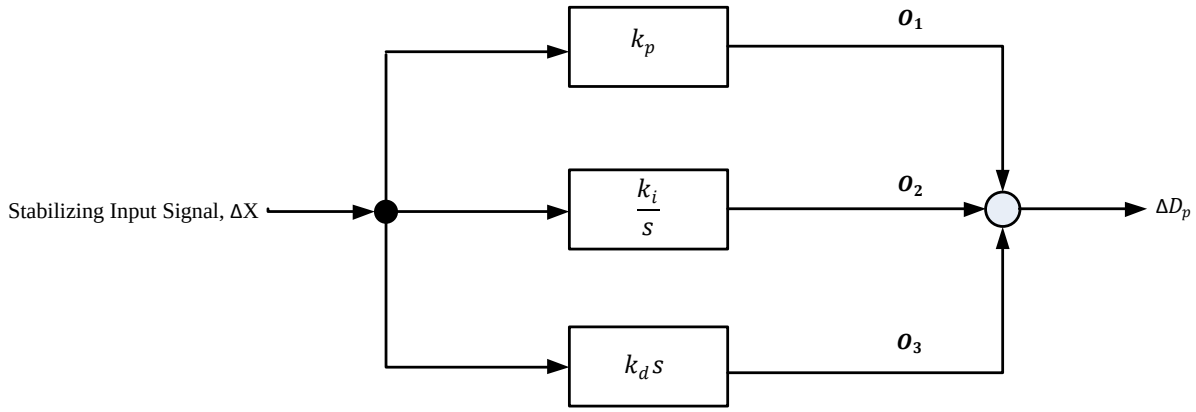

Figure 3-7: PID Controller

The stabilizing input signal to the PID controller were considered to be generator speed deviation, $\Delta\omega$, generator output power, *Pe*, active power flow of the transmission line as the stabilizing input signal. The control signal, ΔD_p is obtained as

$$\Delta D_p = O_1 + O_2 + O_3 \tag{3-2}$$

where,

$$O_1 = k_p.(\Delta X) \tag{3-3}$$

$$\dot{O_2} = k_i.(\Delta X) \tag{3-4}$$

$$O_3 = k_d.(\Delta \dot{X}) \tag{3-5}$$

The PID controller parameters, k_p , k_i & k_d have to be properly designed to get the best out of PWMSC.

Since it is difficult to model the derivative controller it is approximated as $k_d \frac{(s+z)}{(s+p)}$. The location of the pole should be very far in the left plane for proper representation.

The output of the derivative block now is,

$$O_3 = k_d.(\dot{X}_1 + zX_1) \tag{3-6}$$

where, X_1 is an intermediate state. The state equation is,

$$\dot{X}_1 = \Delta X - pX_1 \tag{3-7}$$

3.5 PWMSC controller parameters optimization

Optimum values of PID gains were obtained through a genetic algorithm (GA). The steps in deriving the control are presented in the following.

3.5.1 Objective function

The objective of the PWMSC controller is selected so as to minimize the electromechanical mode oscillation. The following objective functions are proposed for measuring the performance of the PWMSC controller.

$$J_1 = \int_0^{t_{sim}} (\Delta\omega)^2 dt \tag{3-8}$$

$$J_2 = \int_0^{t_{sim}} |\Delta\omega| dt \tag{3-9}$$

$$J_3 = \int_0^{t_{sim}} t|\Delta\omega| dt \tag{3-10}$$

where, $\Delta\omega$ is the speed deviation of the generator.

Time-domain simulation of the nonlinear model of power system incorporating all saturation limits of control signals is carried out for the simulation period to calculate the objective function. It is aimed to minimize the objective functions in order to improve the system response in terms of the settling time and overshoots.

3.5.2 Optimization problem

For minimizing J, the following constraints are considered,

$$0 \leq D_p \leq 1 \tag{3-11}$$

$$k_{p_{min}} \leq k_p \leq k_{p_{max}} \tag{3-12}$$

$$k_{i_{min}} \leq k_i \leq k_{i_{max}} \tag{3-13}$$

$$k_{d_{min}} \leq k_d \leq k_{d_{max}} \tag{3-14}$$

$$p_{min} \leq p \leq p_{max} \tag{3-15}$$

$$z_{min} \leq z \leq z_{max} \tag{3-16}$$

Here, D_p is the on-period duty ratio of the PWMSC switches, which is by definition limited in between 0 to 1. k_p, k_i, k_d, p, z are PID controller parameters which are bounded to their corresponding minimum and maximum values.

Real-coded genetic algorithm (RCGA) is employed to solve this optimization problem and search for optimal set of the controller parameters.

3.5.3 Real-coded genetic algorithm

Genetic algorithms (GAs) are general purpose search algorithms which use principles inspired by natural genetic populations to evolve solutions to problems. The basic idea is to maintain a population of chromosomes which represent candidate solutions to the concrete problem that evolves over time through a process of competition and controlled variation. Each chromosome in the population has an associated fitness to determine which chromosomes are used to form new ones in the competition process which is called selection. The new ones are created using genetic operators such as crossover and

mutation which are described below. GAs have had a great measure of success in search and optimization problems.

3.5.3.1 Crossover

A blend crossover operator (BLX-α) has been employed in this study. This operator starts by choosing randomly a number from the interval $[x_i - \alpha(y_i - x_i), y_i + \alpha(y_i - x_i)]$, where x_i and y_i are the *i*th parameter values of the parent solutions and $x_i < y_i$. To ensure the balance between exploitation and exploration of the search space, α = 0.5 was selected. This operator is depicted in Figure 3-8.

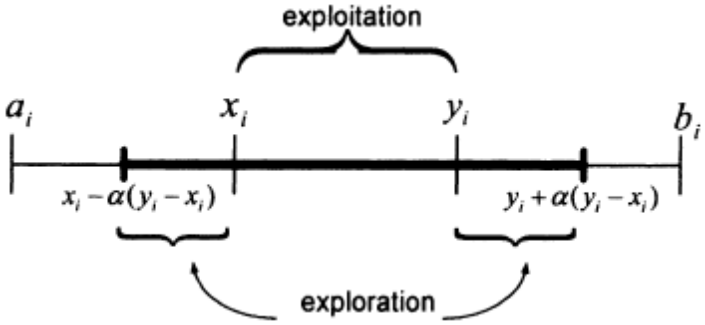

Figure 3-8: Blend crossover operator (BLX-α)

3.5.3.2 Mutation

The random mutation operator has been employed in this study. In this operator, the new value x_i' is a random (uniform) number from the domain $[a_i , b_i]$.

RCGA has been applied to search for optimal settings of the optimized parameters of the proposed controller. In our implementation, the crossover and mutation probabilities of 0.8 and 0.01 respectively are found to be quite satisfactory. The number of individuals in each generation is selected to be 100. In addition, the search will terminate if the best solution does not change for

more than 40 generations or the number of generations reaches 50. The computational flow chart of the proposed design approach is shown in Figure 3-9.

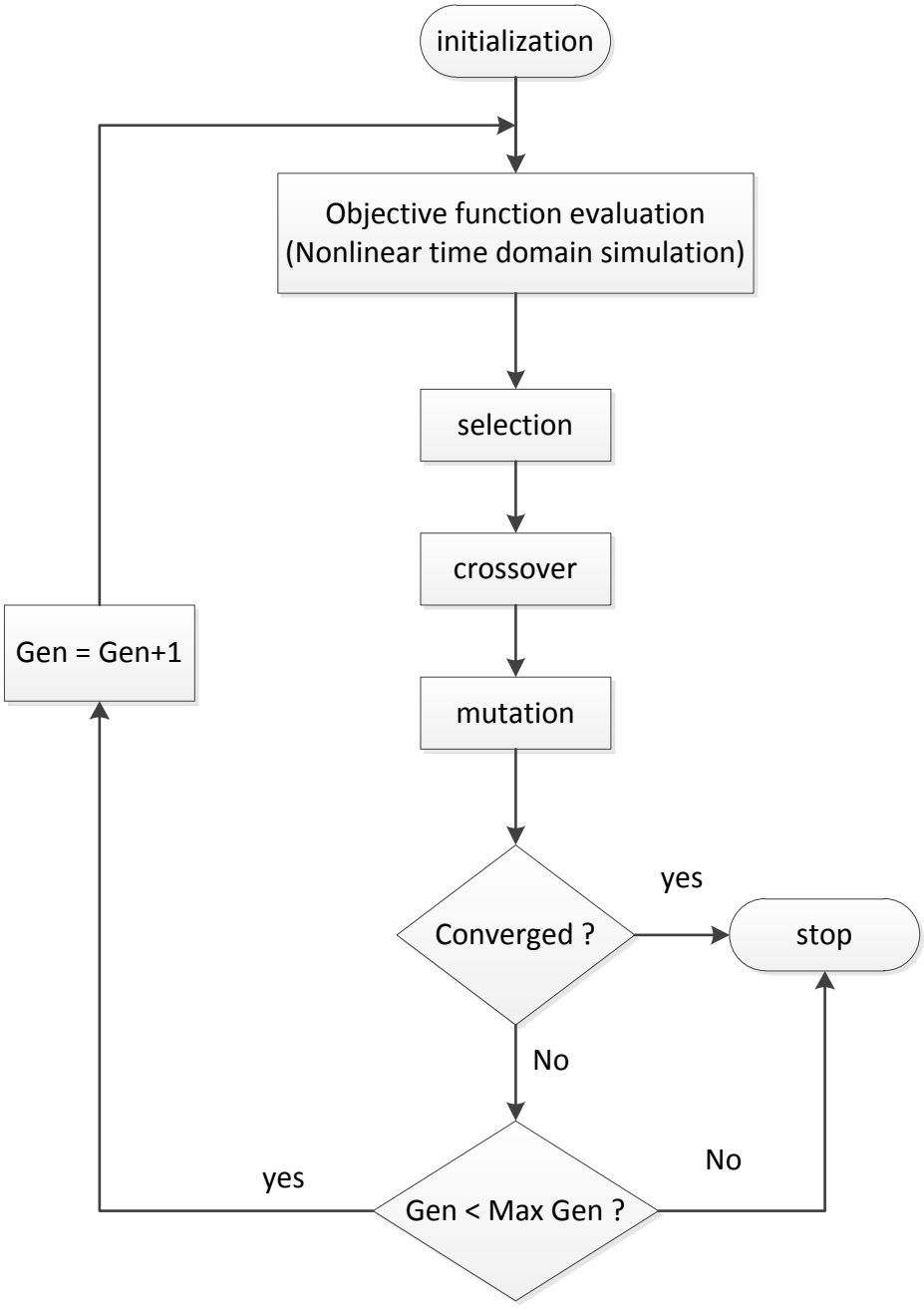

Figure 3-9: Flow chart of proposed Genetic Algorithm

CHAPTER 4

POWER SYSTEM DYNAMIC MODELS WITH PWMSC

Non-linear dynamic models of power systems installed with PWMSC are presented here. In this study, two cases are considered.

1. A single machine infinite bus power system.
2. A multi-machine power system

4.1 Single machine infinite bus power system model

The configuration of the single machine infinite bus (SMIB) power system is illustrated in Figure 4-1. The generator supplies power to the grid over a transmission line which is equipped with the PWMSC.

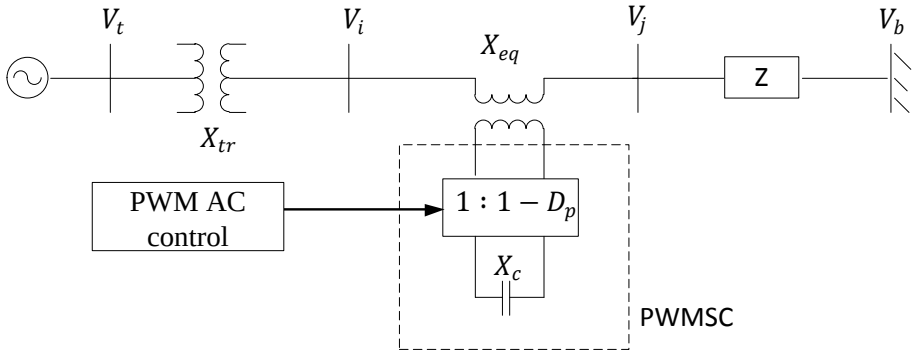

Figure 4-1: Single machine infinite bus system with PWMSC

The dynamic model of the synchronous generator is represented by the fourth-order model including excitation control system. Electromechanical swing equations of the generator are given by:

$$\dot{\delta} = \omega_0(\omega - 1) \tag{4-1}$$

$$\dot{\omega} = \frac{1}{M}\left(P_m - P_e - D(\omega - 1)\right) \tag{4-2}$$

The internal voltage (E'_q) equation is

$$\dot{E'_q} = \frac{1}{T'_{d0}}\left(E_{fd} - E'_q - (x_d - x'_d)i_d\right) \tag{4-3}$$

The IEEE type ST1 is used for the voltage regulator excitation. The block diagram of the excitation system is shown in Figure 4-2.

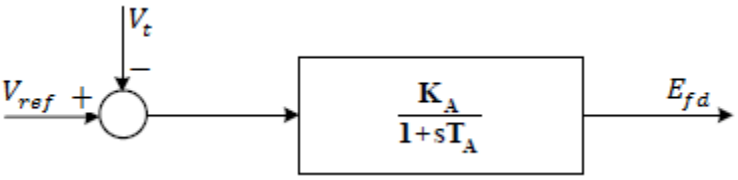

Figure 4-2: Block diagram of IEEE type ST1 excitation system

The excitation system equation is

$$\dot{E_{fd}} = \frac{1}{T_A}\left(K_A\left(V_{ref} - V_t + u_E\right) - E_{fd}\right) \tag{4-4}$$

Here, δ is the rotor angle of the generator, ω_0 is the synchronous speed; ω is the rotor speed, E'_q is the internal voltage of the machine, M is the machine inertia & D is the damping coefficient, P_m and P_e are the input and output powers of the generator, respectively, T'_{d0} is open circuit field time constant of generator, E_{fd} is the field voltage, x_d and x_q are the direct-axis and quadrature-axis reactance, x'_d is the direct-axis transient reactance, i_d,$i_q$and v_d,v_q are d- and q-axis components of the armature current, i and terminal voltage, v_t, K_A and T_A are the gain and time constant of the excitation system.

The set of equations (4-1), (4-2), (4-3) and (4-4) form the non-linear model of SMIB system with PWMSC, where the effect of PWMSC in the transmission line is considered by the equivalent reactance X_{eq} injected by the PWMSC in the transmission line as given in the following equation,

$$X_{eq} = -n^2\left(1 - D_p\right)^2 X_c + X_{LT}$$

This equivalent injected reactance X_{eq} can be controlled by controlling duty ratio, D_p. In order to control D_p both PI and PID controllers have been incorporated. Generator speed deviation, $\Delta\omega$ have been used as stabilizing input signal for the SMIB system. The PID controller configuration in SMIB is shown in Figure 4-3.

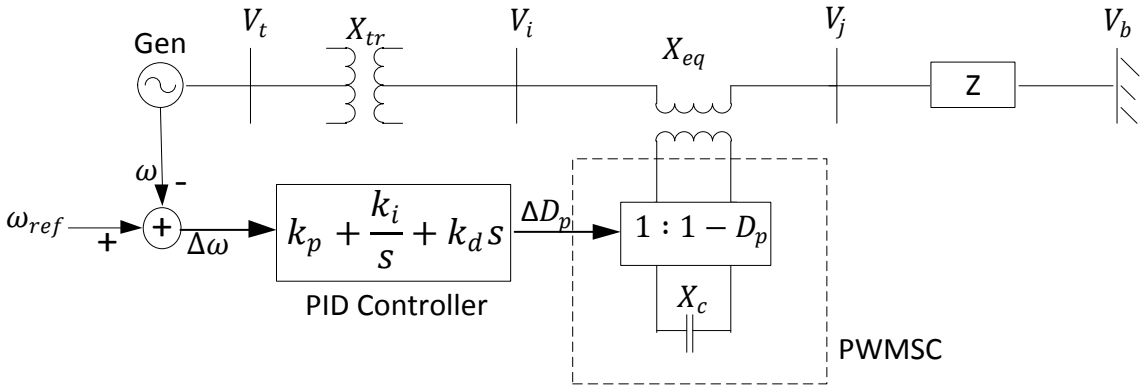

Figure 4-3: SMIB with PID controller

The PID controller controls D_p according to,

$$\Delta D_p = O_1 + O_2 + O_3 \tag{4-5}$$

Where, $O_1 = k_p.(\Delta\omega)$ (4-6)

$$\dot{O_2} = k_i.(\Delta\omega) \tag{4-7}$$

$$O_3 = k_d.(\Delta\dot{\omega}) \tag{4-8}$$

Here, $\Delta\dot{\omega}$ is obtained from Equation (4-2).

PI controller has been implemented with the same configuration but only substituting $k_d = 0$ and thus, $O_3 = 0$ in equation (4-12).

This non-linear model of SMIB system can be written as

$$\dot{x} = f(x, i_d, i_q, P_e, V_t) \tag{4-9}$$

where, x is the vector of state variables, $[\delta, \omega, E'_q, E_{fd}]$ and $[i_d, i_q, P_e, V_t]$ are non-state variables which are calculated from the following,

$$i_d = \frac{-sin\delta.r_i.V_b + (X_{eq}+X_1).(E'_q - V_b.cos\delta)}{{X_{eq}}^2 + X_{eq}.(X_1+X_2) + (X_1.X_2+{r_i}^2)} \tag{4-10}$$

and

$$i_q = \frac{r_i.E'_q - cos\delta.r_i.V_b + (X_{eq}+X_2).V_b.sin\delta}{{X_{eq}}^2 + X_{eq}.(X_1+X_2) + (X_1.X_2+{r_i}^2)} \tag{4-11}$$

Where, $X_1 = x_q + X_{tr} + X_i$ (4-12)

$$X_2 = x'_d + X_{tr} + X_i \tag{4-13}$$

$$Z = r_i + jX_i \tag{4-14}$$

P_e & V_t are calculated from the following equations

$$V_t = \sqrt{(V_d^2 + V_q^2)} \tag{4-15}$$

$$P_e = v_d i_d + v_q i_q \tag{4-16}$$

Where, $v_d = x_q i_q$ (4-17)

$$v_q = E'_q - x'_d i_d \tag{4-18}$$

4.2 Multi-machine power system model with PWMSC

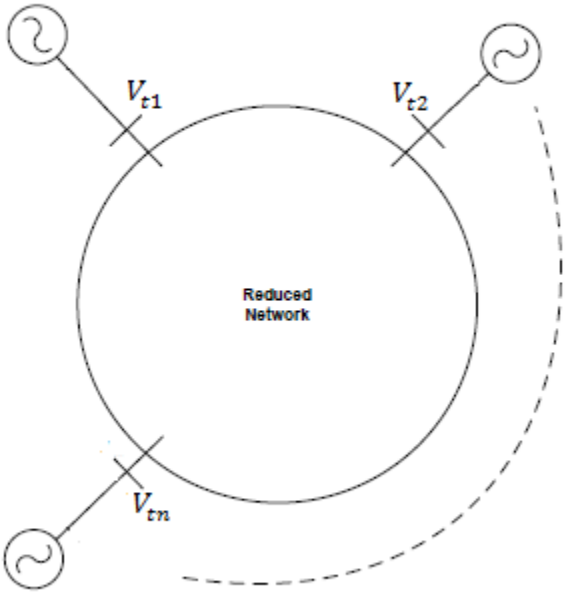

Figure 4-4: Reduced multi-machine system configuration

The model of a multi-machine power system containing the dynamics of synchronous generator, its excitation system, the loads etc., is presented in the following. It is assumed that each generator is connected to the network through its transmission network.

The assumptions made to simplify the mathematical model which describes the non-linear dominant dynamic behavior of a multi-machine power system are,

1. Transient saliency of the generator is neglected (i.e. $x'_d = x'_q$).

2. Governor and turbine dynamics are neglected. This results in constant input mechanical power.

3. The network is in quasi-static state (no transmission line dynamics included).

4. The loads are represented by constant impedance loads. The load buses are eliminated and the network voltage current relationship between the terminal buses of generators is expressed through a reduced bus admittance matrix (Y_b).

The multi-machine power system configuration with the loads eliminated is shown in Figure 4-4. The non-linear dynamics for the i-th machine of the n-machine power system of Figure 4-4 can be written similar to SMIB model equations as,

$$\dot{\delta_i} = \omega_0 \omega_i \tag{4-19}$$

$$\dot{\omega_i} = \frac{1}{M_i}\left(P_{m_i} - P_{e_i} - D_i \omega_i\right) \tag{4-20}$$

$$\dot{E'_{q_i}} = \frac{1}{T'_{d0_i}}\left(E_{fd_i} - E'_{q_i} - \left(x_{d_i} - x'_{d_i}\right) i_{d_i}\right) \tag{4-21}$$

$$\dot{E'_{d_i}} = \frac{1}{T'_{q0_i}}\left(-E'_{d_i} + \left(x_{q_i} - x'_{q_i}\right) i_{q_i}\right) \tag{4-22}$$

$$\dot{E_{fd_i}} = \frac{1}{T_{A_i}}\left(K_{A_i}\left(v_{ref_i} - v_{t_i} + u_{E_i}\right) - E_{fd_i}\right) \tag{4-23}$$

The symbols in (4-19) to (4-23) are exactly the same as in case of single machine system. The variations in d-q internal voltage dynamics have been included in this analysis in line with Anderson's work [64].

This non-linear model for the i-th machine can be expressed in the form,

$$\dot{x_i} = f(x_i, i_{d_i}, i_{q_i}, P_{e_i}, v_{t_i}) \tag{4-24}$$

where, x_i is the state vector for the i-th machine, $[\delta_i, \omega_i, E'_{q_i}, E'_{d_i}, E_{fd_i}]$

The non-linear model of the multi-machine system contains generator currents which are non-state variables. These non-state variables are eliminated by including the voltage-current relationship of the network.

From Figure 4-4,

$$I_L = Y_b V_t \tag{4-25}$$

Here, I_L is the vector of injected currents to the network$[I_{L_1}, I_{L_2}, \ldots\ldots, I_{L_n}]^T$; V_B is the vector of network bus voltages $[V_{t_1}, V_{t_2}, \ldots\ldots, V_{t_n}]^T$ and Y_b is the reduced bus admittance matrix.

The currents and voltages in (4-25) are complex quantities and when broken up into real and imaginary parts, they will be along the natural common frame of reference, called the D-Q coordinates. The state equations in (4-19) to (4-23) for each generator are along their individual d_i-q_i frames of references. In order to combine the network equations (4-25) with the machine equation a transformation of variables is needed. The following two transformations are reported in the literature [64],

a) Transforming generator quantities to common reference frame.

b) Transforming network equations to individual generator reference frames.

In this thesis the second transformation is used; the advantage is that the generator quantities remain unchanged thus making control design somewhat simpler.

Consider the phasor diagram shown in Figure 4-5. Here, D – Q is the common network reference frame and d_i-q_i is the reference frames of individual machines.

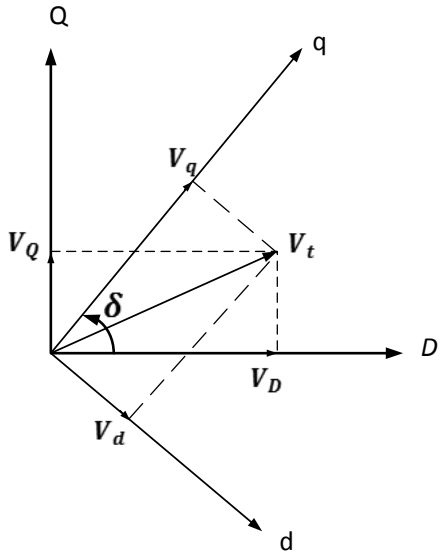

Figure 4-5: Phasor relationship between two frames of references

Let δ_i (the rotor angle for i-th synchronous machine) be the angle between D and q_i. It can be shown from Figure **4-5** that,

$$V_{Di} = V_{di}sin\delta_i + V_{qi}cos\delta_i \tag{4-26}$$

$$V_{Qi} = -V_{di}cos\delta_i + V_{qi}sin\delta_i \tag{4-27}$$

or,

$$V_{Di} + jV_{Qi} = V_{di}sin\delta_i + V_{qi}cos\delta_i + j(-V_{di}cos\delta_i + V_{qi}sin\delta_i) \tag{4-28}$$

$$V_{ti\ D-Q} = e^{j\left(\delta_i - \frac{\pi}{2}\right)}V_{ti\ d-q} \tag{4-29}$$

Here, $V_{ti\ D-Q}$ is the terminal voltage on common reference frame D – Q and $V_{ti\ d-q}$ is the terminal voltage in d – q frame of machine i.

Equation (4-29) can be written as,

$$V_{ti\ D-Q} = T_r V_{ti\ d-q} \tag{4-30}$$

Or $V_{ti\ d-q} = T_r^{-1} V_{ti\ D-Q}$ (4-31)

Where, T_r is known as the transformation matrix and $V_{ti\ D-Q}$, $V_{ti\ d-q}$ are the terminal voltage matrices along the two reference frames. These matrices are shown below.

$$V_{ti\ d-q} = \begin{bmatrix} V_{d1} + jV_{q1} \\ V_{d2} + jV_{q2} \\ . \\ . \\ . \\ V_{dn} + jV_{qn} \end{bmatrix}, \quad V_{ti\ D-Q} = \begin{bmatrix} V_{D1} + jV_{Q1} \\ V_{D2} + jV_{Q2} \\ . \\ . \\ . \\ V_{Dn} + jV_{Qn} \end{bmatrix},$$

$$T_r = \begin{bmatrix} e^{j\left(\delta_1 - \frac{\pi}{2}\right)} & & & \\ & e^{j\left(\delta_2 - \frac{\pi}{2}\right)} & & \\ & & \dots\dots & \\ & & & e^{j\left(\delta_n - \frac{\pi}{2}\right)} \end{bmatrix}$$

Similarly the currents on the network frame can be written as

$$I_{L\ D-Q} = T_r I_{L\ d-q} \quad (4\text{-}32)$$

I_L and V_B in (4-25) are in network frame (D–Q) which can be transformed to (d–q) frame using (4-30) and (4-32) as,

$$T_r I_{L\ d-q} = Y_b T_r V_{ti\ d-q} \quad (4\text{-}33)$$

Pre – multiplying by T_r^{-1} yields,

$$I_{L\ d-q} = (T_r^{-1} Y_b T_r) V_{t\ d-q} \quad (4\text{-}34)$$

Or, $I_{L\ d-q} = Y_m V_{t\ d-q}$ (4-35)

Where, $Y_m = (T_r^{-1}\ Y_b T_r) = G_m + jB_m$ (4-36)

Here, Y_m is the reduced admittance matrix transferred to generator coordinates. For convenience the subscript d–q in (4-35) is dropped from now onwards and is to be assumed that all the variables are referred to generator side unless mentioned otherwise.

Referring to Figure 4-6, it can be seen that the multi-machine case is similar to SMIB case except that the currents and voltages are all vectors and all the reactance are expressed as diagonal matrices.

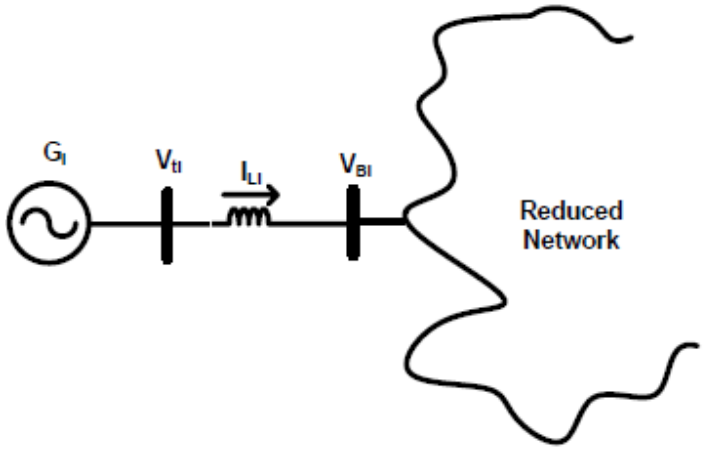

Figure 4-6: Configuration of the i-th generator in n–machine system

The non-state variables in (4-24) are eliminated by breaking (4-35) in d–q components as,

$$I_d + jI_q = (G_m + jB_m)(V_d + jV_q) \tag{4-37}$$

Now, $V_d = e'_d + x'I_q$ (4-38)

$$V_q = e'_q - x'I_d \tag{4-39}$$

Here, $x'_q = x'_d = x'$ (transient saliency neglected)

Substituting (4-38), (4-39) into (4-37) and solving for I_d, I_q we get,

$$I_d = K_4^{-1}K_1^{-1}\{(K_3B_m + G_m)e'_d + (K_3G_m - B_m)e'_q\} \tag{4-40}$$

and $$I_q = K_1^{-1}[B_m e'_d + G_m e'_q - G_m x'I_d] \tag{4-41}$$

Where, $K_1 = 1 - B_m x'$ (4-42)

$$K_3 = G_m x' K_1^{-1} \tag{4-43}$$

$$K_4 = 1 + K_1^{-1} K_3 G_m x' \tag{4-44}$$

Now, $$V_t = \sqrt{\left(V_d^2 + V_q^2\right)} \tag{4-45}$$

Where, V_d & V_q can be found from (4-38) & (4-39) respectively after obtaining I_d, I_q from (4-40), (4-41). And P_e can be calculated from the following equation.

$$P_e = V_d I_d + V_q I_q \tag{4-46}$$

The effect of PWMSC in the transmission line is considered by the equivalent reactance X_{eq} as given in equation (3-1),

$$X_{eq} = -n^2\left(1 - D_p\right)^2 X_c + X_{LT}$$

This equivalent reactance X_{eq} is seen from the primary side of the coupling transformer injected by the PWMSC. So, this X_{eq} is added to the transmission line reactance where the PWMSC is connected. If the PWMSC is connected in the transmission line between bus i & bus j, then

So, $$X_{ij} = X_{ij} + X_{eq} \tag{4-47}$$

Then, the reduced bus admittance matrix (Y_b) is formed for this multi-machine system eliminating the load buses retaining only the generator buses. This Y_b is then transferred to generator coordinates admittance matrix (Y_m) through (4-36) .

This new Y_m will affect the calculations of non-state variables, i_{d_i}, i_{q_i}, P_{e_i}, v_{t_i} in equations (4-40), (4-41), (4-46) & (4-45) respectively and the nonlinear model of this multi-machine system as well.

4.2.1 PWMSC installed Multi-machine power system with PID controller

A PID controller has been employed to control the degree of compensation of the PWMSC controller. Three different stabilizing input signals have been used for the PID controller in the multi-machine case in order to evaluate the efficiency of these signals as tracking signals. Moreover, as generator speed is not available at all locations of the system performance of other signals have been investigated.

4.2.1.1 Speed deviation Δω as input to PID controller

The speed deviation of generator-i of the multi-machine system was taken as the stabilizing input signal to the PID controller of PWMSC.

PID controller dynamics can be written as

$$\Delta D_p = O_1 + O_2 + O_3 \tag{4-48}$$

where, $O_1 = k_p.(\Delta\omega_i)$ (4-49)

$$\dot{O_2} = k_i.(\Delta\omega_i) \tag{4-50}$$

$$O_3 = k_d.(\Delta\dot{\omega}_i) \tag{4-51}$$

Here, k_p , k_i & k_d are the PID controller parameters and the expression of $\Delta\dot{\omega}_i$ is obtained from (4-20).

PI controller was also employed by making $O_3 = k_d = 0$ and simplifying PID controller dynamics to,

$$\Delta\dot{D}_p = k_p.\Delta\dot{\omega}_2 + k_i.(\Delta\omega_2) \tag{4-52}$$

4.2.1.2 Active power output deviation, ΔP_e as input to PID controller

The performance of active power output deviation, ΔP_e as a stabilizing input to PID controller is also explored. The active power output deviation of generator-i is tracked to regulate the duty ratio, D_p of the PWMSC.

Here, D_p is regulated according to,

$$\Delta D_p = O_1 + O_2 + O_3 \tag{4-53}$$

Where, $O_1 = k_p.(\Delta P_{e_i})$ (4-54)

$$\dot{O}_2 = k_i.(\Delta P_{e_i}) \tag{4-55}$$

$$O_3 = k_d \frac{(s+z)}{(s+p)}.(\Delta \dot{P}_{e_i}) \tag{4-56}$$

Here, k_d is replaced by $k_d \frac{(s+z)}{(s+p)}$ in order to avoid the differentiation of the active power output deviation, ΔP_{e_i} which is not readily available.

So, Equation (4-56) can be decomposed into

$$O_3 = k_d.(\dot{X}_1 + zX_1) \tag{4-57}$$

Where, X_1 is an intermediate state variable and

$$\dot{X}_1 = \Delta P_{e_i} - pX_1 \tag{4-58}$$

Here, we don't need to determine the expression of $\Delta \dot{P}_{e_2}$.

$$\Delta P_{e_i} = P_{e_{i_{ref}}} - P_{e_i} \tag{4-59}$$

$$P_{e_i} = v_{d_i} i_{d_i} + v_{q_i} i_{q_i} \tag{4-60}$$

$P_{e_{2_{ref}}}$ is considered as P_{e_2} at steady state.

The governing equation of the PI controller is obtained from (4-53) by putting $O_3 = 0$.

4.2.1.3 Change in transmission line active power flow ΔP_{ij} as stabilizing input signal to PID controller

Change in active power flow of transmission line is also used as stabilizing input signal to PID controller. If the PWMSC is connected in the transmission line between bus-i & bus-j, change in active power flow from bus-i to bus-j was taken as the stabilizing input signal to the PID controller of PWMSC. Where, active power flow from bus-i to bus-j at steady state is taken as reference.

$$P_{ij} = real\left\{(v_i - v_j).\ conj\left((v_i - v_j).y_{ij}\right)\right\} \tag{4-61}$$

$$\Delta P_{ij} = P_{ij_{ref}} - P_{ij} \tag{4-62}$$

$P_{ij_{ref}}$ is P_{ij} at steady state.

The PID controller equations can be written as,

$$\Delta D_p = O_1 + O_2 + O_3 \tag{4-63}$$

Where, $O_1 = k_p.(\Delta P_{ij})$ (4-64)

$$\dot{O_2} = k_i.(\Delta P_{ij}) \tag{4-65}$$

$$O_3 = k_d \frac{(s+z)}{(s+p)}.(\Delta \dot{P}_{ij}) \tag{4-66}$$

Equation (4-66) can be decomposed into

$$O_3 = k_d.(\dot{X}_1 + zX_1) \tag{4-67}$$

Here, X_1 is an intermediate state variable and

$$\dot{X}_1 = \Delta P_{ij} - pX_1 \tag{4-68}$$

CHAPTER 5

SIMULATION RESULTS: SINGLE MACHINE INFINITE BUS SYSTEM WITH PWMSC

5.1 PWMSC with PI controller

The single machine infinite bus system given in Figure 4-1 was simulated to test the damping performance of the PWMSC controllers. A PI controller, as shown in Figure 5-1 was used to control the PWMSC reactor. The system data & operating condition is given in Appendix-A. The input to the PI controller was considered to be generator speed deviation.

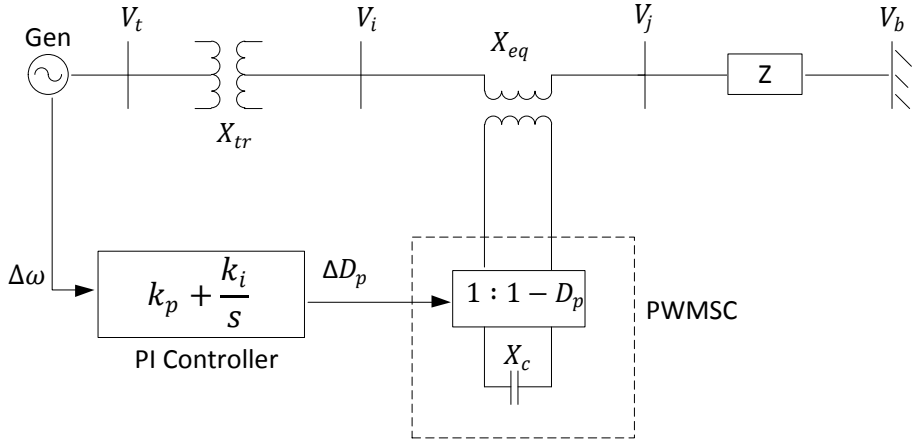

Figure 5-1: SMIB with PI controller

The system performance has been tested by simulating the power system model for a disturbance of 30% torque input pulse of 0.2s duration applied after 1 sec.

The effect of PWMSC device inserted in the SMIB system without stabilizing control is shown in Figure 5-2 and Figure 5-3. From the figures it is clearly visible that the PWMSC device decreases the power system oscillations and improves the stability of the system without any stabilizing control.

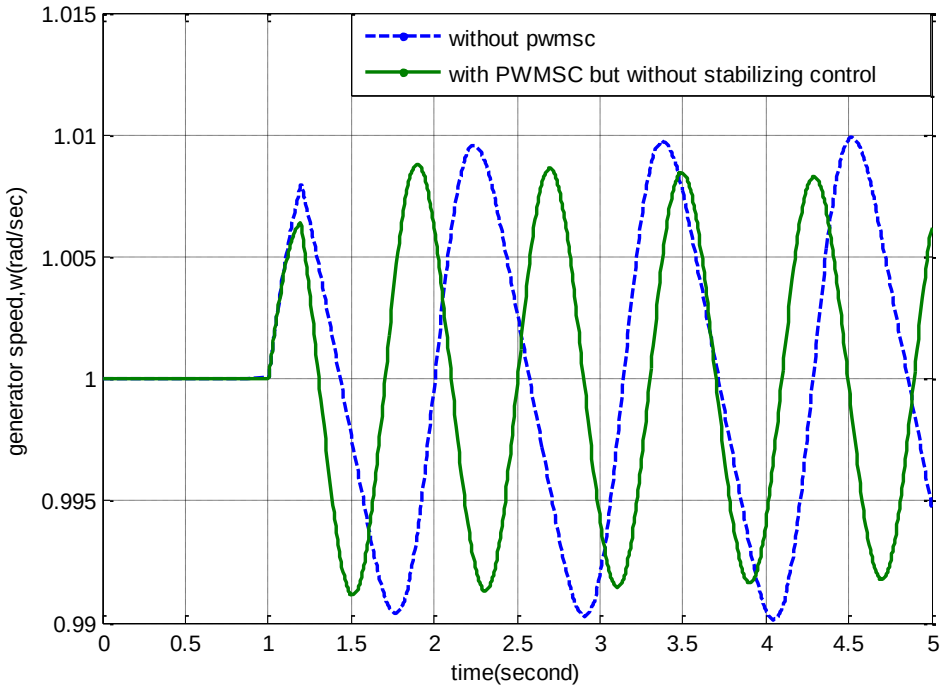

Figure 5-2: Effect of PWMSC device on SMIB system generator speed

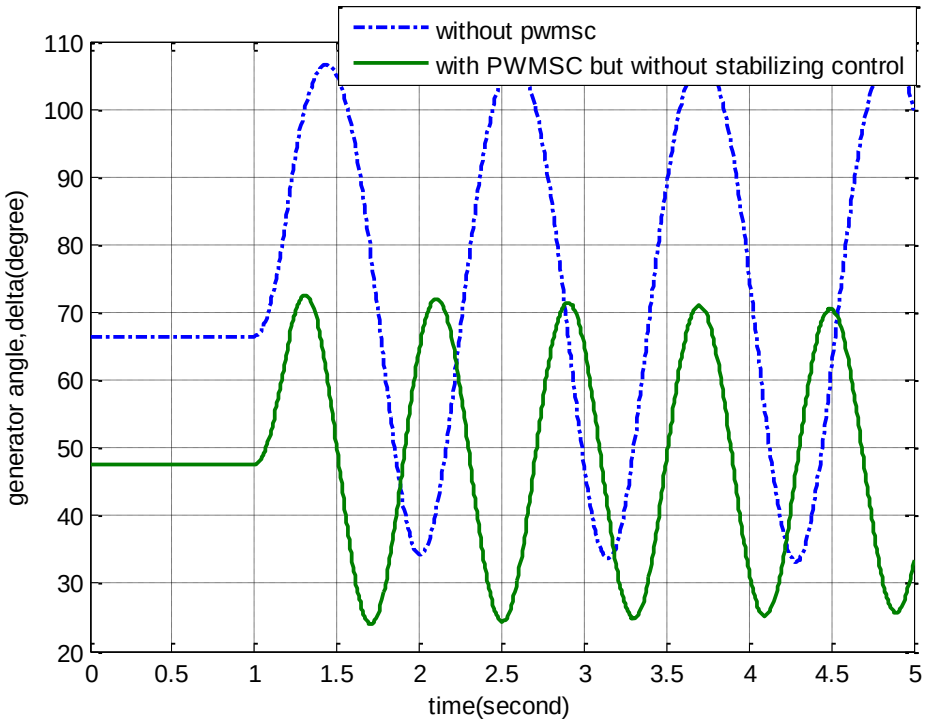

Figure 5-3: Effect of PWMSC device on SMIB system generator angle

In order to get the best out of the PWMSC device, the stabilizing control has to be incorporated. Here, the PI controller is employed to serve this purpose. To optimize the PI controller parameters (k_p, k_i) Real-coded genetic algorithm (RCGA) has been employed. The objective functions with the constraints are given in (3-8) to (3-16). The maximum & minimum values of k_p, k_i considered in this optimization algorithm are selected as,

$$k_{p_{min}} = -1000, \qquad k_{p_{max}} = 1000, \qquad k_{i_{min}} = -1000, \qquad k_{i_{max}} = 1000$$

The optimum gains obtained for the three objective functions are summarized in the following table.

Table 5-1: Optimum gain parameters for the SMIB system in 5.1

Objective functions	$J_1 = \int_0^{t_{sim}} (\Delta\omega)^2 dt$	$J_2 = \int_0^{t_{sim}} \lvert\Delta\omega\rvert dt$	$J_3 = \int_0^{t_{sim}} t\lvert\Delta\omega\rvert dt$
Optimum parameters	k_p =-1000 $k_i = -997.46$	$k_p = -980.44$ $k_i = 283.35$	k_p =–647.47 k_i =274.59

The simulation results obtained for these three sets of optimum parameters for a 30% torque pulse for 0.2s are shown in Figure 5-4, Figure 5-5, Figure 5-6 and Figure 5-7.

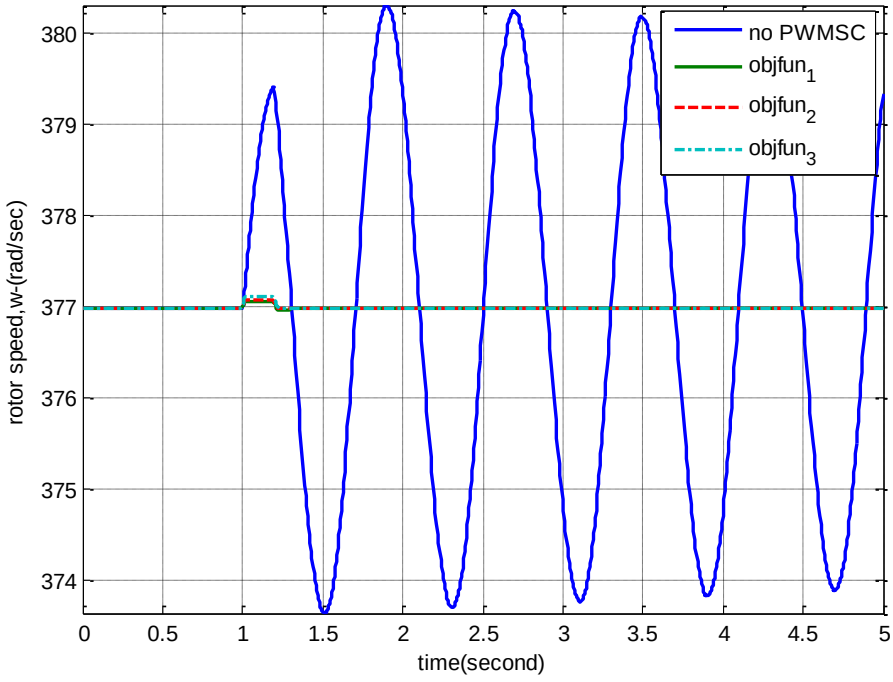

Figure 5-4: Nonlinear system response of rotor speed for three cases of the SMIB system with a torque input pulse disturbance in the generator

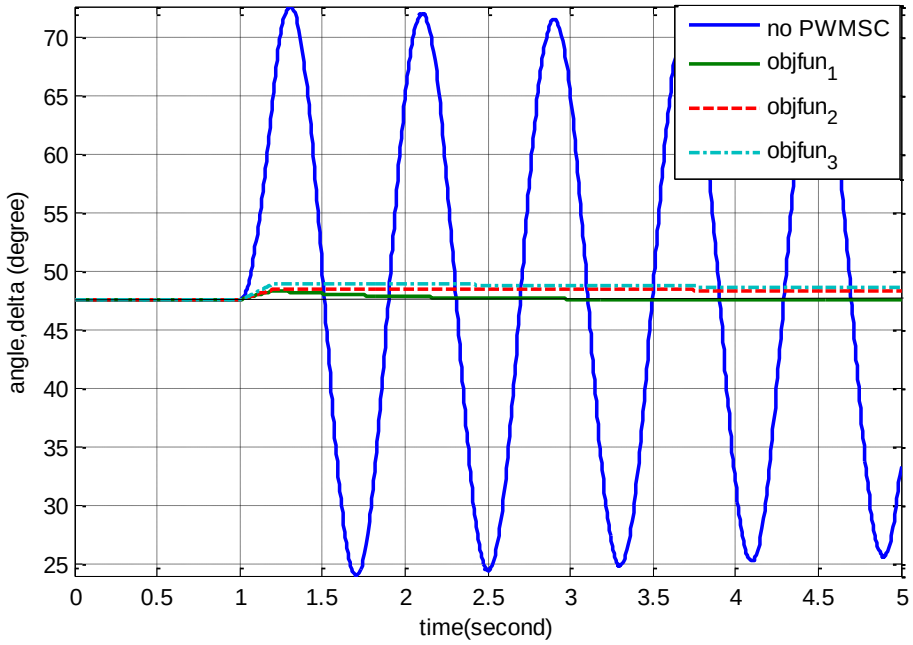

Figure 5-5: Nonlinear system response of rotor angle for three cases of the SMIB system with a torque input pulse disturbance in the generator.

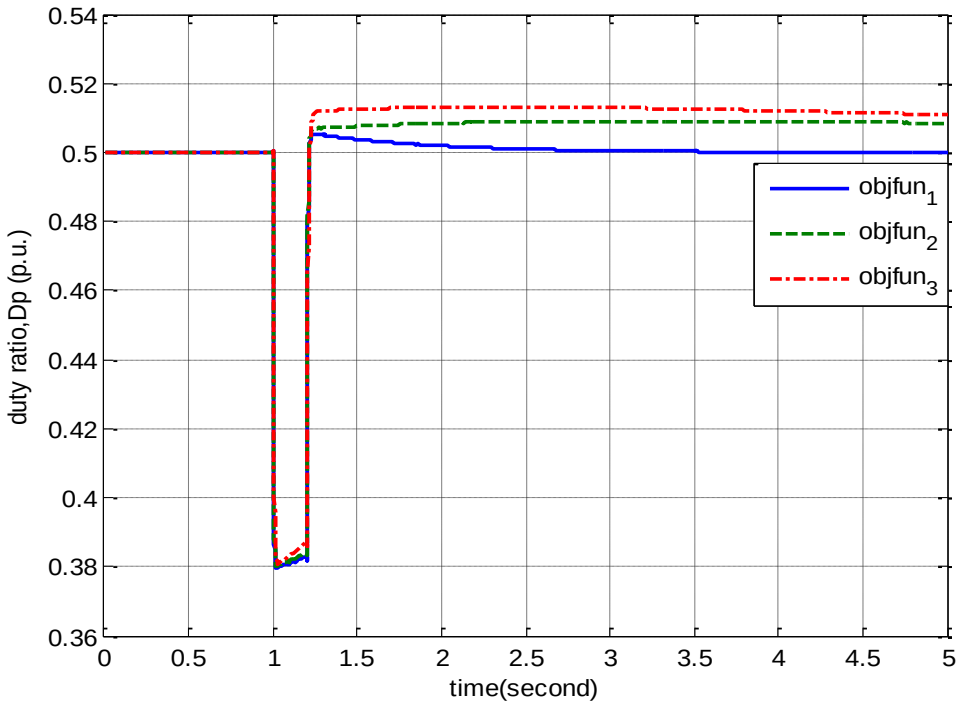

Figure 5-6: Control signal (duty ratio) of the PWMSC for three cases of the SMIB system with a torque input pulse disturbance in the generator.

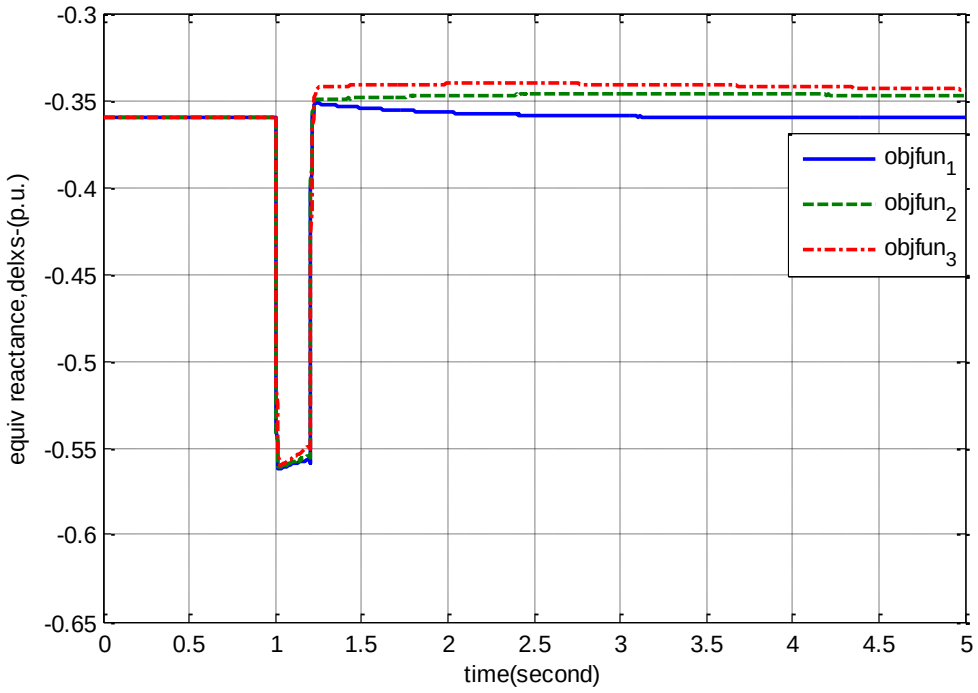

Figure 5-7: Equivalent reactance of the PWMSC for three cases of the SMIB system with a torque input pulse disturbance in the generator

Figure 5-4 and Figure 5-5 shows the variation of rotor speed and rotor angles, respectively, while Figure 5-6 and Figure 5-7 shows the control signal and the equivalent reactance, of the PWMSC. Responses obtained for the three different sets of optimum parameters corresponding to three objective functions are plotted to compare the suitability of the objective functions.

From Figure 5-5, Figure 5-6 and Figure 5-7 can be seen that the response with objective function J_1 settles back to its steady-state position faster than other objective functions J_2 and J_3. But in Figure 5-4 the generator rotor speed response shows that the settling time for J_2 *and* J_3 is lower than J_1 but their percent overshoot is higher.

However, all three responses show that the PWMSC controller has an outstanding performance in damping electromechanical oscillations.

Though the results obtained are excellent, they are obtained at the cost of very high gain parameters (k_p, k_i). That's why another optimum parameter search is done with limiting the k_p, k_i values to lower limits as given below,

$$k_{p_{min}} = -100, \qquad k_{p_{max}} = 100, \qquad k_{i_{min}} = -100, \qquad k_{i_{max}} = 100$$

The parameters are optimized with the objective function $J_1 = \int_0^{t_{sim}} (\Delta\omega)^2 dt$ only. The optimization results are given below,

$$k_p = -80, \qquad k_i = -10$$

The simulation results with this PI configuration are shown Figure 5-8 to Figure 5-12.

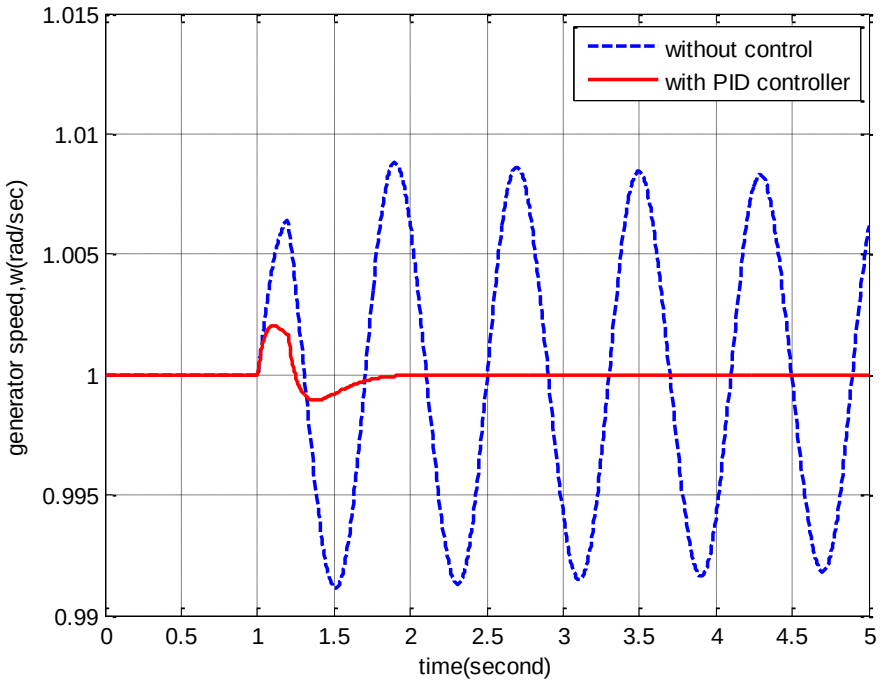

Figure 5-8: Nonlinear system response of rotor speed of the SMIB system with PI controller for a torque input pulse disturbance in the generator

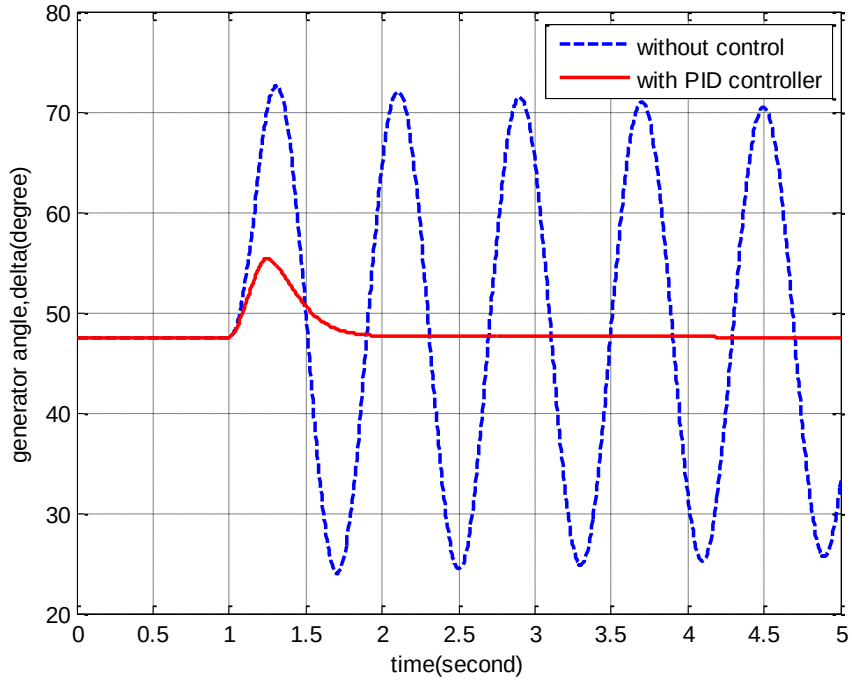

Figure 5-9: Nonlinear system response of rotor angle for the SMIB system with PI controller for a torque input pulse disturbance in the generator

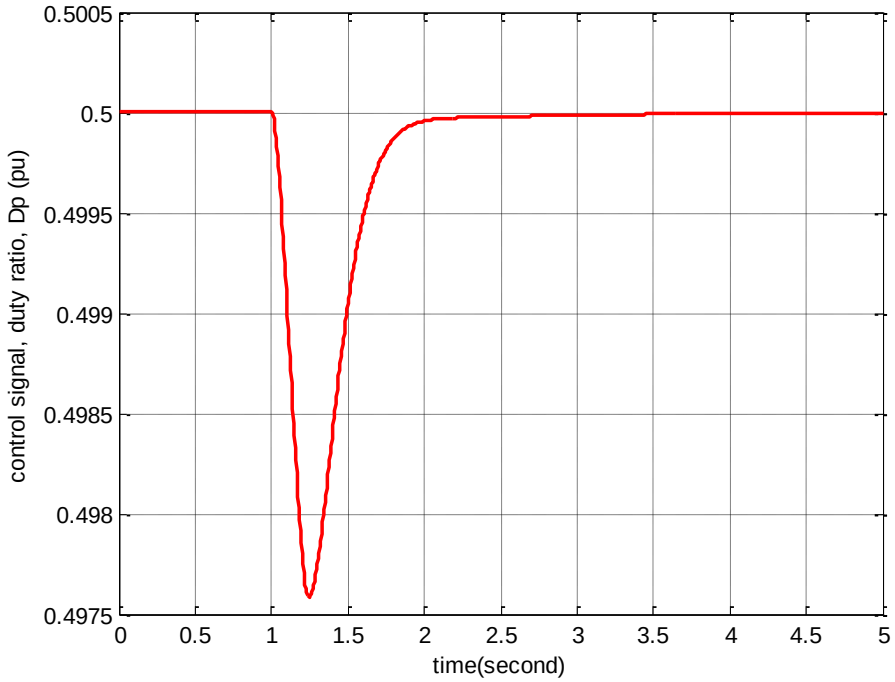

Figure 5-10: Control signal (duty ratio) of the PWMSC for the SMIB system with PI controller for a torque input pulse disturbance in the generator

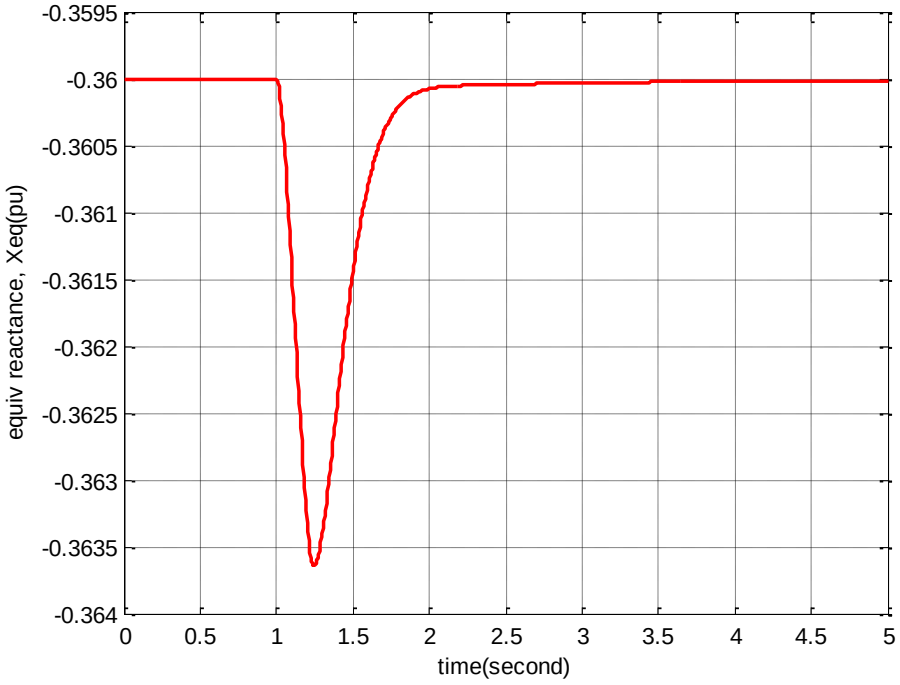

Figure 5-11: Equivalent reactance of the PWMSC for the SMIB system with PI controller for a torque input pulse disturbance in the generator

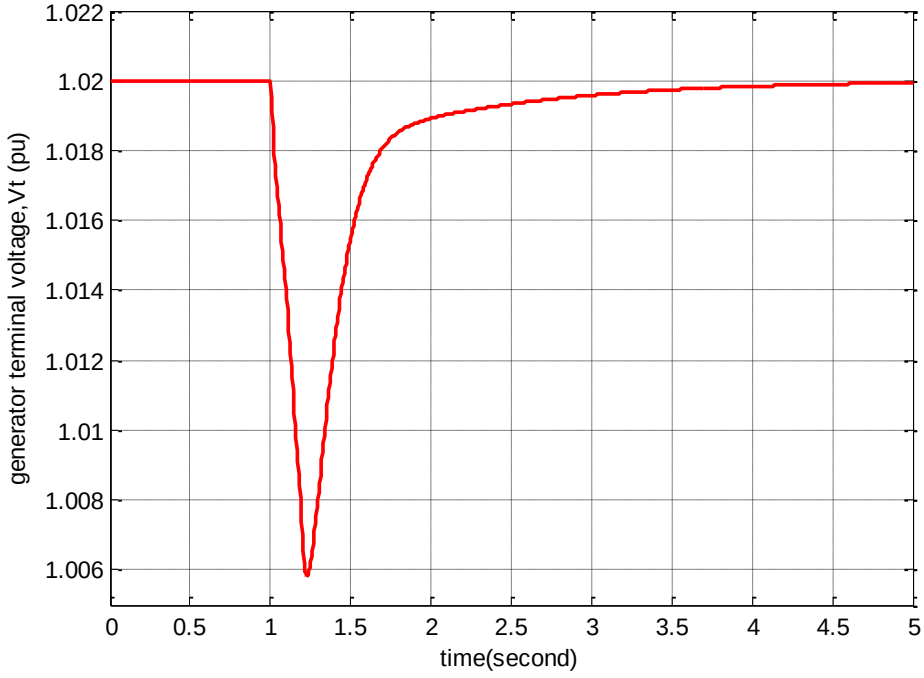

Figure 5-12: Generator terminal voltage, V_t for the SMIB system with PI controller for a torque input pulse disturbance in the generator

These results show quite satisfactory damping performance of the system with relatively very lower gains of k_p and k_i.

5.2 PWMSC with PID controller

The single machine infinite bus system installed with PWMSC is also tested with PID controller with generator speed deviation as stabilizing signal as shown in Figure 4-3. The system data & operating condition are given in Appendix A.

The PWMSC controller was tested as the SMIB system incorporating a PID controller considering a disturbance of 30% torque input pulse of 0.2s duration.

The maximum & minimum values of k_p, k_i , k_d considered in the RCGA optimization are,

$$k_{p_{min}} = -100, \quad k_{p_{max}} = 100, \quad k_{i_{min}} = -100, \quad k_{i_{max}} = 100,$$

$$k_{d_{min}} = -10, \; k_{d_{max}} = 10$$

The parameters are optimized with the objective function $J_1 = \int_0^{t_{sim}} (\Delta\omega)^2 dt$ only. The optimization results are given below,

$$k_p = -80, \qquad k_i = -10, \quad k_d = 0.0911$$

The simulation results with this PID configuration are shown Figure 5-13 to Figure 5-17.

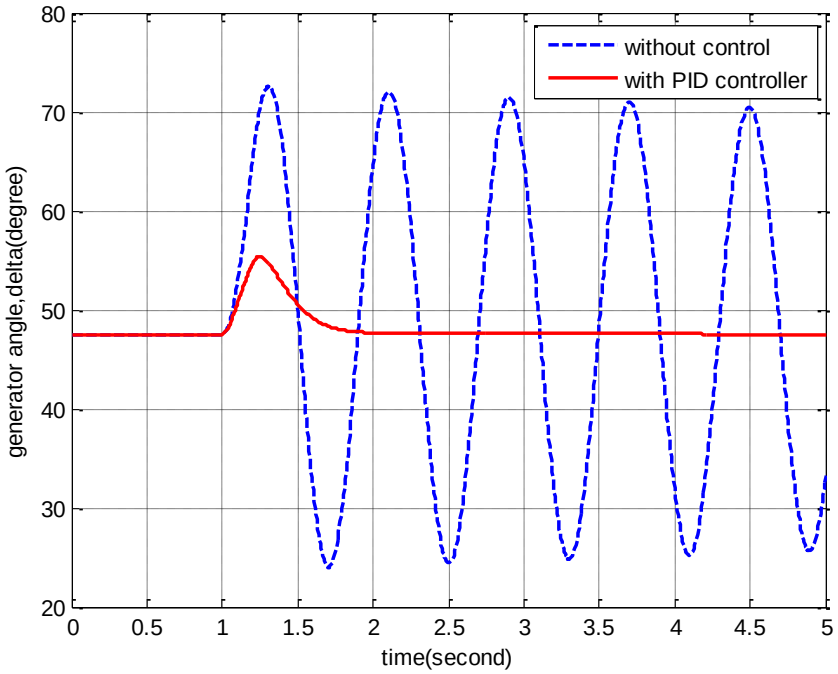

Figure 5-13: Nonlinear system response of rotor speed of the SMIB system with PID controller for a torque input pulse disturbance in the generator

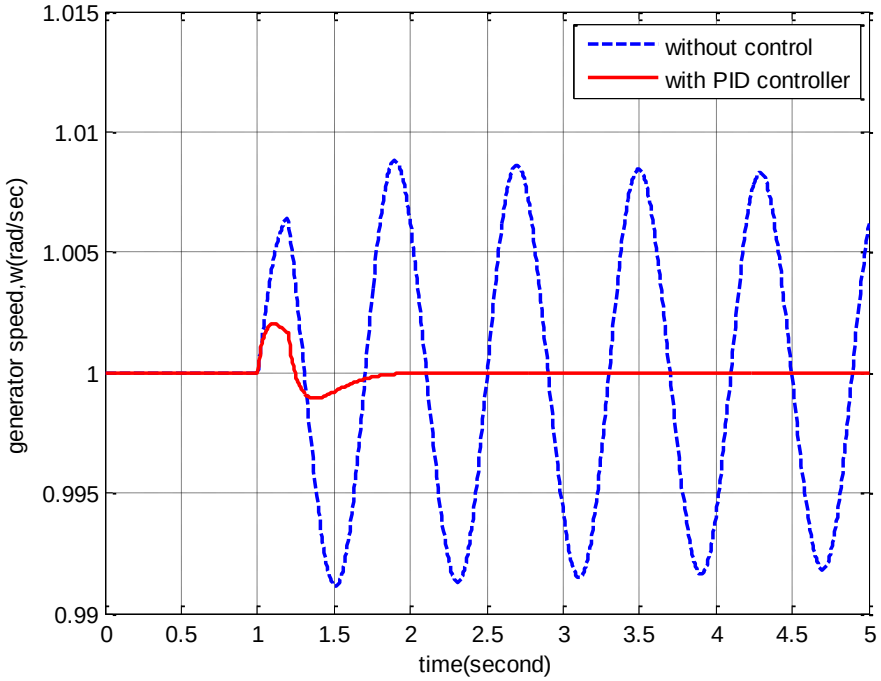

Figure 5-14: Nonlinear system response of rotor speed of the SMIB system with PID controller for a torque input pulse disturbance in the generator

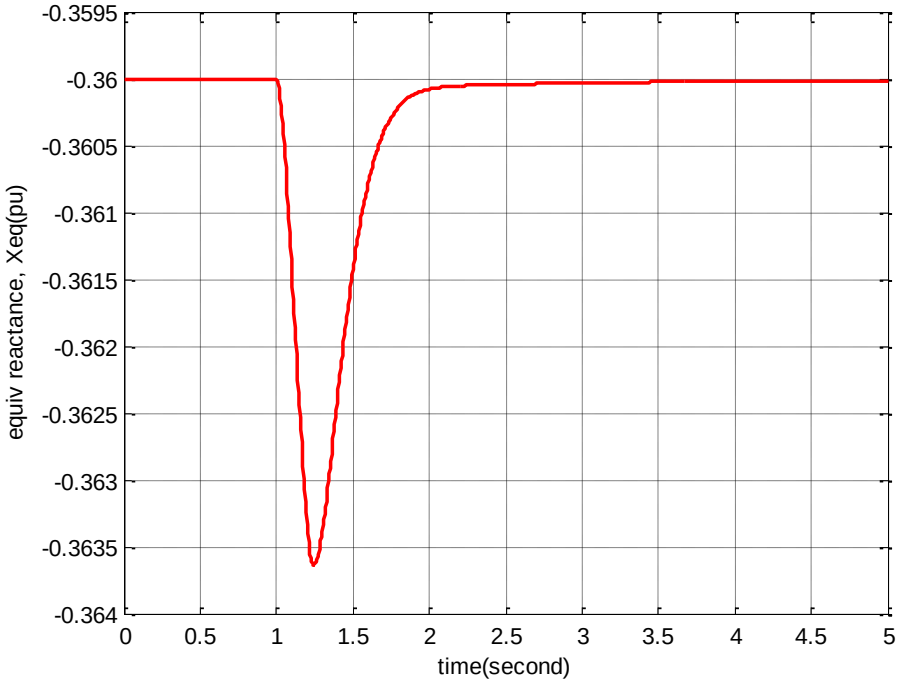

Figure 5-15: Equivalent reactance of the PWMSC of the SMIB system with PID controller for a torque input pulse disturbance in the generator

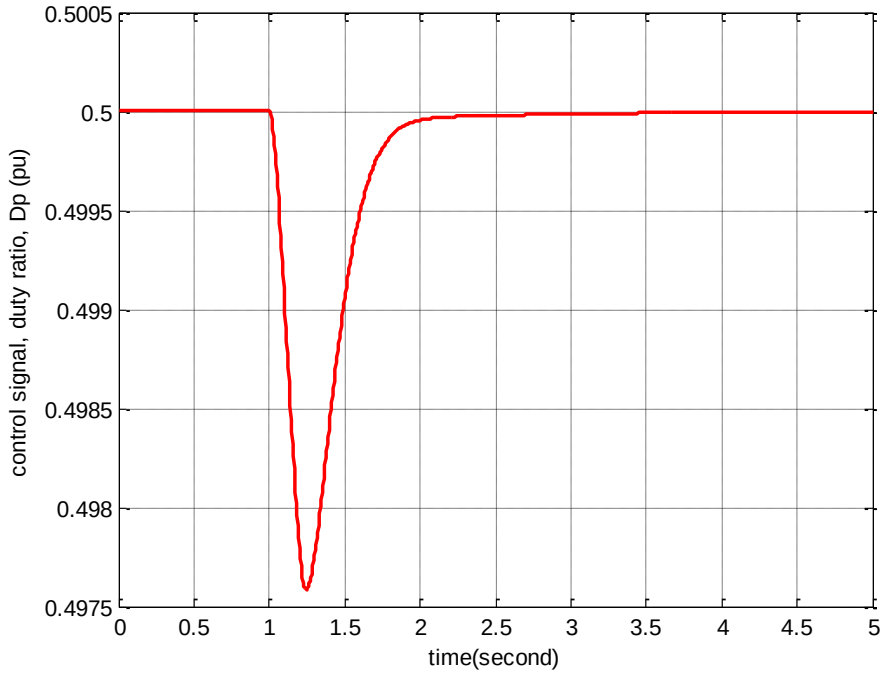

Figure 5-16: Control signal (duty ratio) of the PWMSC of the SMIB system with PID controller for a torque input pulse disturbance in the generator

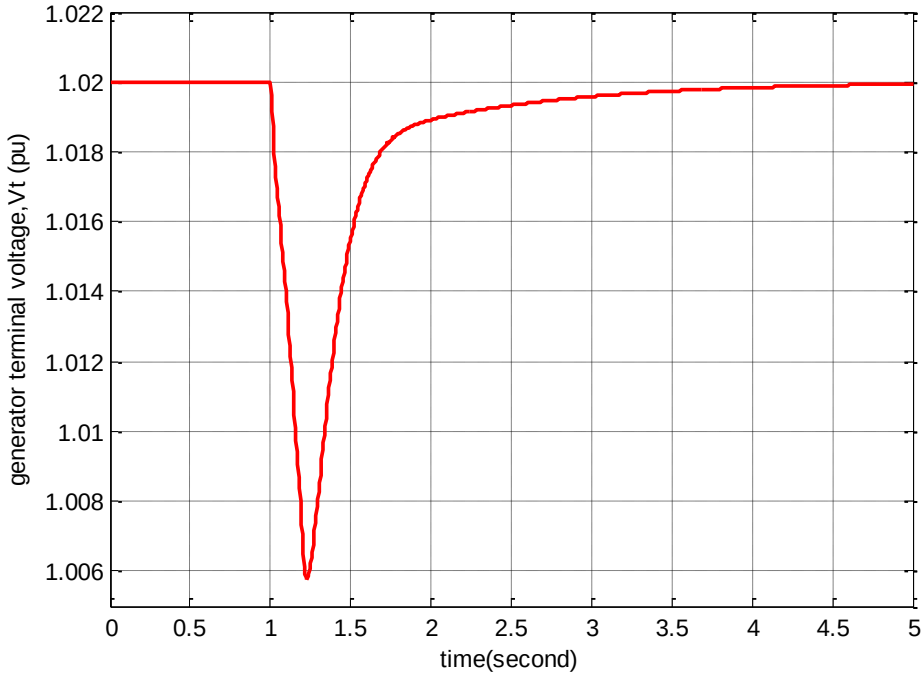

Figure 5-17: Generator terminal voltage, V_t of the SMIB system with PID controller for a torque input pulse disturbance in the generator

These results show quite satisfactory damping performance of the system but use of PID controller doesn't show significant improvement over PI controller.

5.3 Three phase fault study of the SMIB system

The robustness of the PWMSC controllers was checked by experiencing the SMIB system a three phase fault as shown in Figure 5-18. A three phase fault was simulated at the infinite bus for three cycles (0.05 sec). Here, a PID controller is employed to add stabilizing control of the PWMSC. Deviation of speed of the generator is taken as stabilizing input signal to the PID controller. Simulation results are shown in Figure 5-19 to Figure 5-23.

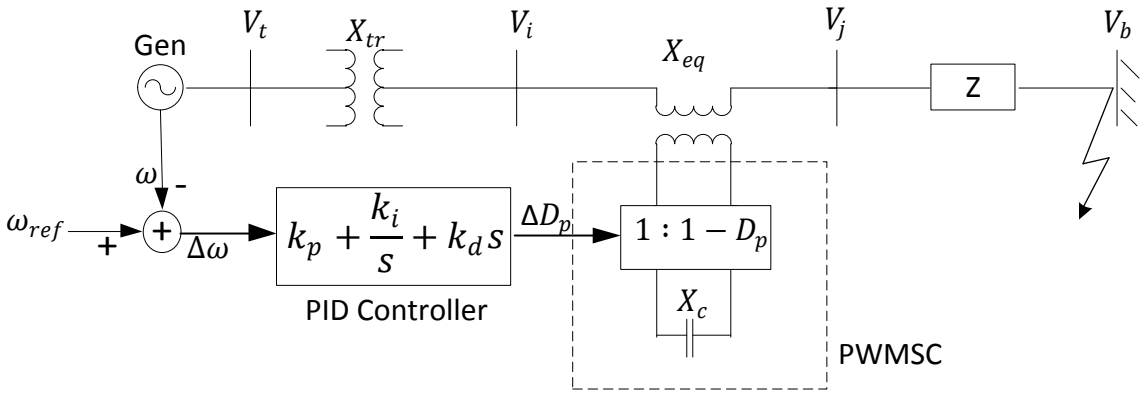

Figure 5-18: Three phase fault study of the SMIB system with PID controller

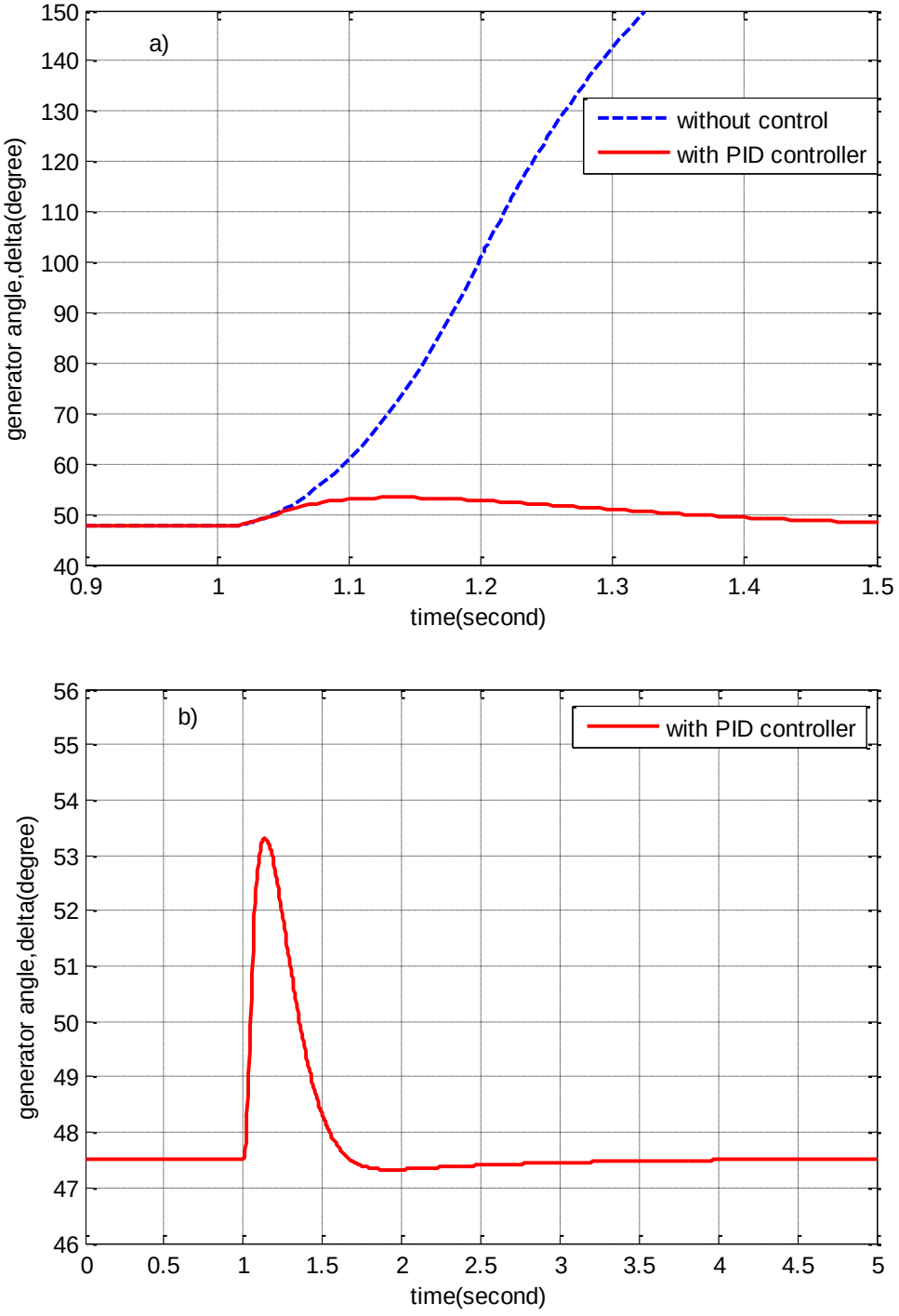

Figure 5-19: Response of generator angle of SMIB system for a three phase fault a) comparison of with or without stabilizing control, b) with PID controller

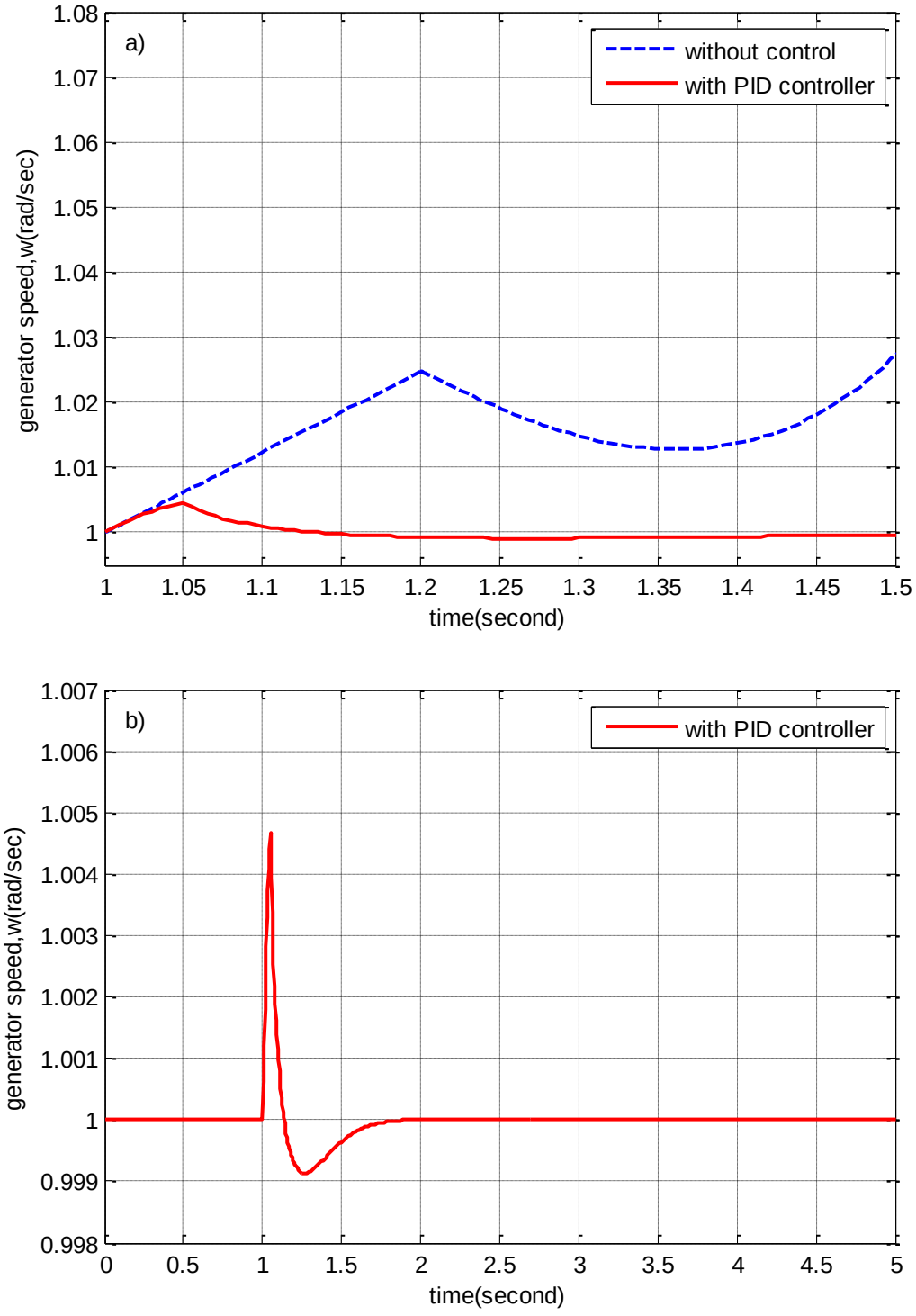

Figure 5-20: Response of generator speed of SMIB system for a three phase fault a) comparison of with or without stabilizing control, b) with PID controller

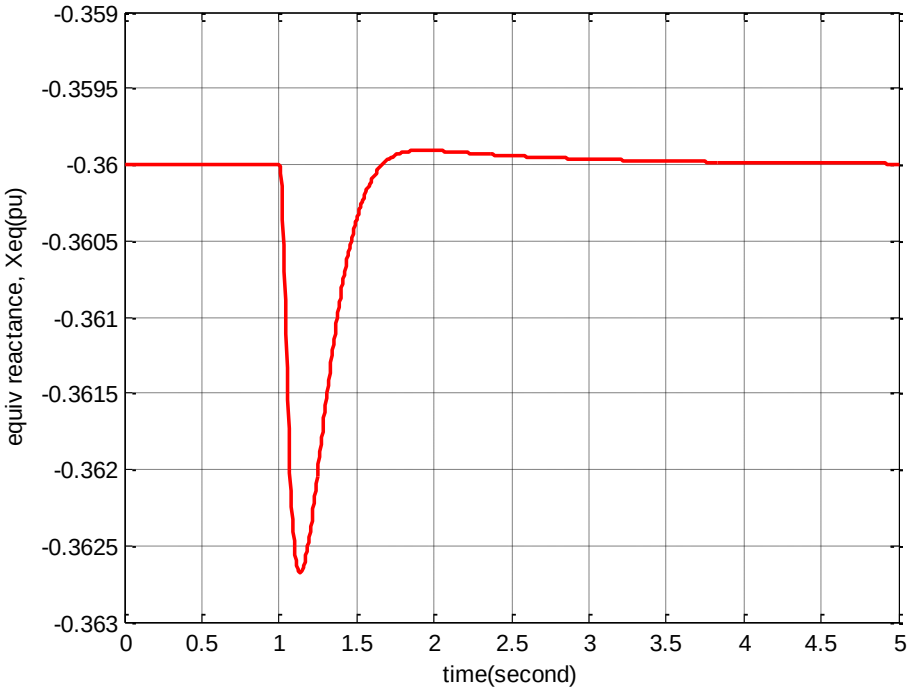

Figure 5-21: Equivalent reactance of the PWMSC of the SMIB system for a three phase fault

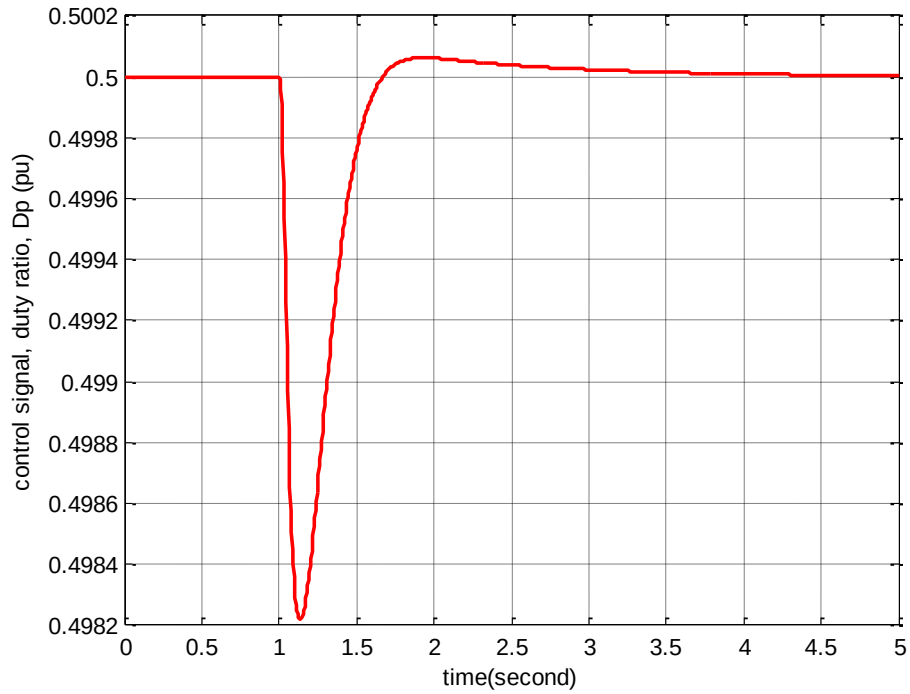

Figure 5-22: Control signal of the PWMSC of the SMIB system for a three phase fault

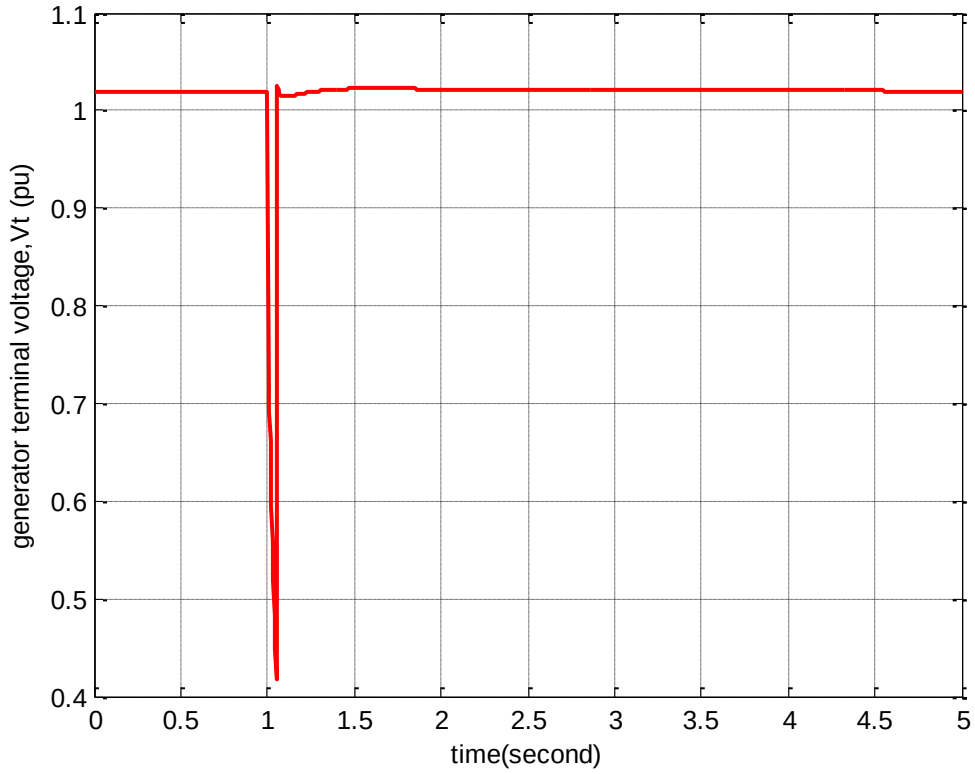

Figure 5-23: Terminal voltage of the generator of the SMIB system for a three phase fault

From the simulation results shown in Figure 5-19 and Figure 5-20, it has been observed that the SMIB system without stabilizing control goes unstable when it experiences a three phase fault. The SMIB system with PID controller shows excellent performance in damping electromechanical oscillations.

CHAPTER 6

SIMULATION RESULTS: MULTI-MACHINE POWER SYSTEM WITH PWMSC

A 4 generator, 12 bus multi-machine system with 4 constant impedance loads is used as a test system. The multi-machine power system is equipped with PWMSC in the transmission line between bus 2 & bus 9 as shown in Figure 6-1. Generators are operating at their nominal operating points with nominal loading. All the bus data, generator data, line data, load data and nominal operating points are given in Appendix B.

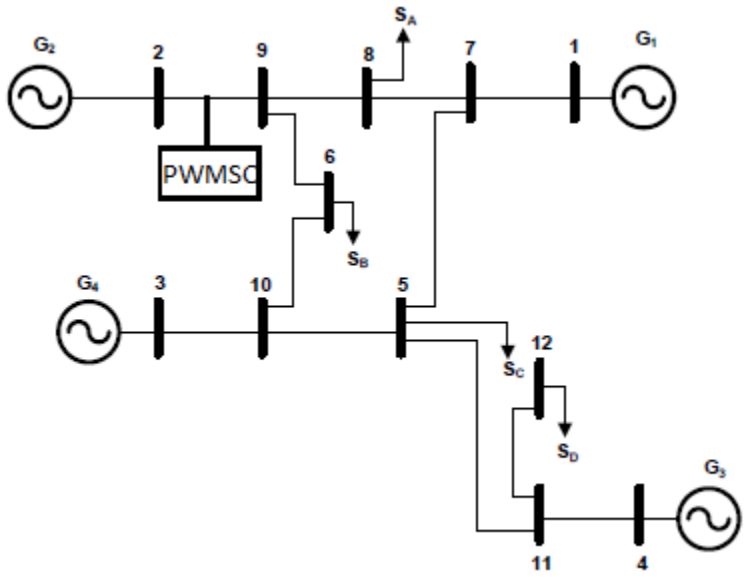

Figure 6-1: Multi-machine power system installed with PWMSC

Nonlinear model of the multi-machine system is simulated in MATLAB. In order to test the performance of the PWMSC controllers, a three phase fault of 0.1s is applied at bus 8

and the faulty line between bus-8 and bus-9 is tripped. After 0.1 sec the fault is cleared and the line is restored to service.

6.1 PWMSC controlled by PI controller

The equivalent reactance, X_{eq} injected in the transmission line of the multi-machine system is dependent upon the duty ratio, $D_p$of the PWMSC. The duty ratio (or X_{eq}) is controlled by a PI controller whose structure is shown in Figure 3-7, omitting k_d ($k_d = 0$).

Three different stabilizing input signals have been tested for the PI controller. For each configuration, the controller parameters (k_p, k_i) are optimized using real-coded genetic algorithm (RCGA).

6.1.1 Speed deviation, Δω as input to PI controller

The PI controller configuration in the multi-machine system with generator speed deviation, $\Delta\omega$ as stabilizing input is shown in Figure 6-2.

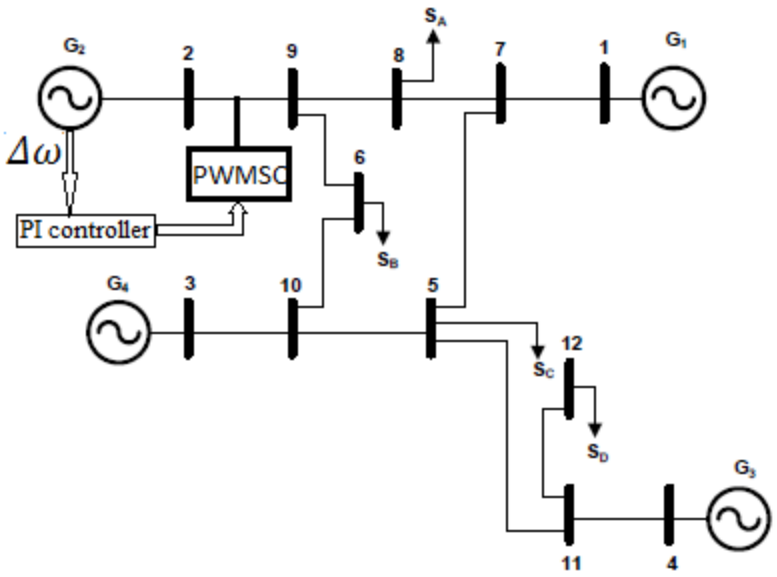

Figure 6-2: Speed deviation, Δω as input to PI controller: multi-machine power system

The maximum & minimum values of the controller parameters (k_p, k_i) considered in the optimization algorithm are,

$$k_{p_{min}} = -1000, \qquad k_{p_{max}} = 1000, \qquad k_{i_{min}} = -1000, \qquad k_{i_{max}} = 1000$$

The optimum parameters obtained from this algorithm for two objective functions are given in the following table.

Table 6-1 : Optimum gain parameters for the multi-machine system in 6.1.1

Objective functions	$J_1 = \int_0^{t_{sim}} (\Delta\omega)^2 dt$	$J_2 = \int_0^{t_{sim}} \lvert\Delta\omega\rvert dt$
Optimum parameters	k_p =-30.69 $k_i = 6$	$k_p = -30.64$ $k_i = 0$

The simulation results are shown in Figure 6-3 to Figure 6-7.

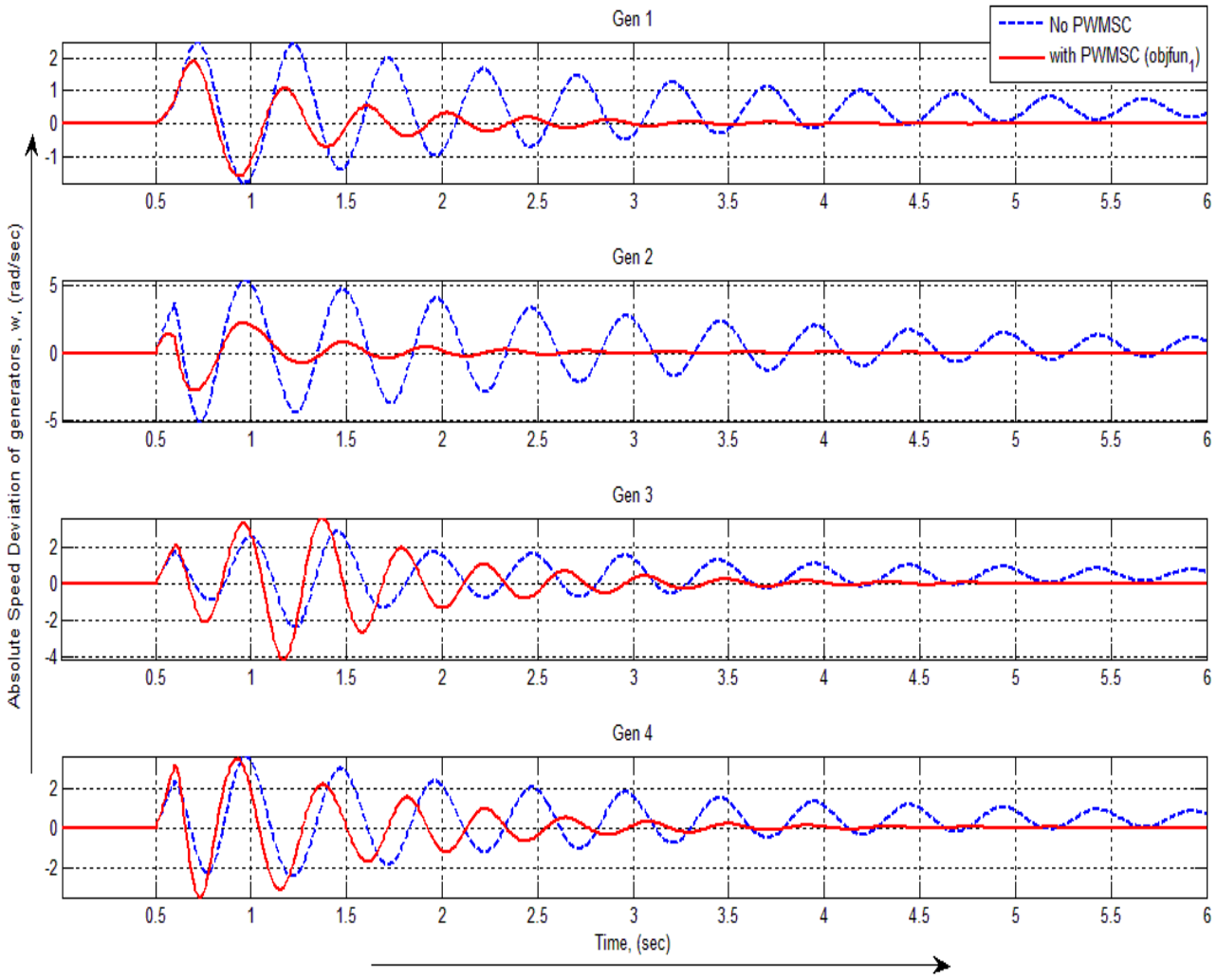

Figure 6-3: Rotor speed of generators of multi-machine system with PI controller following a 3 phase fault in bus 8

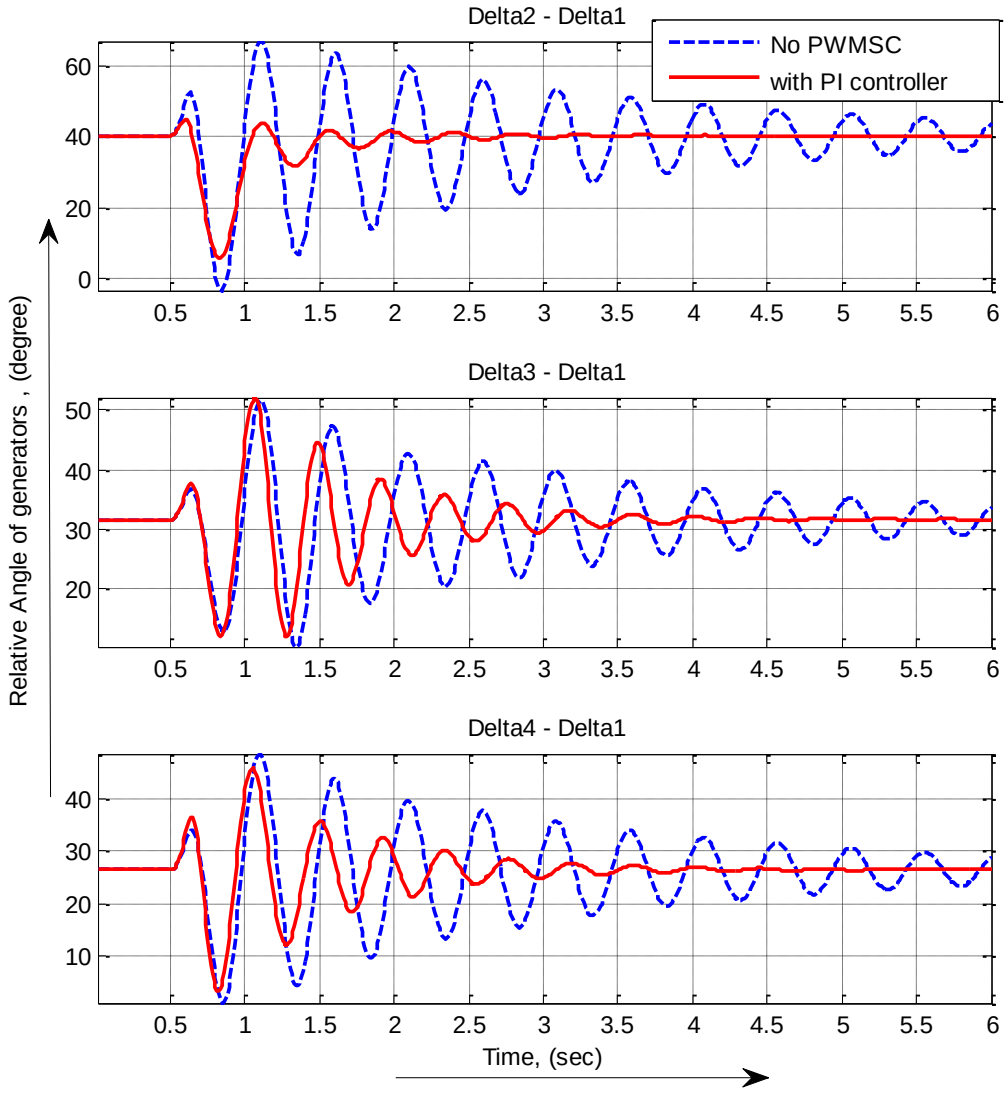

Figure 6-4: Relative angle of generators with respect to Gen-1 in multi-machine system with PI controller following a 3 phase fault in bus 8

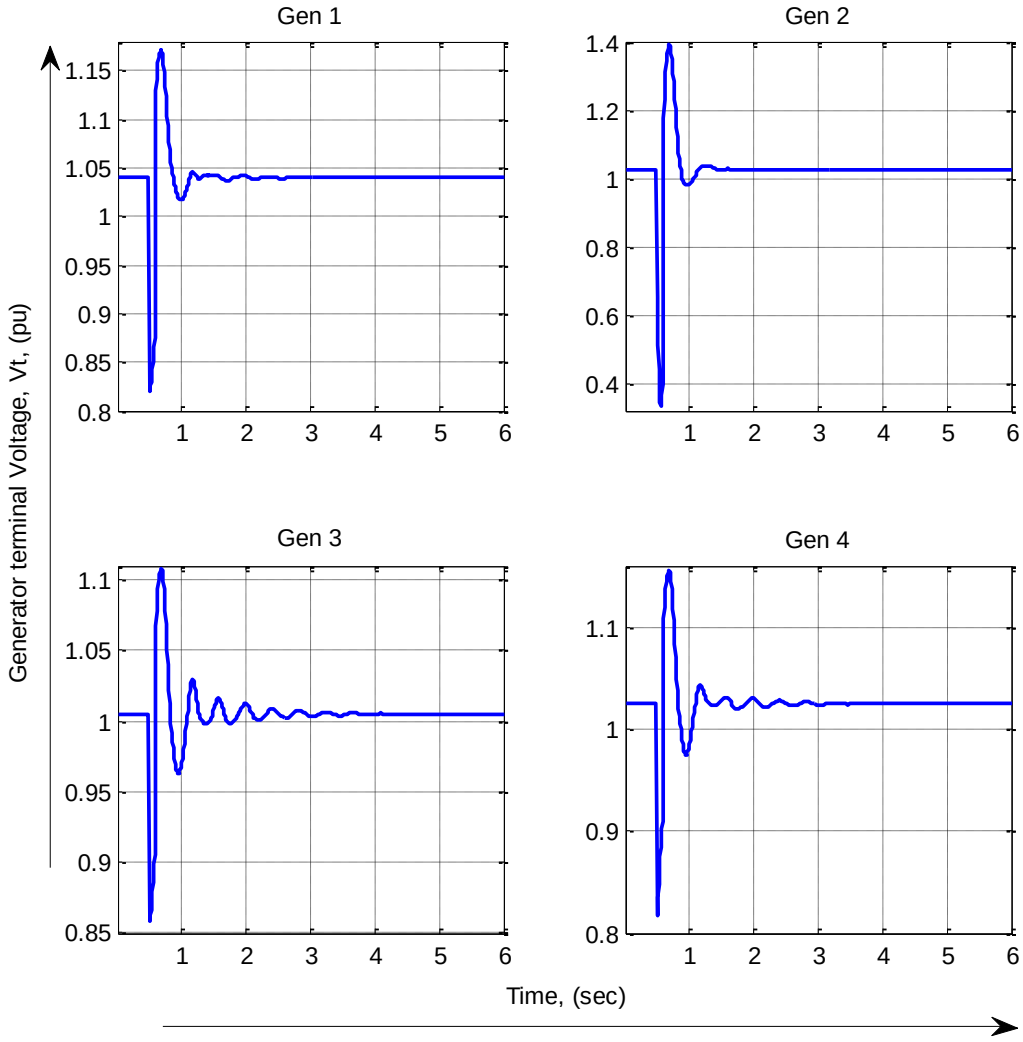

Figure 6-5: Terminal voltages of generators of multi-machine system with PI controller following a 3 phase fault in bus 8

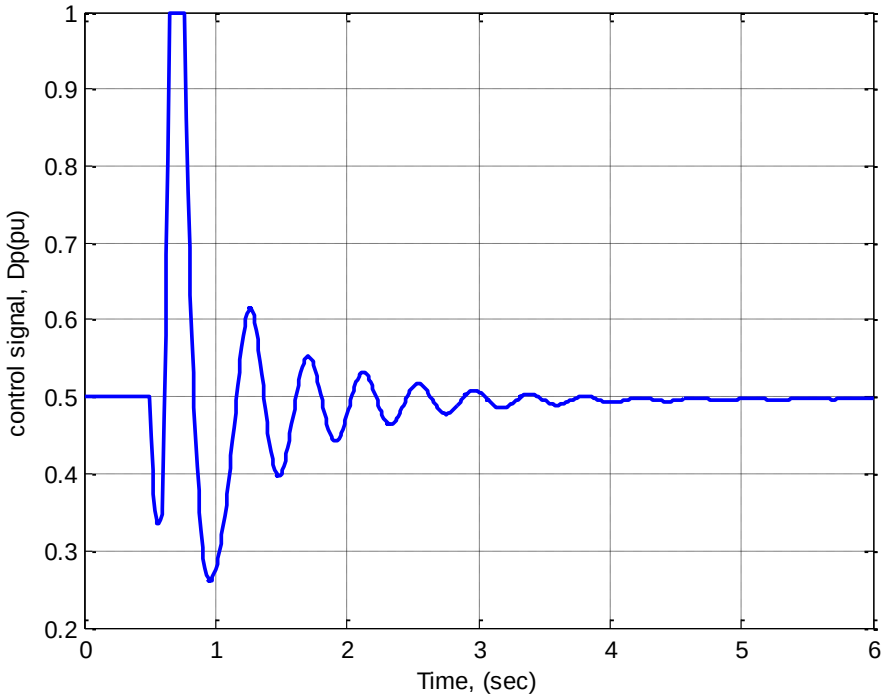

Figure 6-6: Control signal of PWMSC with PI controller following a 3 phase fault in multi-machine system

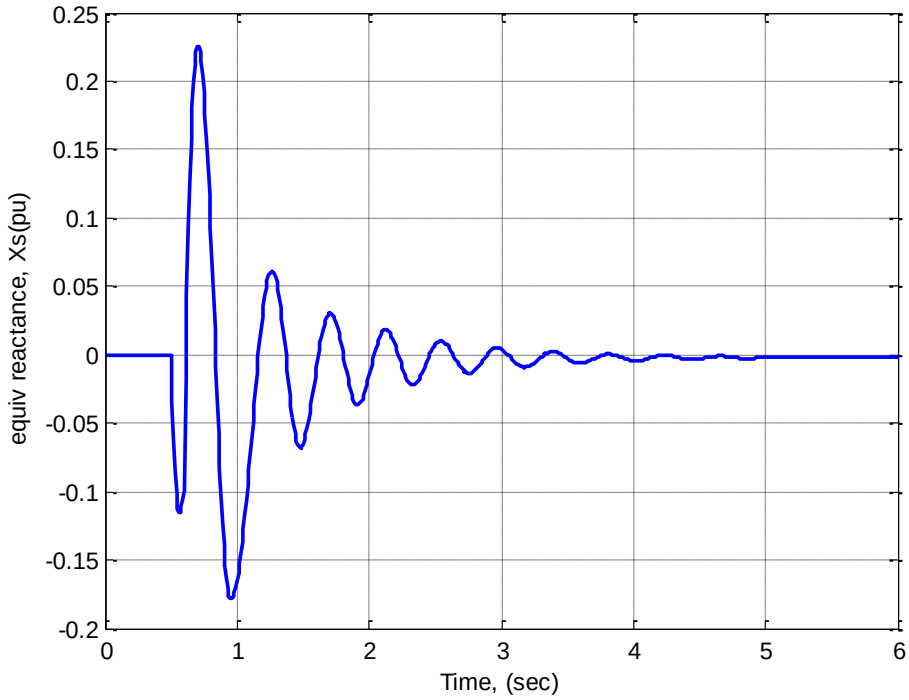

Figure 6-7: Equivalent reactance seen from transmission line of multi-machine system with PI controller following a 3 phase fault in bus 8

From Figure 6-3 to Figure 6-7, nonlinear model response of the generators & the PWMSC controller are shown for objective function, $J_1 = \int_0^{t_{sim}} (\Delta\omega)^2 dt$. This objective function gave better response compared to the other. Results indicate that the performance of the system in damping electromechanical mode oscillation is excellent. Responses of the generator speed deviation in Figure 6-3 & relative angle of generators shown in Figure 6-4 ,while the terminal voltage of generators, especially gen-2 as shown in Figure 6-5 and the control signal, duty ratio,D_p of the PWMSC is as shown in Figure 6-6 which is slightly over modulated.

6.1.2 Active power output deviation, ΔP_e as input to PI controller

The PI controller configuration in the multi-machine system with active power output deviation of generator-2, ΔP_{e_2} as stabilizing input is shown in Figure 6-8.

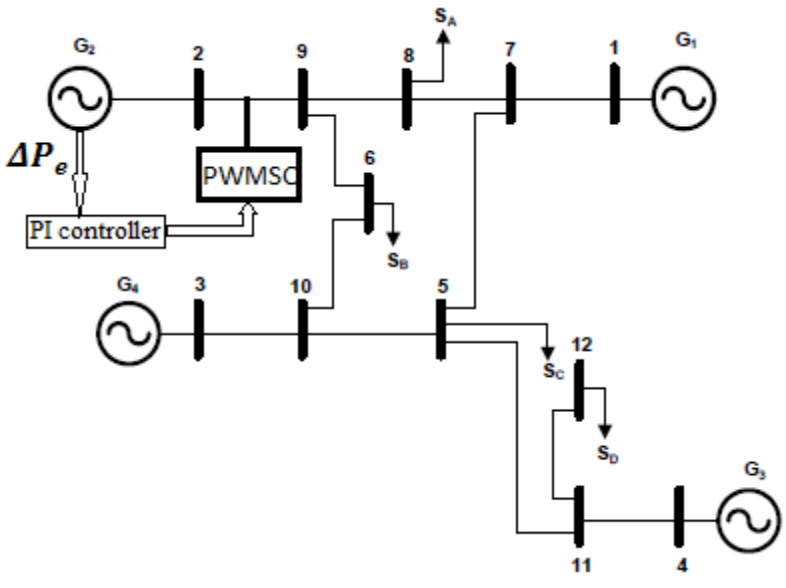

Figure 6-8: Active power output deviation, ΔP_e as input to PI controller: multi-machine power system

Nonlinear model of the multi-machine system shown in Figure 6-8 was simulated with PI controller dynamics given in equations (4-53) to (4-60). But, it has been observed in the simulation results that the PI controller doesn't give satisfactory results if we want to mitigate the electromechanical oscillations by tracking the generator active power output deviation ΔP_e.

6.1.3 Change in transmission line active power flow ΔP_{29} as stabilizing input signal to PID controller

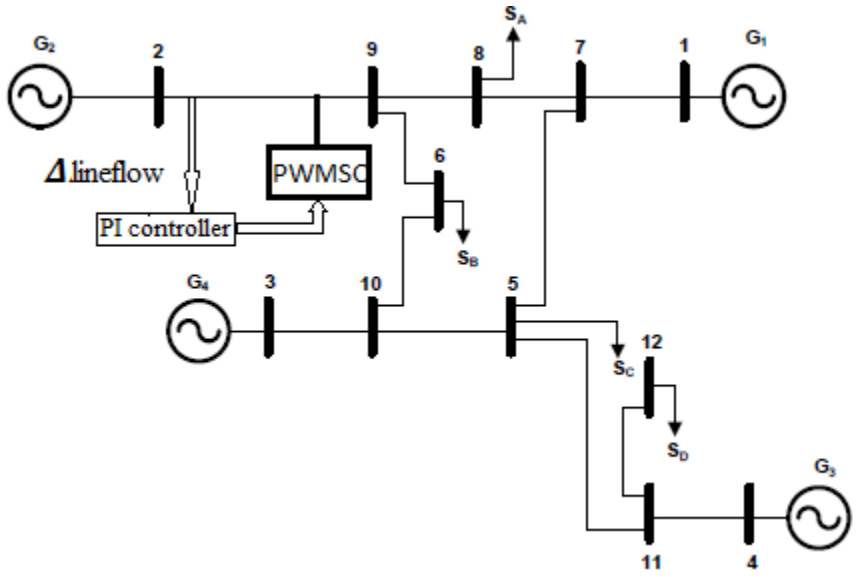

Figure 6-9: Change in active power flow of line as Stabilizing input signal to PI controller: multi-machine power system

The PI controller configuration in the multi-machine system with change in active power flow of transmission line between bus2 and bus-9, ΔP_{29} as stabilizing input is shown in Figure 6-9.

The PI controller dynamics were incorporated from equations (4-61) to (4-68). But the simulation results obtained for this controller configuration was not satisfactory.

6.2 PWMSC with PID controller

A PID controller shown in Figure 3-7 is employed to regulate the PWMSC switch's duty ratio D_p and thus controlling the equivalent reactance X_{eq} injected by the PWMSC.

Figure 6-10 displays the PID controller strategy adopted here. Speed deviation of generator-2, $\Delta\omega_2$ has been used here as stabilizing input to the controller.

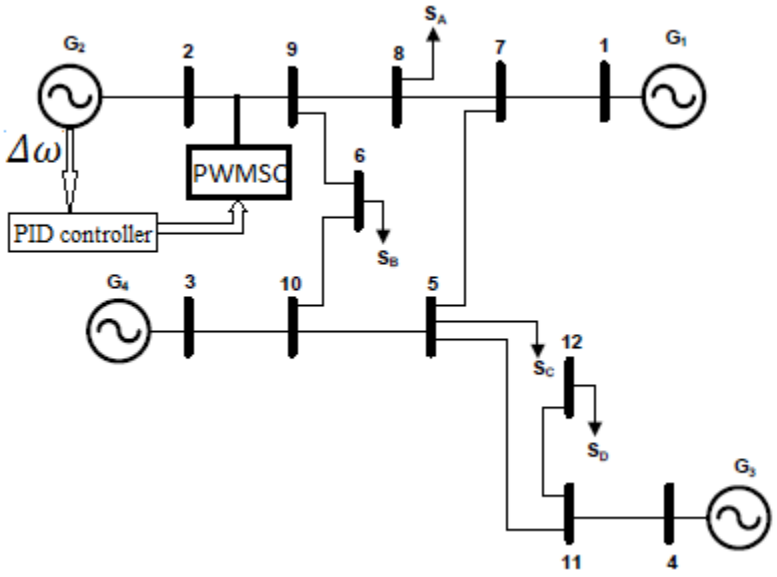

Figure 6-10: Speed deviation, Δω as input to PID controller: multi-machine power system

The PID controller parameters (k_p , k_i , k_d) were optimized using real-coded genetic algorithm (RCGA). The maximum & minimum values of k_p, k_i and k_d considered in this optimization algorithm are given below.

$$k_{p_{min}} = -1000, \qquad k_{p_{max}} = 1000, \qquad k_{i_{min}} = -1000, \qquad k_{i_{max}} = 1000$$

$$k_{d_{min}} = -100, \qquad k_{d_{max}} = 100$$

The optimum parameters obtained from this algorithm for two objective functions are given in the following table.

Table 6-2 : Optimum gain parameters for the multi-machine system in 6.2

Objective functions	$J_1 = \int_0^{t_{sim}} (\Delta\omega)^2 dt$	$J_2 = \int_0^{t_{sim}} \lvert\Delta\omega\rvert dt$
Optimum parameters	k_p =-30.69 $k_i = 6$ $k_d = -0.646$	$k_p = -30.64$ $k_i = 0$ $k_d = 0$

The simulation results are shown in Figure 6-11 to Figure 6-15.

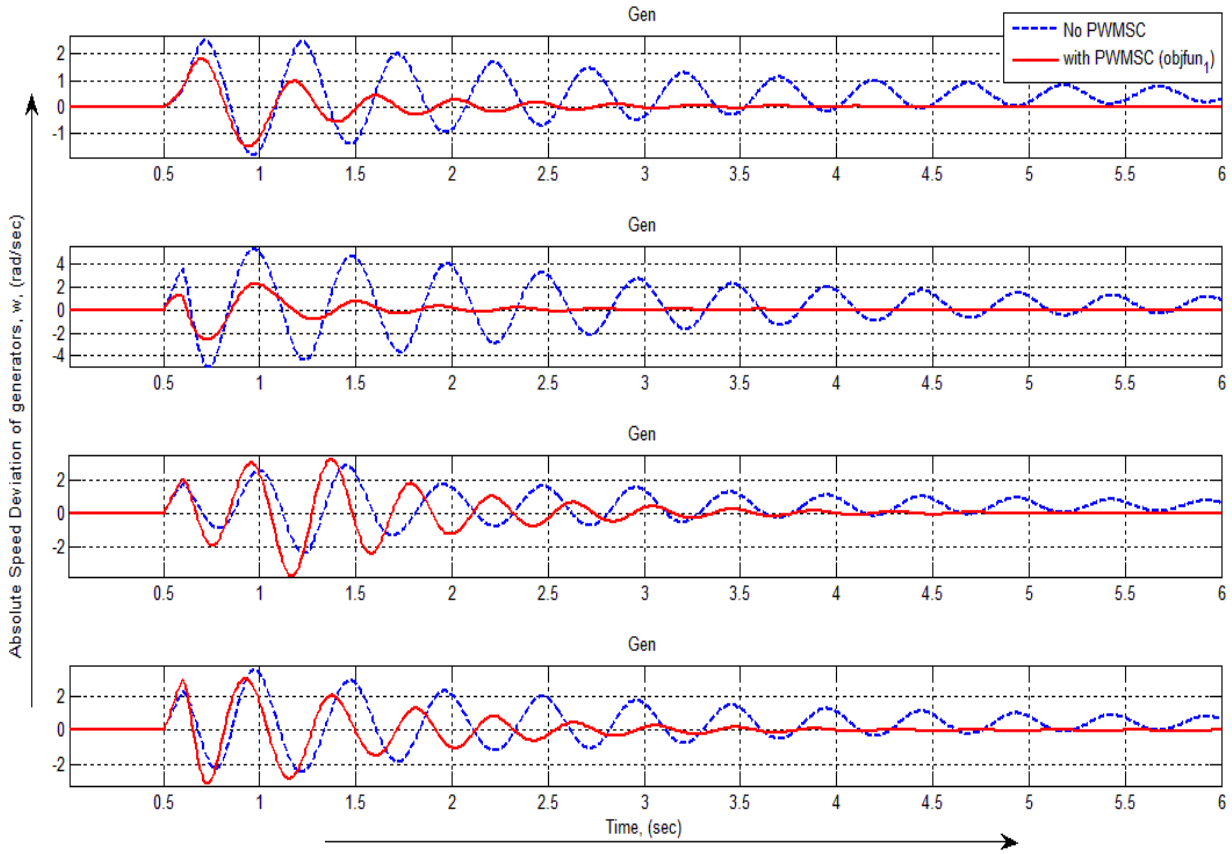

Figure 6-11: Rotor speed of generators of multi-machine system with PID controller following a 3 phase fault in bus 8

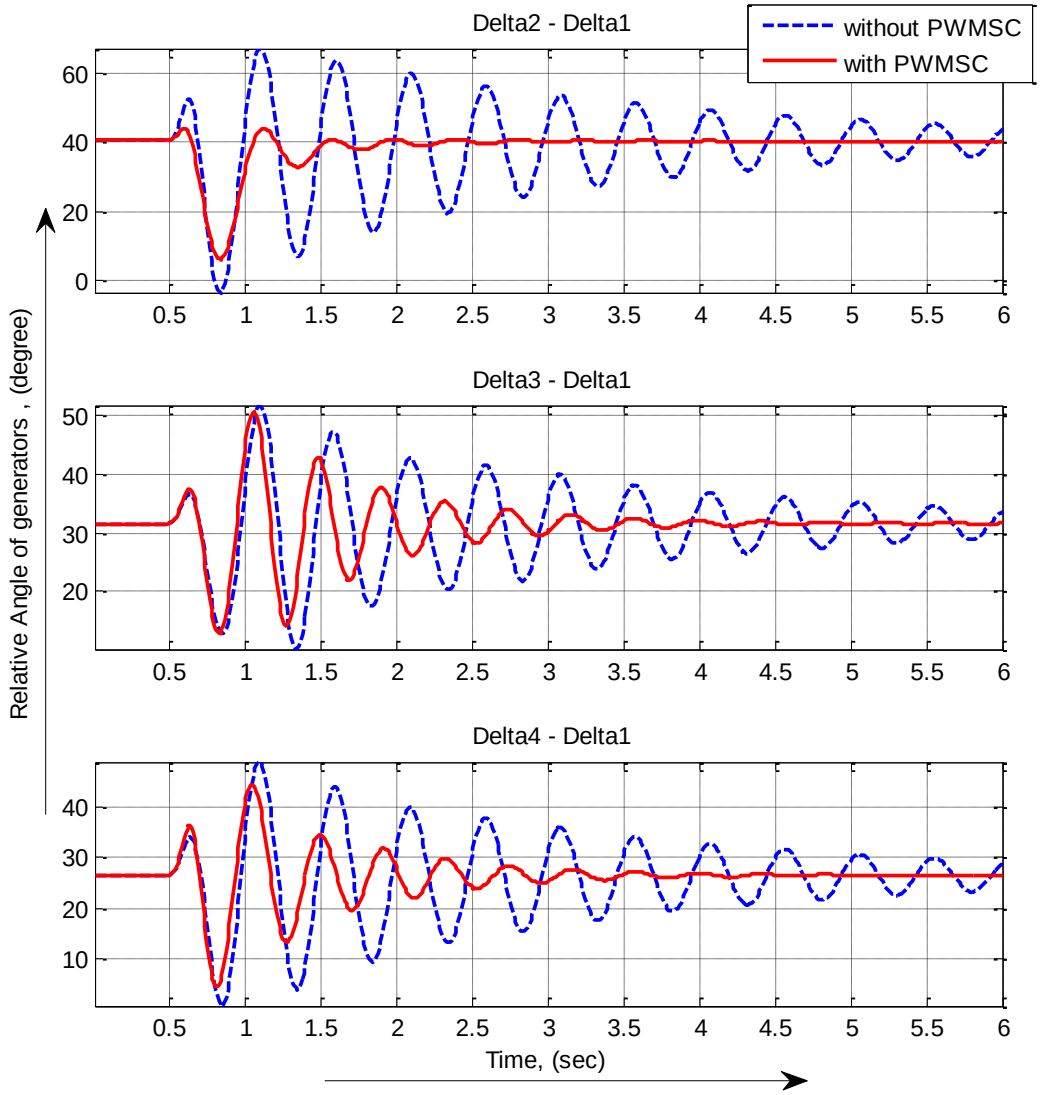

Figure 6-12: Relative angle of generators with respect to Gen-1 in multi-machine system with PID controller following a 3 phase fault in bus 8

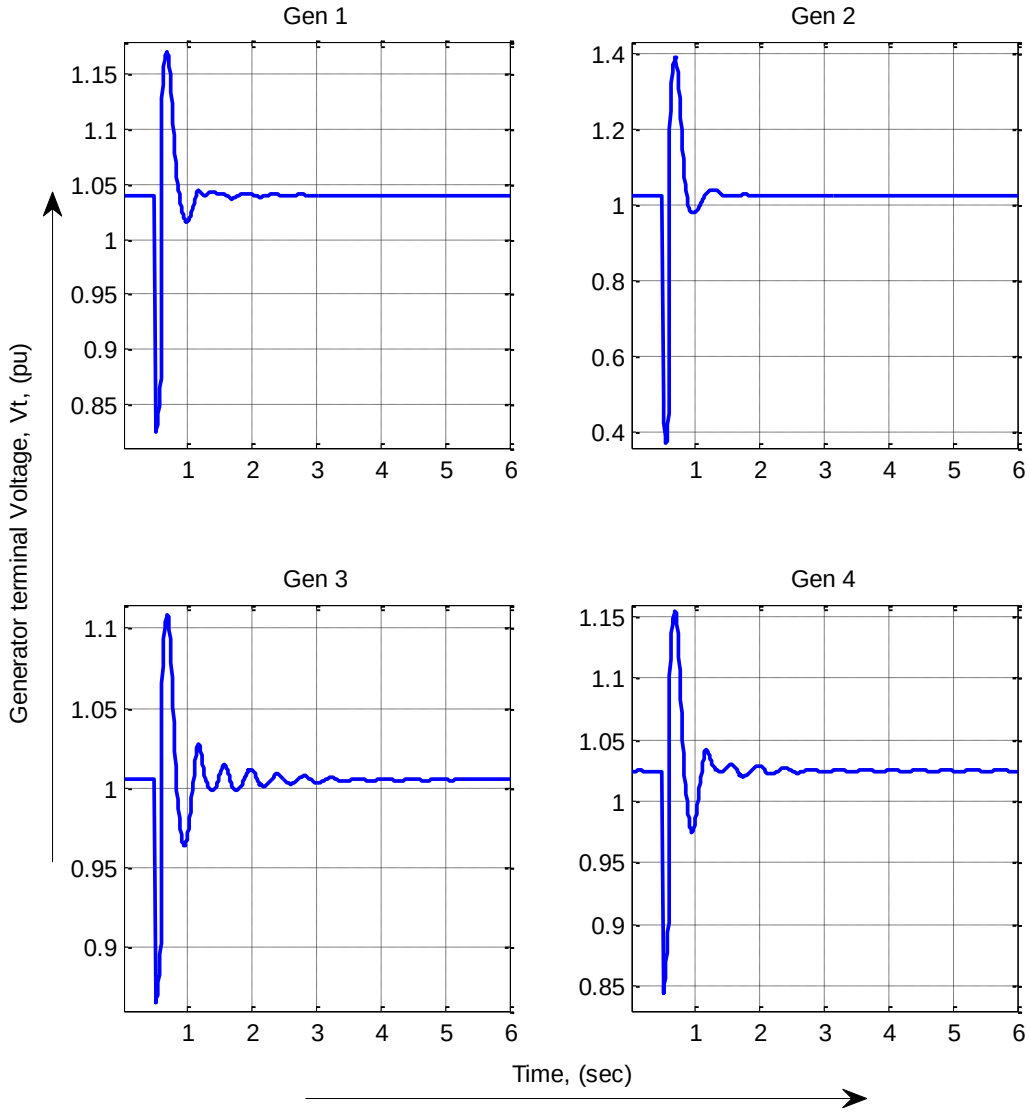

Figure 6-13: Terminal voltages of generators of multi-machine system with PID controller following a 3 phase fault

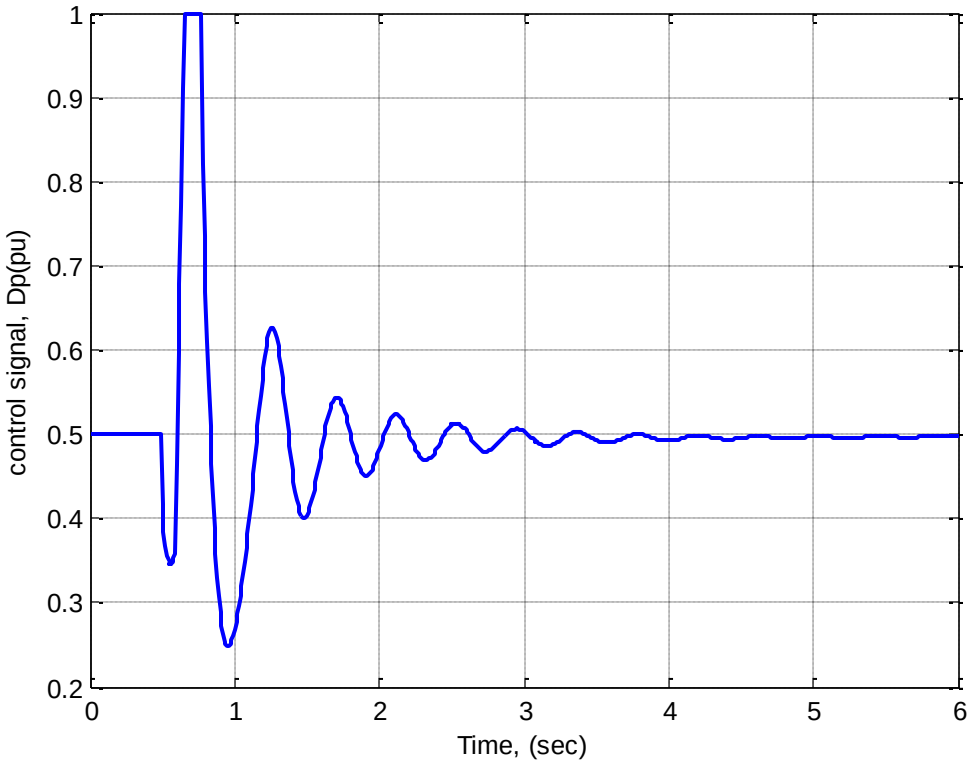

Figure 6-14: Control signal of PWMSC with PID controller following a 3 phase fault in multi-machine system

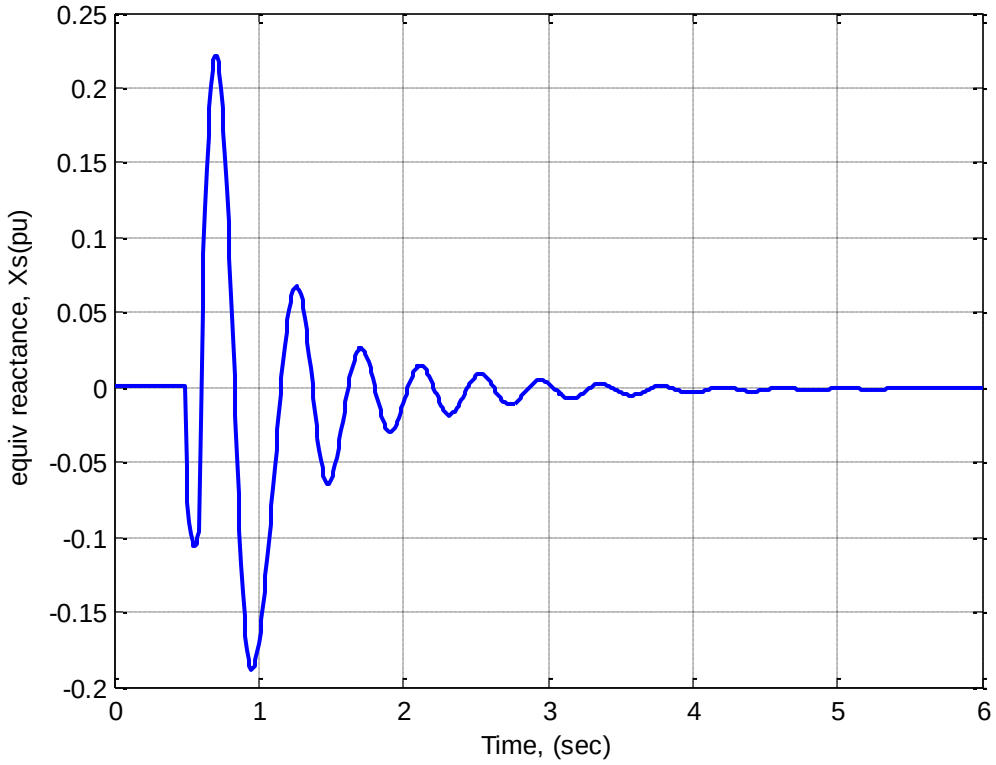

Figure 6-15: Equivalent reactance seen from transmission line of multi-machine system with PID controller following a 3 phase fault

From Figure 6-11 to Figure 6-15, nonlinear model response of the generators & the PWMSC controller are shown only for objective function, $J_1 = \int_0^{t_{sim}} (\Delta\omega)^2 dt$ for the sake of clearness of the figures. And this objective function, J_1 gave better response than the objective function, J_2. Responses of the generator speed deviation in Figure 6-11 & relative angle of generators shown in Figure 6-12 are quite satisfactory. There is some excursion in the terminal voltage of generators, especially gen-2 as shown in Figure 6-13 and the control signal, duty ratio, D_p of the PWMSC is slightly over modulated as shown in Figure 6-14.

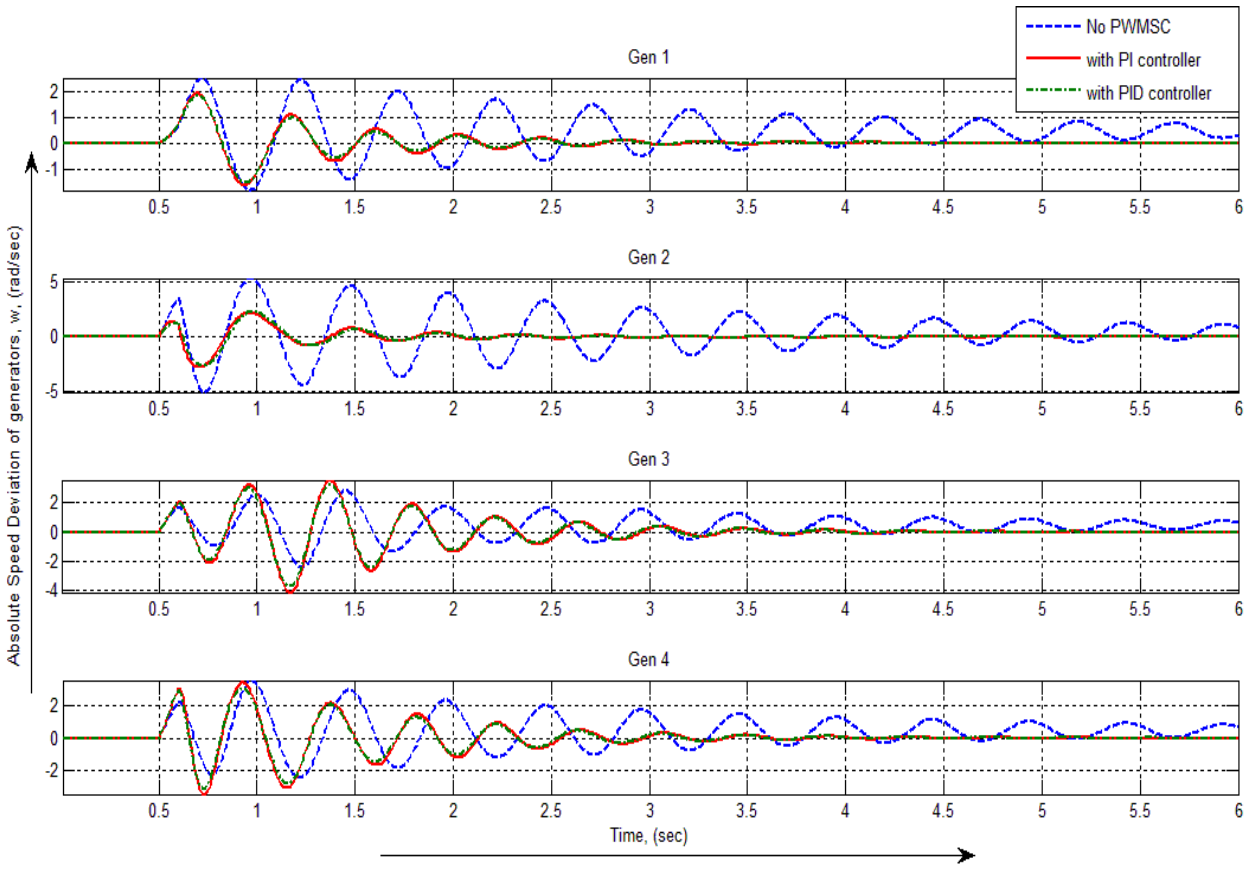

Figure 6-16: Comparison between PI & PID controller in damping generator speed oscillation of multi-machine system

A comparison of PI & PID controller in damping generator speed oscillation of multi-machine system is shown in Figure 6-16. After comparing all the results of PI & PID controller it has been observed that, the PID controller has contribution in decreasing the overshoot of the nonlinear system response following a three-phase fault. But the contribution of the PID controller is not as attractive as the expenditure & complexity it will cost.

Generator active power output deviation, ΔP_e and change in active power flow of transmission line, ΔP_{29} was also tried as stabilizing input signals to the PID controller,

but didn't yield satisfactory results in terms of damping electromechanical mode oscillations.

6.2.1 Simulation results of torque input pulse disturbance in the multi-machine system

The multi-machine system shown in Figure 6-10 is experienced with a disturbance of 10% torque input pulse of 0.1s duration applied on gen-2.

Controller gain parameters are selected as k_p =-30.69, $k_i = -15$, $k_d = 0$

The simulation results are shown in Figure 6-17 to Figure 6-21 which are quite satisfactory.

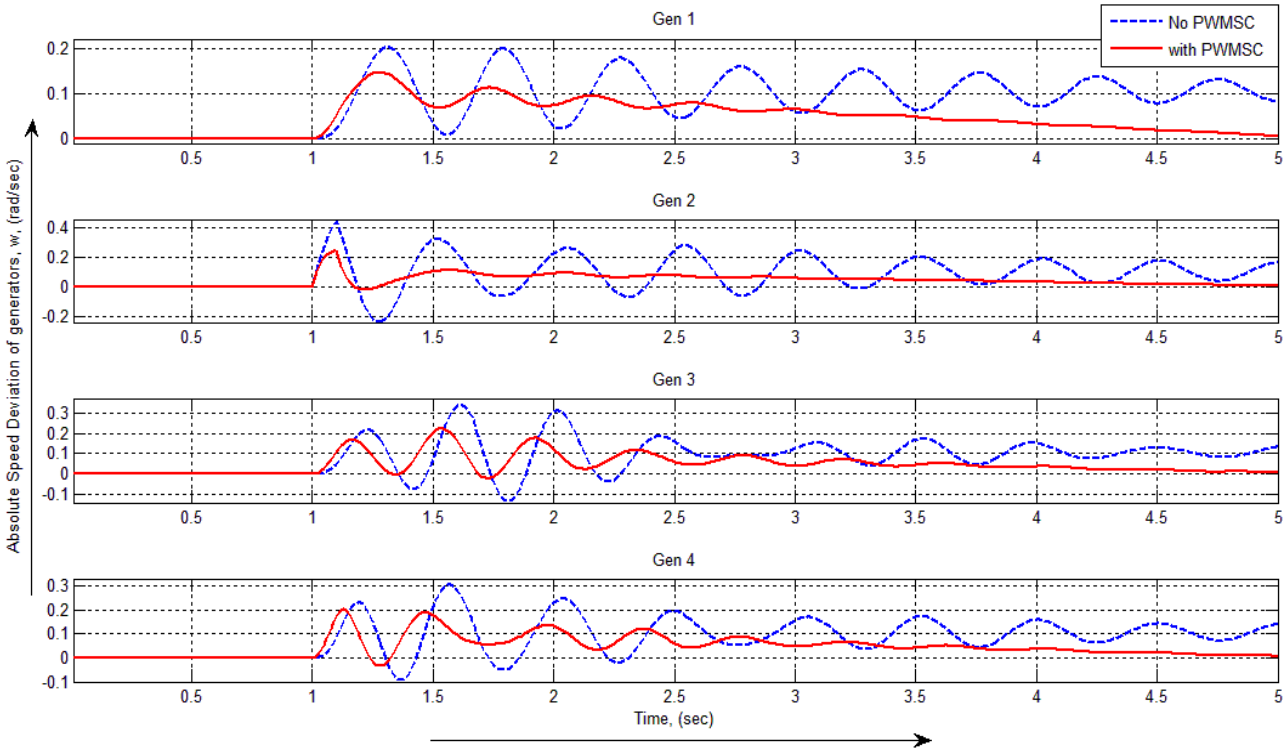

Figure 6-17: Rotor speed of generators of multi-machine system with a torque input pulse disturbance in the generator-2

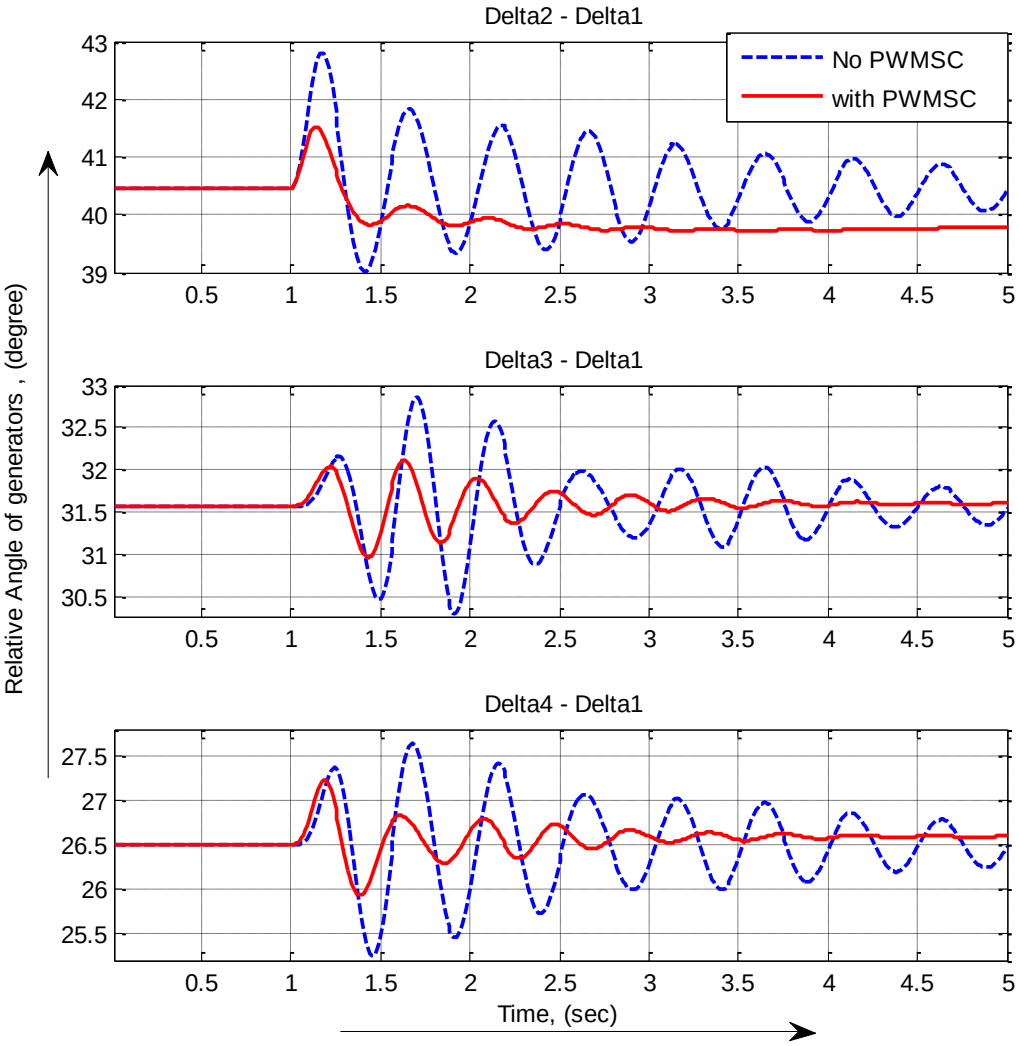

Figure 6-18: Rotor angle of generators of multi-machine system with a torque input pulse disturbance in the generator-2

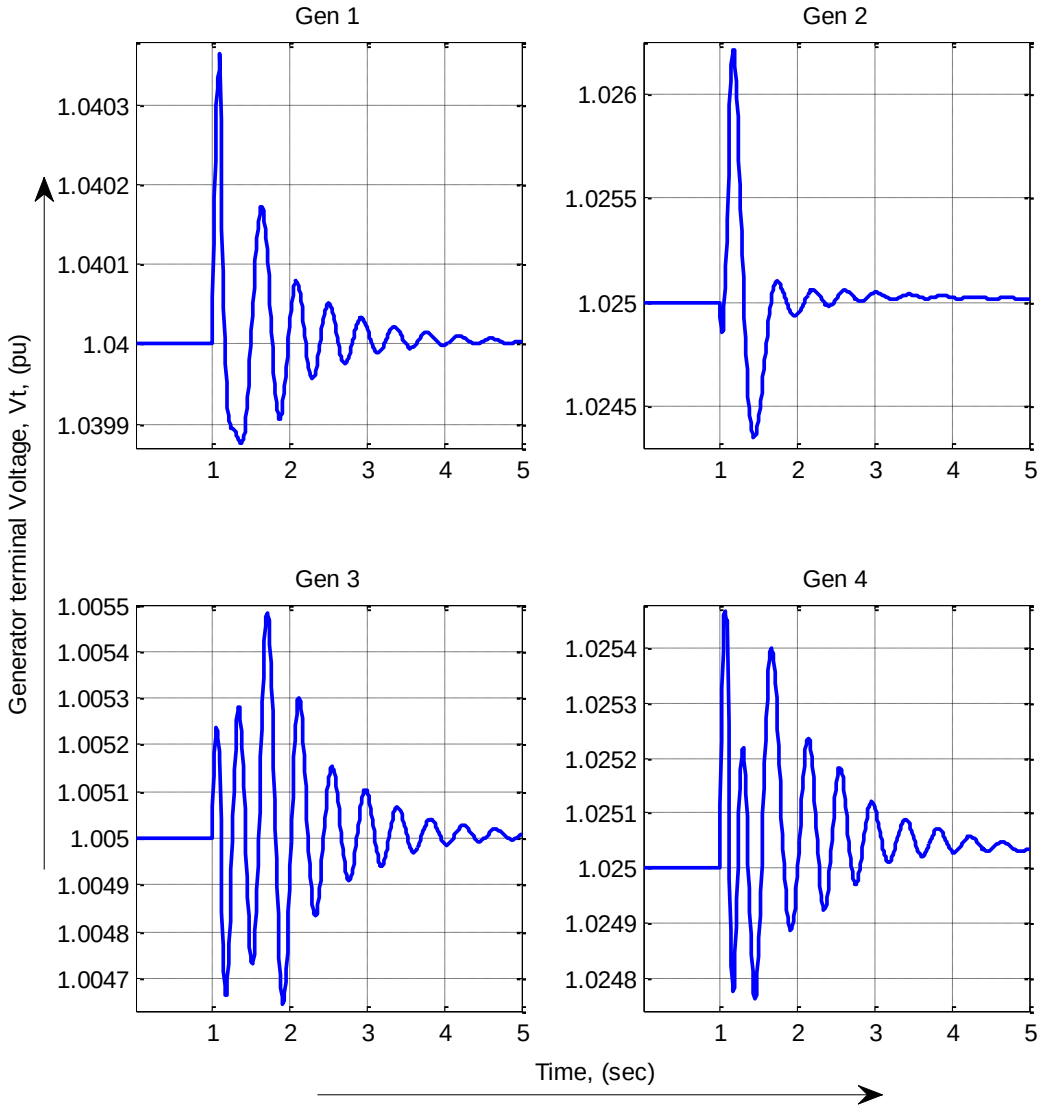

Figure 6-19: Generator terminal voltages of generators of multi-machine system with a torque input pulse disturbance in the generator-2

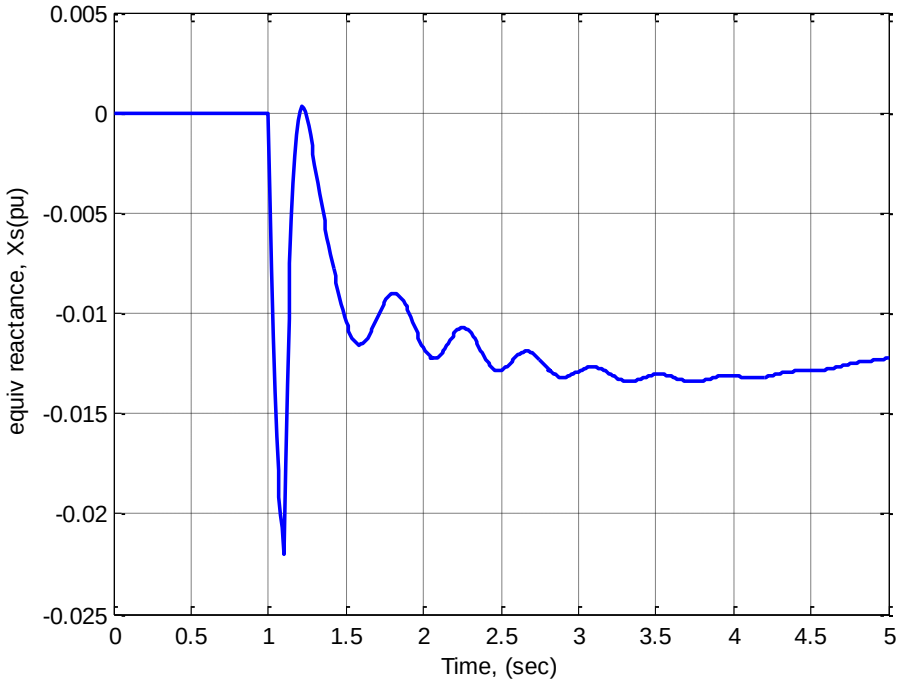

Figure 6-20: Equivalent reactance of the PWMSC in the multi-machine system with a torque input pulse disturbance in the generator-2

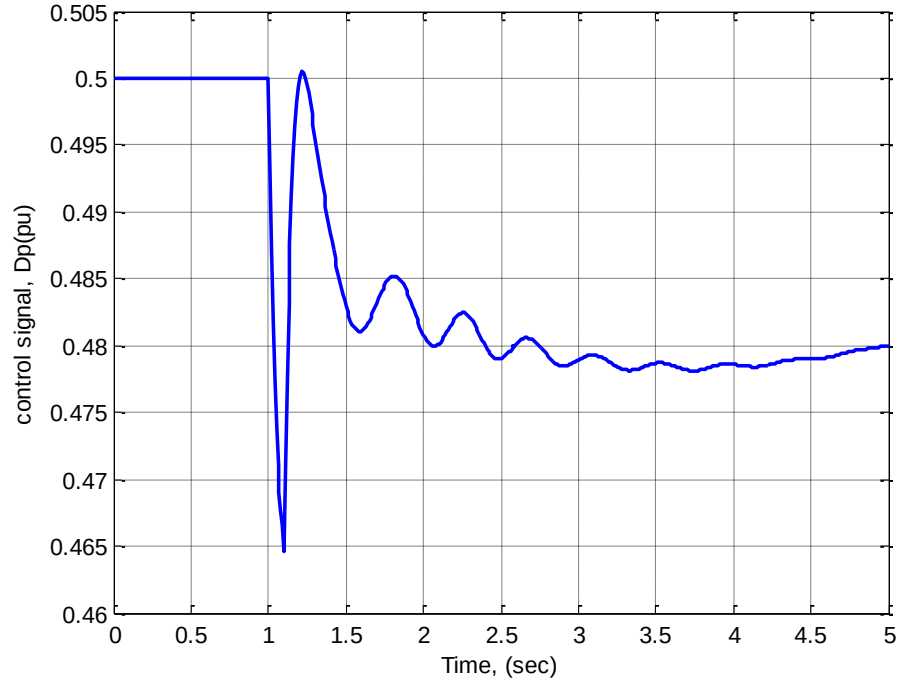

Figure 6-21: Control signal of the PWMSC with PID controller in the multi-machine system with a torque input pulse disturbance in the generator-2

6.3 Effect of PWMSC and fault locations

To test the robustness of the PWMSC controller it has been tested for a three phase fault at different locations and the PWMSC is also placed at different locations in the multi-machine system. Specifically 2 cases have been considered.

6.3.1 Case-1: Different fault location

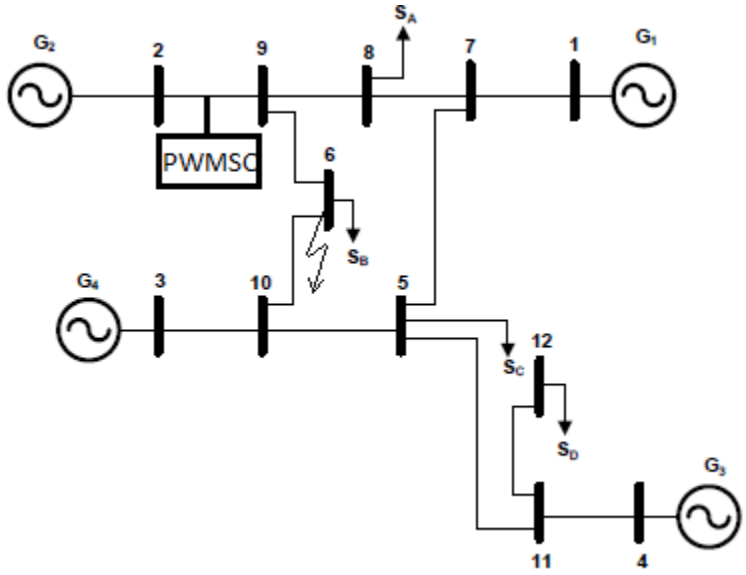

Figure 6-22: Multi-machine system considered for case-1

A three phase fault is applied at bus 6 for 0.1 sec in the multi-machine system as shown in Figure 6-22 and the faulty line between bus 9 and bus 6 is tripped. After 0.1 sec the fault is cleared and the faulty line is restored to service. Here, the PWMSC is connected in the same position i.e. between bus-2 and bus-9 and a PID controller is associated with the PWMSC with gains found in previous section. Simulation results are shown in Figure 6-23 to Figure 6-27.

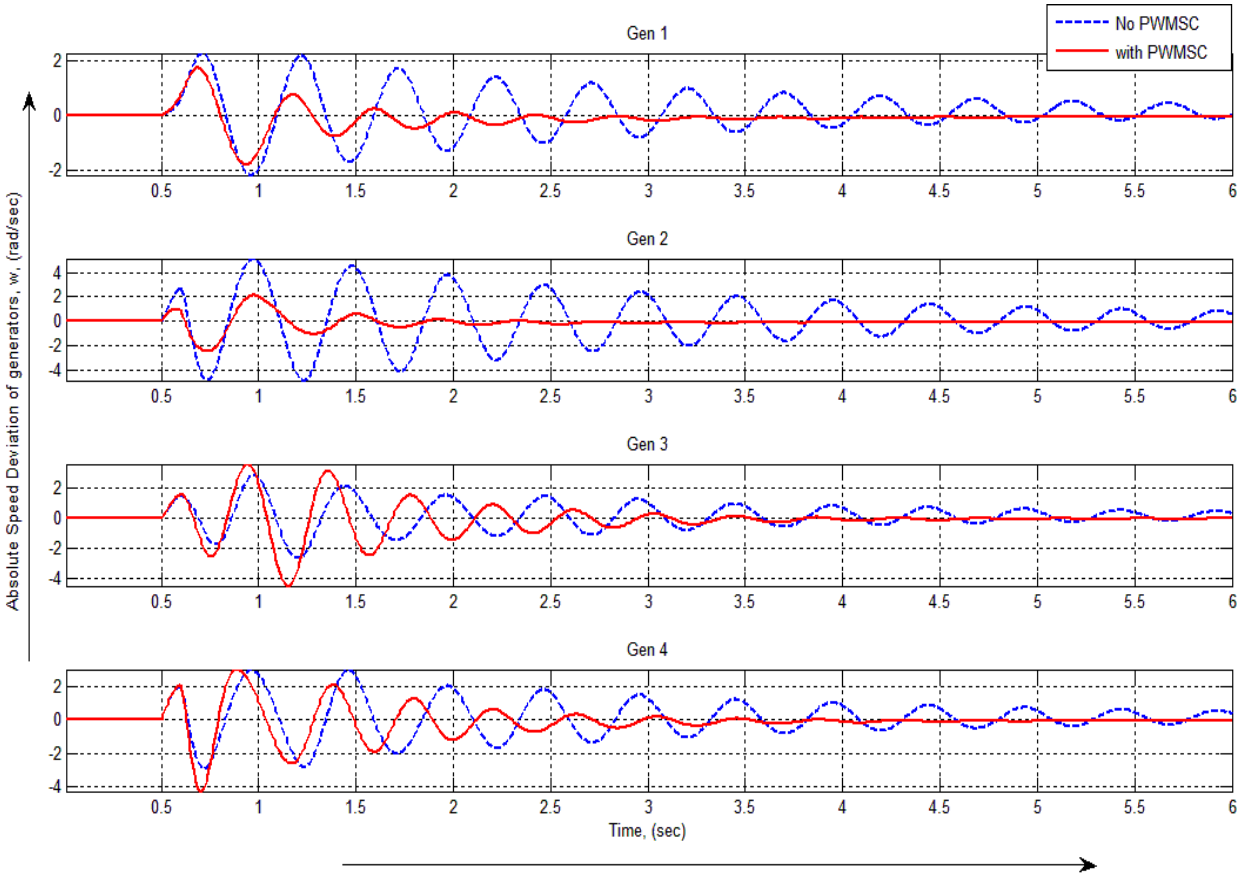

Figure 6-23: Rotor speed of generators of multi-machine system with PID controller following a 3 phase fault (case 1)

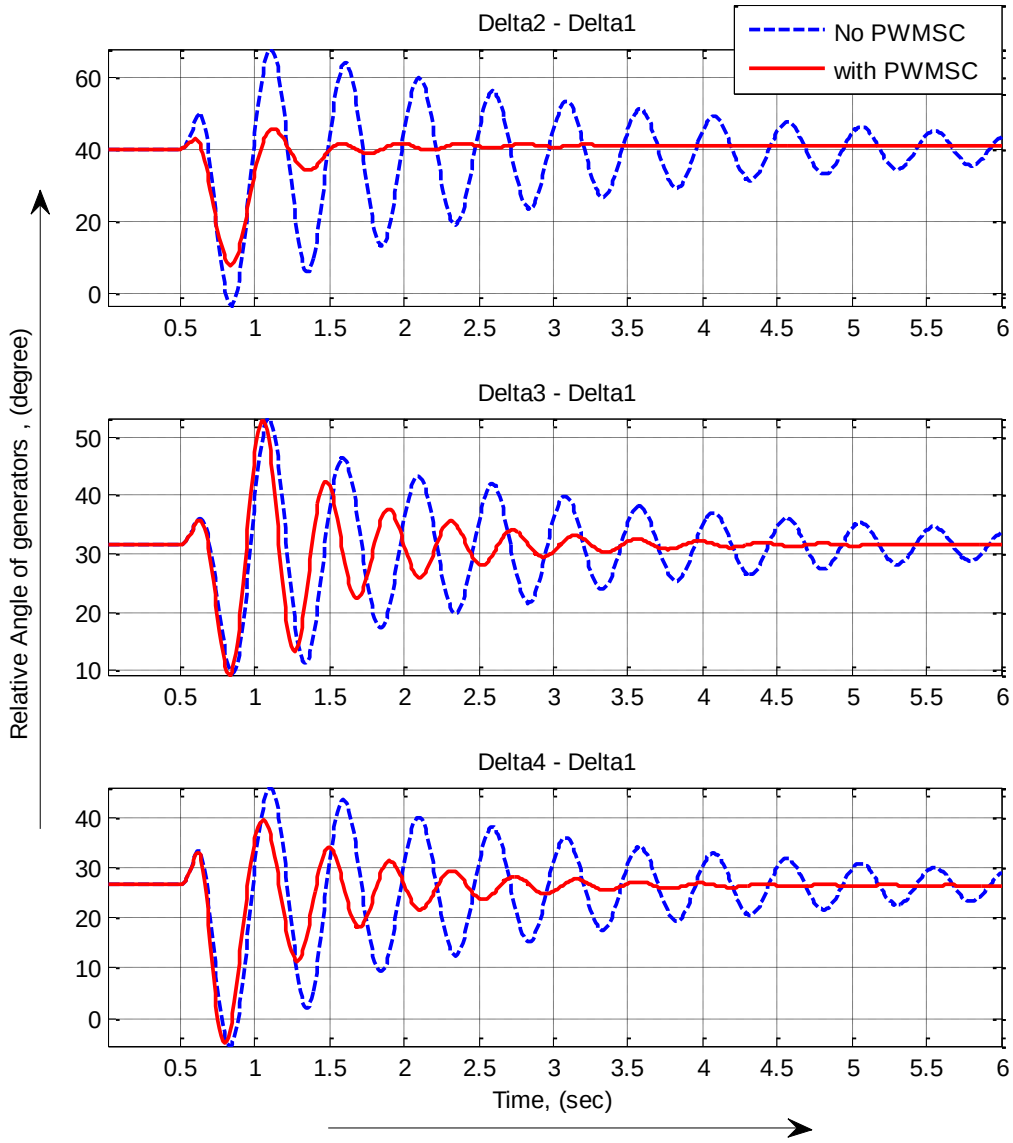

Figure 6-24: Relative angle of generators with respect to Gen-1 in multi-machine system with PID controller following a 3 phase fault (case 1)

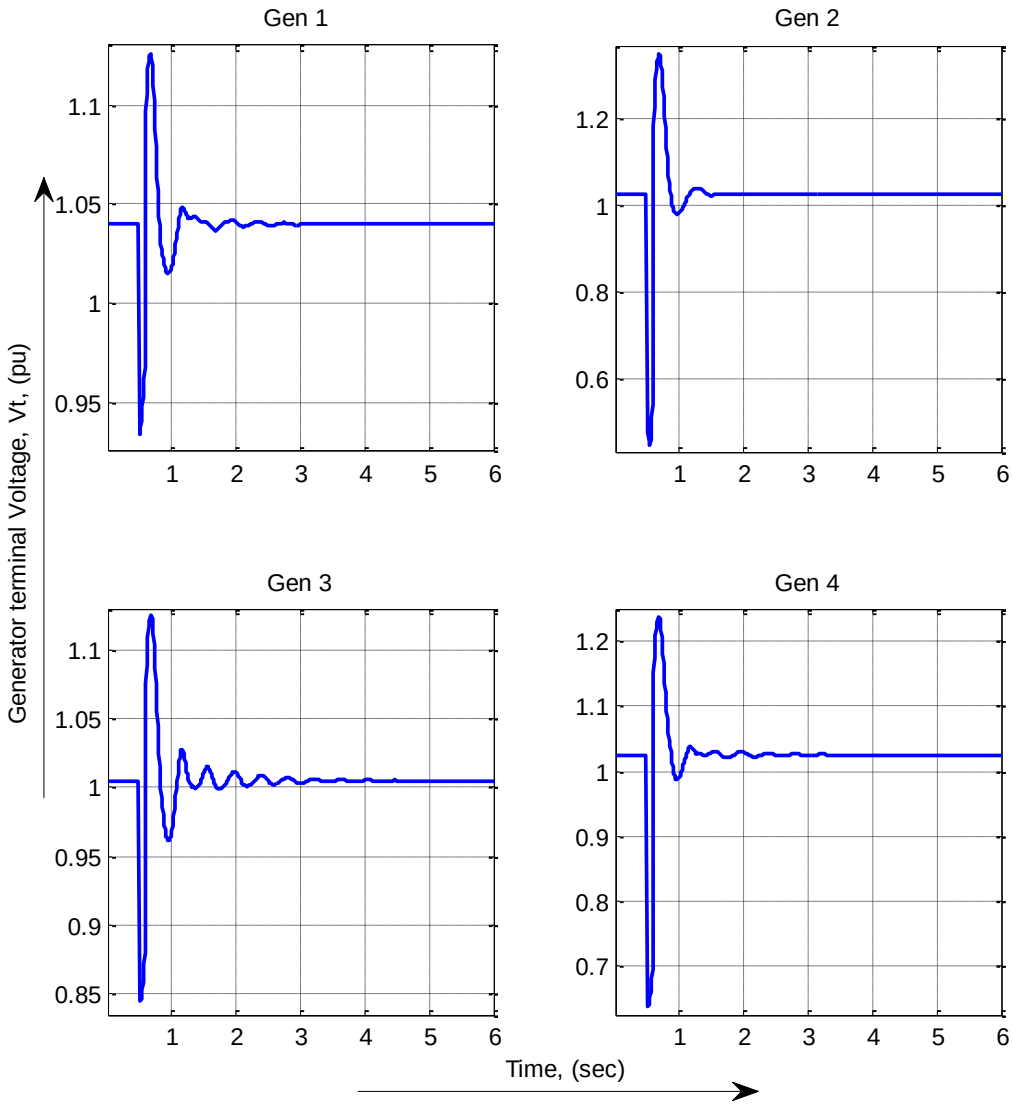

Figure 6-25: Terminal voltages of generators of multi-machine system with PID controller following a 3 phase fault (case 1)

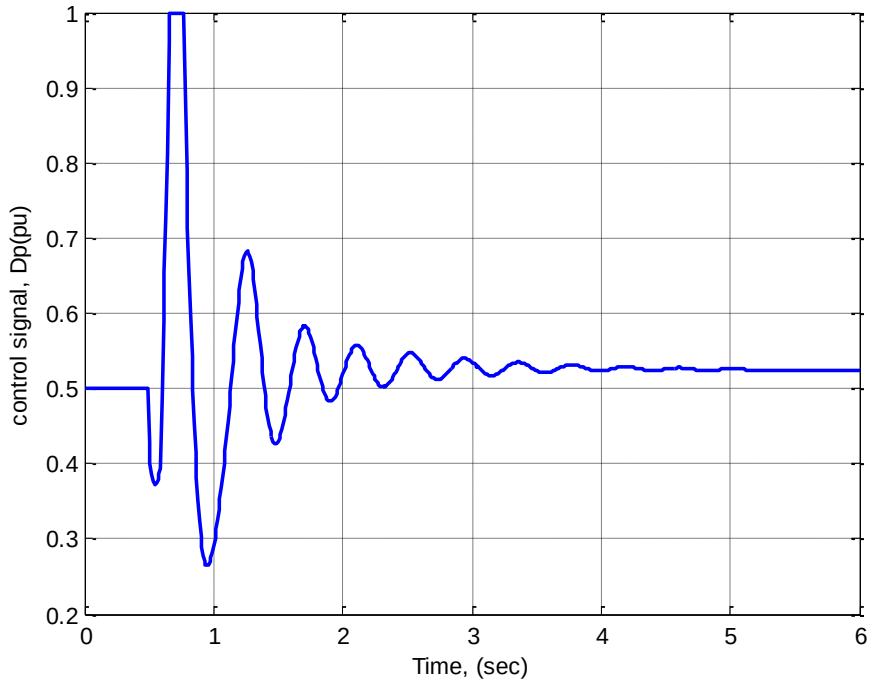

Figure 6-26: Control signal of PWMSC employing PID controller following a 3 phase fault in multi-machine system (case 1)

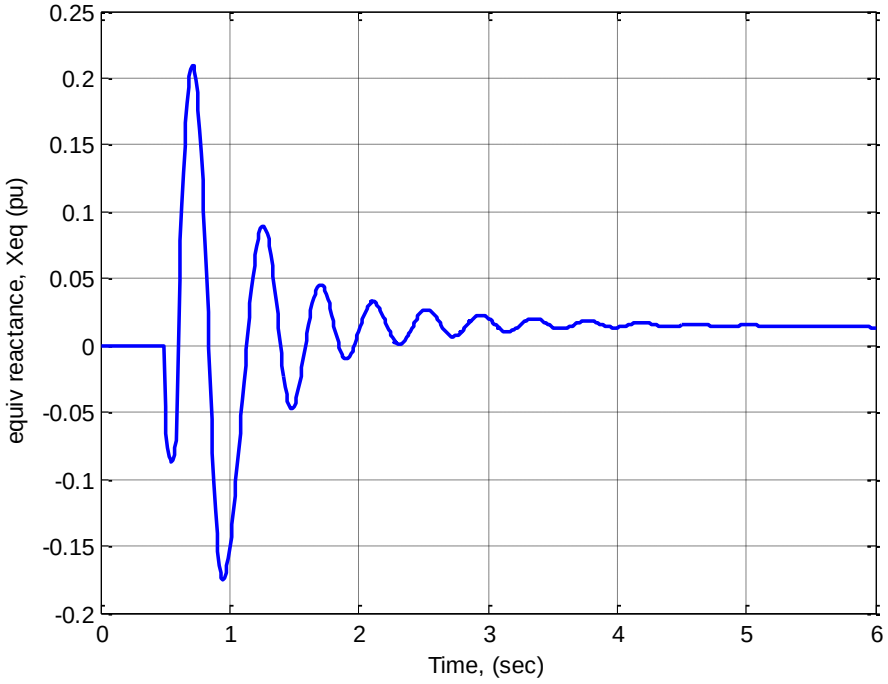

Figure 6-27: Equivalent reactance of PWMSC with PID controller following a 3 phase fault in multi-machine system (case 1)

The nonlinear simulation results obtained for this case is quite satisfactory.

6.3.2 Case-2: Different PWMSC location

The PWMSC is connected between bus 3 & bus 10 and a three phase fault is applied at bus 6 at for 0.1 sec and the faulty line between bus 9 & bus 6 is tripped. Then, after 0.1 sec the fault is cleared & the line is restored to service. This configuration is shown in Figure 6-28.

Here, a PID controller is employed to control the PWMSC series compensation and the rotor speed of generator-3 $\Delta\omega_3$ is used as stabilizing input to the PID controller.

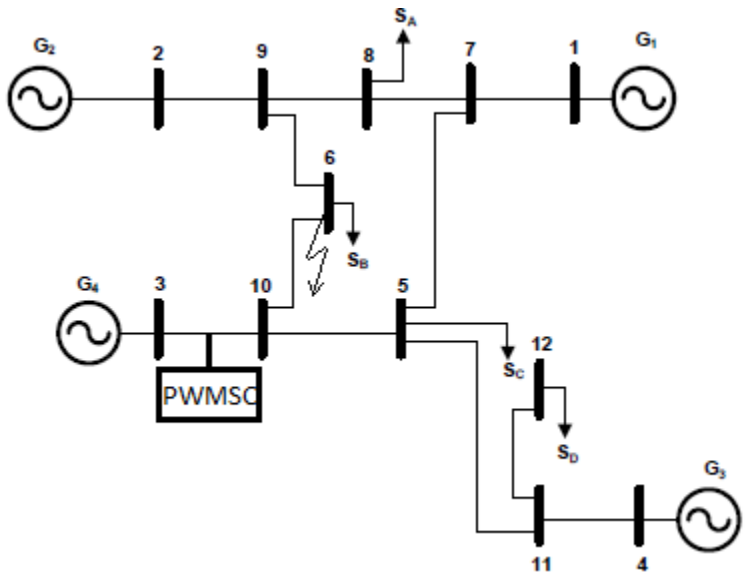

Figure 6-28: Multi-machine system considered for case-2

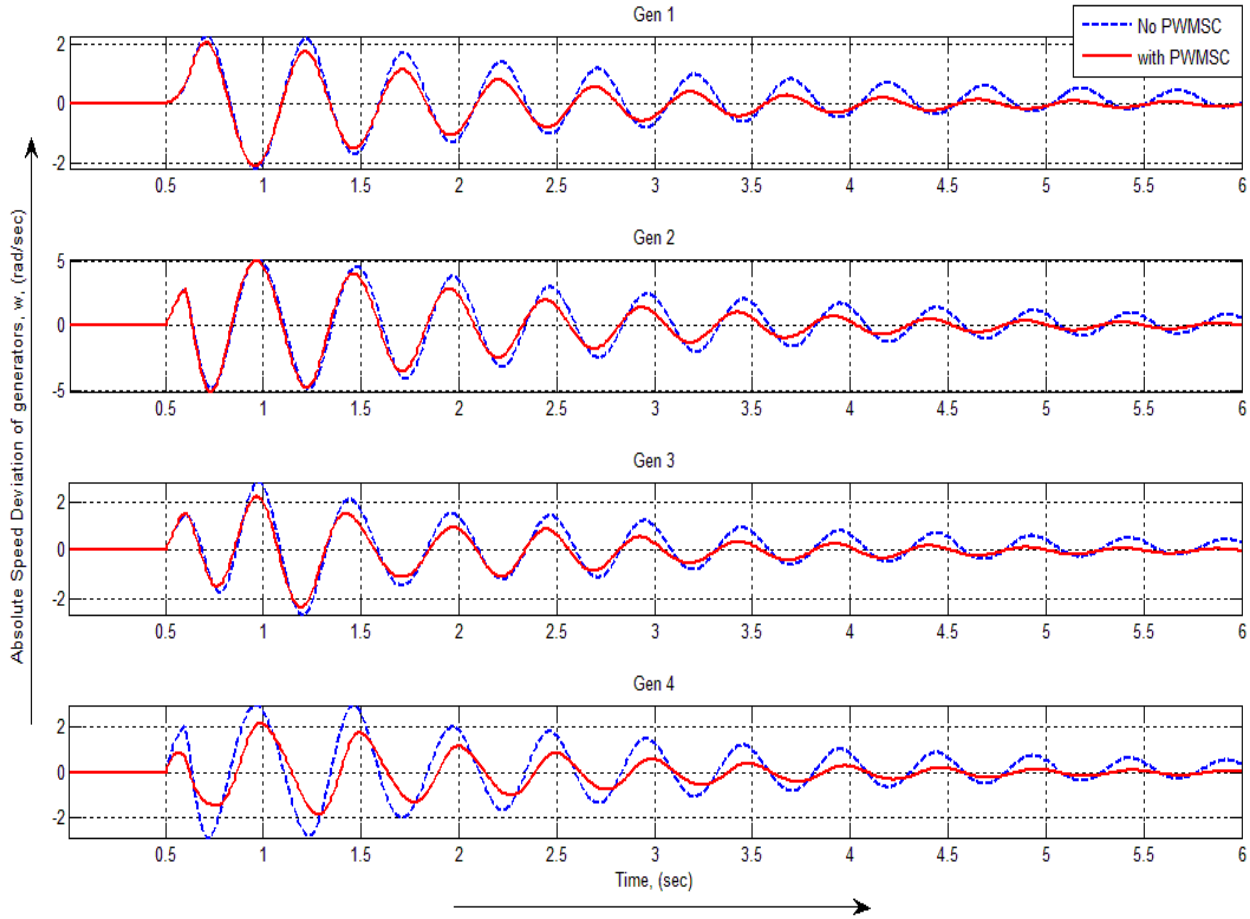

Figure 6-29: Rotor speed of generators of multi-machine system with PID controller following a 3 phase fault (case 2)

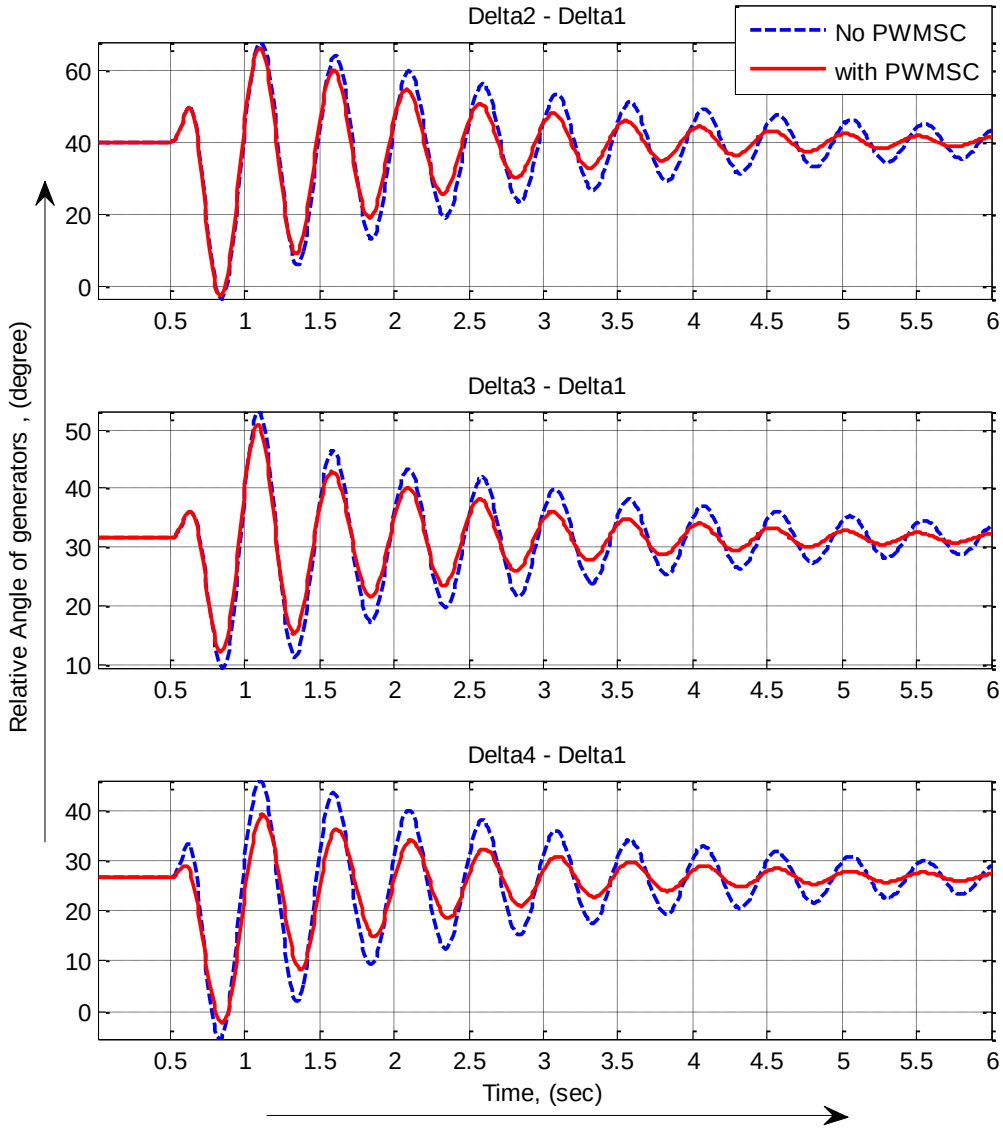

Figure 6-30: Relative angle of generators with respect to Gen-1 in multi-machine system with PID controller following a 3 phase fault (case 2)

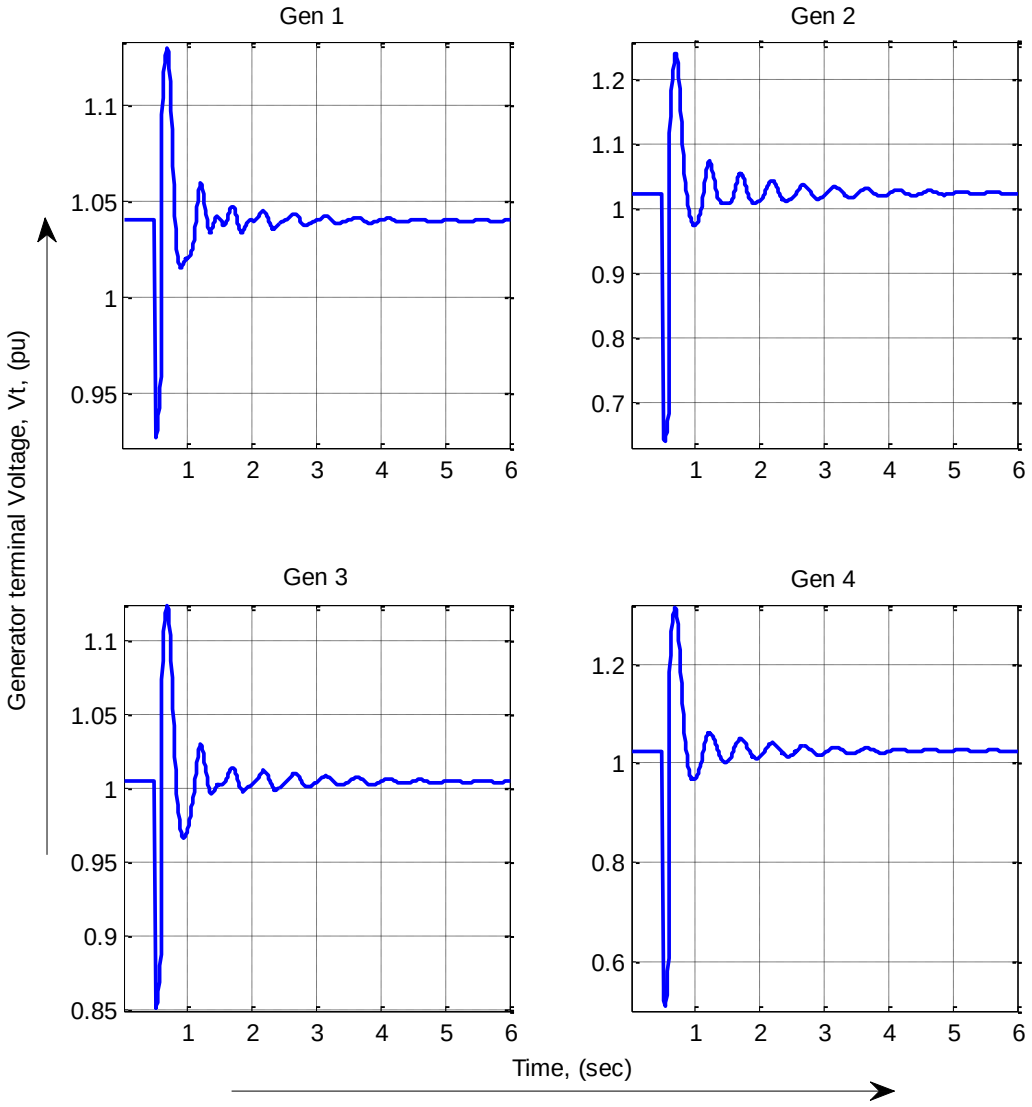

Figure 6-31: Terminal voltages of generators of multi-machine system with PWMSC following a 3 phase fault (case 2)

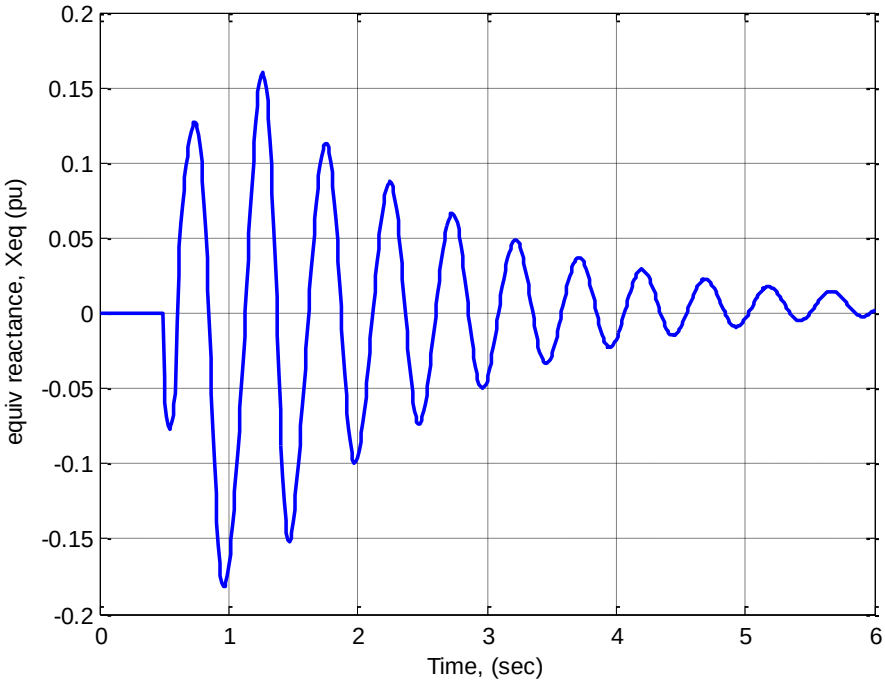

Figure 6-32: Equivalent reactance of PWMSC with PID controller following a 3 phase fault in multi-machine system (case 2)

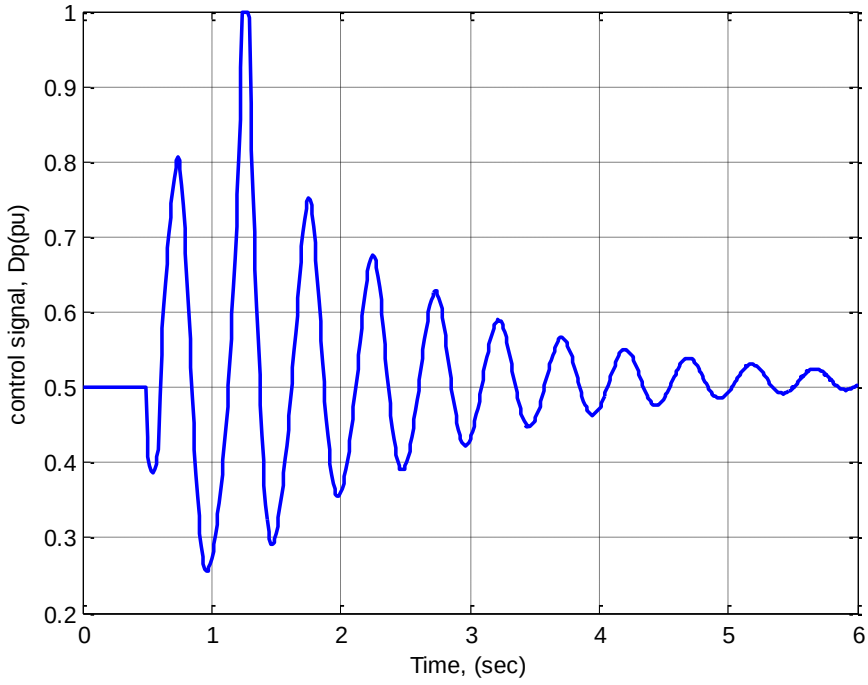

Figure 6-33: Control signal of PWMSC employing PID controller following a 3 phase fault in multi-machine system (case 2)

The simulations results shown in Figure 6-29 to Figure 6-33 does not depict as good performance as the PWMSC has shown in case 1 or previous cases when it was connected in between bus-2 and bus-9. It seems that, this is due to the larger size of generator-2 and thus, larger controllability of gen-2 over the network.

CHAPTER 7

CONCLUSIONS AND FUTURE WORKS

Dynamic performance of a single machine infinite bus power system as well as multi-machine power system installed with PWMSC has been investigated. Non-linear and linear models of both single machine as well as multi-machine power system have been derived. A comparative study has been carried out with proportional- integral (PI) and proportional- integral-derivative (PID) controllers installed in generator speed control loop, generator active power control loop and transmission line active power control loop to investigate the damping performance of the controllers and test the suitability of the different feedback control loops. The PI controller with generator speed as stabilizing signal demonstrated to provide very good damping to the system transients. PID controller has shown slightly better damping than PI controllers but care should be taken so that the system does not become over-sensitive. The generator active power and transmission line active power flow, however, does not provide significant damping to the system. For optimization of the controller parameters, genetic algorithm has been used with three objective functions. Speed deviation of the generator was taken as error signal and the integral of squared error, integral of absolute error and integral of time multiplied absolute error was taken as performance indices. All of these have shown satisfactory results in optimizing the parameters. But the optimization results obtained with the integral of squared error-objective function is better than other two. The controller was also tested for different fault locations in the multi-machine power system as well as different locations of the PWMSC itself. PWMSC has advantages over the

conventional FACTS devices such as simpler power circuit structure, simpler control strategy, withstanding high temperatures, compactness in size, no low order harmonic generations, etc.

7.1 Recommendations for future research

The research in this area can be further advanced in the following suggested directions.

- An online self-tuning adaptive control technique can be developed to enhance the dynamic performance of a power system installed with PWMSC and make it applicable in practical power systems.
- A method can be developed to find the optimal location and size of the PWMSC for a particular power system.
- Keeping in view that generator speed is not available at all locations of the multi-machine system, techniques can be adopted to synthesize speed from locally available signals.
- Only PI & PID controller is used in this work. Other types of controllers can also be explored.

APPENDIX

A. Single machine infinite bus system data

Generator data

M =6; D=0; T'_{d0}=3.6134; x_d =0.7; x_q =0.5; x'_d=0.24; *freq*=60;

Exciter data:

K_A= 3; T_A=0.01;

Transmission line data:

X_{tr}=0.15; *Z= 0.7 + j0.07*;

PWMSC data:

X_{tp}=0.015; n=1; X_c=1.5;

Operating condition:

P_e=0.9; V_t=1.02; p.f.= 0.95;

B. Multi-machine system data

Table B-1: Generator data

Gen no	xd	xq	xd1	xq1	H	Tdo1	Tqo1	Ka	Ta	Rs	KE	TE	KF	TF
1	0.146	0.0969	0.0608	0.0969	23.64	8.96	0.31	20	0.2	0	1	0.314	0.063	0.35
2	0.8953	0.8645	0.1198	0.1969	6.4	6	0.535	20	0.2	0	1	0.314	0.063	0.35
3	1.3125	1.2578	0.1813	0.25	3.01	5.89	0.6	20	0.2	0	1	0.314	0.063	0.35
4	1.3125	1.2578	0.1813	0.25	3.01	5.89	0.6	20	0.2	0	1	0.314	0.063	0.35

Table B-2 : generators nominal operating condition

Gen no.	MW	Mvar	Qmin	Qmax
1	34.8	17.85	-50	50
2	105	46.6	-50	75
3	50	30	-20	30
4	60	5	-10	10

Table B-3: nominal loadings

Bus No.	MW	Mvar
5	77.5	30
6	52.5	25
8	72.5	27
12	48.75	15

Table B-4: Transmission line data

From Bus #	To Bus #	R (p.u.)	X (p.u.)	1/2 B (p.u.)	Line code
1	7	0	0.05	0	1
2	9	0	0.05	0	1
4	10	0	0.05	0	1
3	11	0	0.05	0	1
11	12	0.018	0.35/3	0.0175	1
11	5	0.009	0.40/4	0.035	1
5	10	0.009	0.35/3	0.035	1
10	6	0.009	0.27/2	0.035	1
6	9	0.009	0.43/4	0.035	1
9	8	0.009	0.33/3	0.049	1
8	7	0	0.4/3	0.035	1
7	5	0.009	0.4/3	0.035	1

PWMSC data:

X_{tp}=0.15; n=1; X_c=0.6;

REFERENCES

[1] P. Kundur, "Power system control and stability," *The EPRI Power Engineering Series,* 1994.

[2] P. Kundur, M. Klein, G. J. Rogers, and M. S. Zywno, "Application of power system stabilizers for enhancement of overall system stability," *Power Systems, IEEE Transactions on,* vol. 4, pp. 614-626, 1989.

[3] N. Mithulananthan, C. A. Canizares, J. Reeve, and G. J. Rogers, "Comparison of PSS, SVC, and STATCOM controllers for damping power system oscillations," *Power Systems, IEEE Transactions on,* vol. 18, pp. 786-792, 2003.

[4] A. M. Stankovic, P. C. Stefanov, G. Tadmor, and D. J. Sobajic, "Dissipativity as a unifying control design framework for suppression of low frequency oscillations in power systems," *Power Systems, IEEE Transactions on,* vol. 14, pp. 192-199, 1999.

[5] Y.-N. Yu, *Electric power system dynamics* vol. 150: Academic press New York, 1983.

[6] F. P. DeMello and C. Concordia, "Concepts of Synchronous Machine Stability as Affected by Excitation Control," *Power Apparatus and Systems, IEEE Transactions on,* vol. PAS-88, pp. 316-329, 1969.

[7] S. B. Crary and J. B. McClure, "Supplementary control of prime-mover speed governors," *Electrical Engineering,* vol. 61, pp. 209-213, 1942.

[8] A. H. M. A. Rahim and H. M. Al-Maghraby, "Dynamic braking resistor for control of subsynchronous resonant modes," in *Power Engineering Society Summer Meeting, 2000. IEEE*, 2000, pp. 1930-1935 vol. 3.

[9] W. Yu, R. R. Mohler, W. A. Mittelstadt, and D. J. Maratukulam, "Variable-structure braking-resistor control in a multimachine power system," *Power Systems, IEEE Transactions on,* vol. 9, pp. 1557-1562, 1994.

[10] M. H. Ali, T. Murata, and J. Tamura, "Augmentation of transient stability by fuzzy-logic controlled braking resistor in multi-machine power system," in *Power Tech, 2005 IEEE Russia*, 2005, pp. 1-7.

[11] M. H. Ali, T. Murata, and J. Tamura, "The effect of temperature rise of the fuzzy logic-controlled braking resistors on transient stability," *Power Systems, IEEE Transactions on,* vol. 19, pp. 1085-1095, 2004.

[12] S. M. Rovnyak, K. Mei, and G. Li, "Fast load shedding for angle stability control," in *Power Engineering Society General Meeting, 2003, IEEE*, 2003, p. 2279 Vol. 4.

[13] C. W. Taylor, F. R. Nassief, and R. L. Cresap, "Northwest Power Pool Transient Stability and Load Shedding Controls for Generation-Load Imbalances," *Power Apparatus and Systems, IEEE Transactions on,* vol. PAS-100, pp. 3486-3495, 1981.

[14] T. J. E. Miller, *Reactive power control in electric systems*: Wiley, 1982.

[15] J. J. Grainger and W. D. Stevenson, *Power system analysis* vol. 621: McGraw-Hill New York, 1994.

[16] N. G. Hingorani, L. Gyugyi, and M. El-Hawary, *Understanding FACTS: concepts and technology of flexible AC transmission systems* vol. 1: IEEE press New York, 2000.

[17] E. Acha, C. R. Fuerte-Esquivel, H. Ambriz-Perez, and C. Angeles-Camacho, *FACTS: modelling and simulation in power networks*: John Wiley & Sons, 2004.

[18] E. Larsen, C. Bowler, B. Damsky, and S. Nilsson, "Benefits of thyristor controlled series compensation," in *INTERNATIONAL CONFERENCE ON LARGE HIGH VOLTAGE ELECTRIC SYSTEMS*, 1992, pp. 14/37/38-04.

[19] E. Larsen, K. Clark, S. Miske, and J. Urbanek, "Characteristics and rating considerations of thyristor controlled series compensation," *IEEE Transactions on Power Delivery,* vol. 9, pp. 992-1000, 1994.

[20] G. G. Karady, T. H. Ortmeyer, B. R. Pilvelait, and D. Maratukulam, "Continuously regulated series capacitor," *Power Delivery, IEEE Transactions on,* vol. 8, pp. 1348-1355, 1993.

[21] J. M. Ramirez and J. M. Gonzalez, "Steady-state and transient stability studies with an ac-ac PWM series compensator," in *Power Engineering Society General Meeting, 2007. IEEE*, 2007, pp. 1-8.

[22] G. Venkataramanan and B. Johnson, "Pulse width modulated series compensator," *IEE Proceedings-Generation, Transmission and Distribution,* vol. 149, pp. 71-75, 2002.

[23] F. Mancilla-David, S. Bhattacharya, and G. Venkataramanan, "A comparative evaluation of series power-flow controllers using DC-and AC-link converters," *Power Delivery, IEEE Transactions on,* vol. 23, pp. 985-996, 2008.

[24] D. Vincenti, H. Jin, and P. Ziogas, "Design and implementation of a 25-kVA three-phase PWM AC line conditioner," *Power Electronics, IEEE Transactions on,* vol. 9, pp. 384-389, 1994.

[25] L. A. Lopes and G. Joos, "Pulse width modulated capacitor for series compensation," *Power Electronics, IEEE Transactions on,* vol. 16, pp. 167-174, 2001.

[26] A. Alesina and M. Venturini, "Intrinsic amplitude limits and optimum design of 9-switches direct PWM AC-AC converters," in *PESC'88-Annual IEEE Power Electronics Specialists Conference*, 1988, pp. 1284-1291.

[27] L. Huber, D. Borojevic, and N. Burany, "Analysis, design and implementation of the space-vector modulator for forced-commutated cycloconvertors," *Electric Power Applications, IEE Proceedings B,* vol. 139, pp. 103-113, 1992.

[28] K. H. Chu and C. Pollock, "PWM-controlled series compensation with low harmonic distortion," *Generation, Transmission and Distribution, IEE Proceedings-*, vol. 144, pp. 555-563, 1997.

[29] S. A. K. Bhat and J. Vithayathil, "A Simple Multiple Pulsewidth Modulated AC Chopper," *Industrial Electronics, IEEE Transactions on,* vol. IE-29, pp. 185-189, 1982.

[30] P. D. Ziogas, D. Vincenti, and G. Joos, "A practical PWM AC controller topology," in *Industry Applications Society Annual Meeting, 1992., Conference Record of the 1992 IEEE,* 1992, pp. 880-887 vol.1.

[31] J. Hua, G. Goos, and L. Lopes, "An efficient switched-reactor-based static VAr compensator," *Industry Applications, IEEE Transactions on,* vol. 30, pp. 998-1005, 1994.

[32] A. Safari, H. Shayanfar, A. Kazemi, and H. Shayeghi, "Dynamic Modeling of PWM-Based AC Link Series Compensator," *Arabian Journal for Science and Engineering*, pp. 1-11, 2013.

[33] G. Venkataramanan, "Three-phase vector switching converters for power flow control," *Electric Power Applications, IEE Proceedings* -, vol. 151, pp. 321-333, 2004.

[34] O. Simon, J. Mahlein, M. N. Muenzer, and M. Bruckmarm, "Modern solutions for industrial matrix-converter applications," *Industrial Electronics, IEEE Transactions on,* vol. 49, pp. 401-406, 2002.

[35] P. Wheeler, J. Clare, L. Empringham, M. Apap, and M. Bland, "Matrix converters," in *Matrix Converters, IEE Seminar on (Digest No. 2003/10100)*, 2003, pp. 1/1-1/12.

[36] F. Mancilla-David and G. Venkataramanan, "A pulse width modulated AC link unified power flow controller," in *Power Engineering Society General Meeting, 2005. IEEE*, 2005, pp. 1314-1321 Vol. 2.

[37] J. M. Ramirez, J. M. Gonzales, and M. L. Crow, "Steady state formulation of FACTS devices based on ac/ac converters," *Generation, Transmission & Distribution, IET,* vol. 1, pp. 619-631, 2007.

[38] L. A. C. Lopes, G. Joos, and O. Boon-Teck, "A PWM quadrature-booster phase shifter for AC power transmission," *Power Electronics, IEEE Transactions on,* vol. 12, pp. 138-144, 1997.

[39] B. K. Johnson and G. Venkataramanan, "A hybrid solid state phase shifter using PWM AC converters," *Power Delivery, IEEE Transactions on,* vol. 13, pp. 1316-1321, 1998.

[40] J. M. Gonzalez and J. M. Ramirez, "AC/AC series converter in transient stability studies," in *Power Symposium, 2007. NAPS '07. 39th North American*, 2007, pp. 205-211.

[41] M. Ned, T. M. Undeland, and W. P. Robbins, "Power electronics: converters, applications, and design," *Jonh Wiley*, 1995.

[42] H. Mori and Y. Goto, "A parallel tabu search based method for determining optimal allocation of FACTS in power systems," in *Power System Technology, 2000. Proceedings. PowerCon 2000. International Conference on*, 2000, pp. 1077-1082 vol.2.

[43] S. Gerbex, R. Cherkaoui, and A. J. Germond, "Optimal location of FACTS devices to enhance power system security," in *Power Tech Conference Proceedings, 2003 IEEE Bologna*, 2003, p. 7 pp. Vol.3.

[44] M. Saravanan, S. M. R. Slochanal, P. Venkatesh, and P. S. Abraham, "Application of PSO technique for optimal location of FACTS devices considering system loadability and cost of installation," in *Power Engineering Conference, 2005. IPEC 2005. The 7th International*, 2005, pp. 716-721 Vol. 2.

[45] L. J. Cai, I. Erlich, and G. Stamtsis, "Optimal choice and allocation of FACTS devices in deregulated electricity market using genetic algorithms," in *Power Systems Conference and Exposition, 2004. IEEE PES*, 2004, pp. 201-207 vol.1.

[46] E. E. El-Araby, N. Yorino, and H. Sasaki, "A comprehensive approach for FACTS devices optimal allocation to mitigate voltage collapse," in *Transmission and Distribution Conference and Exhibition 2002: Asia Pacific. IEEE/PES*, 2002, pp. 62-67 vol.1.

[47] D. Zhao-Yang, W. Youyi, D. J. Hill, and Y. V. Makarov, "A new approach to power system VAr planning aimed at voltage stability enhancement with feedback control," in *Electric Power Engineering, 1999. PowerTech Budapest 99. International Conference on*, 1999, p. 33.

[48] S. Gerbex, R. Cherkaoui, and A. J. Germond, "Optimal location of multi-type FACTS devices in a power system by means of genetic algorithms," *Power Systems, IEEE Transactions on*, vol. 16, pp. 537-544, 2001.

[49] L. Ippolito and P. Siano, "Selection of optimal number and location of thyristor-controlled phase shifters using genetic based algorithms," *Generation, Transmission and Distribution, IEE Proceedings-*, vol. 151, pp. 630-637, 2004.

[50] M. M. Farsangi, H. Nezamabadi-pour, S. Yong-hua, and K. Y. Lee, "Placement of SVCs and Selection of Stabilizing Signals in Power Systems," *Power Systems, IEEE Transactions on*, vol. 22, pp. 1061-1071, 2007.

[51] Y. Mansour, X. Wilsun, F. Alvarado, and R. Chhewang, "SVC placement using critical modes of voltage instability," *Power Systems, IEEE Transactions on,* vol. 9, pp. 757-763, 1994.

[52] E. Larsen and J. Chow, "SVC control design concepts for system dynamic performance," *Application of Static Var Systems for System Dynamic Performance,* pp. 36-53, 1987.

[53] Z. Qihua and J. Jin, "Robust SVC controller design for improving power system damping," *Power Systems, IEEE Transactions on,* vol. 10, pp. 1927-1932, 1995.

[54] Q. Zhao and J. Jiang, "A TCSC damping controller design using robust control theory," *International Journal of Electrical Power & Energy Systems,* vol. 20, pp. 25-33, 1998.

[55] N. Martins and L. T. G. Lima, "Determination of suitable locations for power system stabilizers and static VAR compensators for damping electromechanical oscillations in large scale power systems," *Power Systems, IEEE Transactions on,* vol. 5, pp. 1455-1469, 1990.

[56] P. Pourbeik and M. J. Gibbard, "Damping and synchronizing torques induced on generators by FACTS stabilizers in multimachine power systems," *Power Systems, IEEE Transactions on,* vol. 11, pp. 1920-1925, 1996.

[57] S. E. M. De Oliveira, "Synchronizing and damping torque coefficients and power system steady-state stability as affected by static VAr compensators," *Power Systems, IEEE Transactions on,* vol. 9, pp. 109-119, 1994.

[58] S. Lee and C.-C. Liu, "An output feedback static var controller for the damping of generator oscillations," *Electric power systems research,* vol. 29, pp. 9-16, 1994.

[59] P. Zhang, A. R. Messina, A. Coorick, and B. J. Cory, "Selection of locations and input signals for multiple SVC damping controllers in large scale power systems," in *Power Engineering Society 1999 Winter Meeting, IEEE,* 1999, pp. 667-670 vol.1.

[60] A. Ekwue, H. Wan, D. Cheng, and Y. Song, "Singular value decomposition method for voltage stability analysis on the National Grid system (NGC)," *International Journal of Electrical Power & Energy Systems,* vol. 21, pp. 425-432, 1999.

[61] A. Hamdan, "An investigation of the significance of singular value decomposition in power system dynamics," *International Journal of Electrical Power & Energy Systems,* vol. 21, pp. 417-424, 1999.

[62] M. M. Farsangi, Y. H. Song, and K. Y. Lee, "Choice of FACTS device control inputs for damping interarea oscillations," *Power Systems, IEEE Transactions on,* vol. 19, pp. 1135-1143, 2004.

[63] M. M. Farsangi, S. Yong-hua, and K. Y. Lee, "On selection of supplementary input signals for STATCOM to damp inter-area oscillations in power systems," in *Power Engineering Society General Meeting, 2005. IEEE*, 2005, pp. 3068-3073 Vol. 3.

[64] P. M. Anderson and AA Fouad, " Power System Control and Stability," ed: IEEE PRESS, 1994.

VITAE

- Romman Ahmed Mostafa Kamal
- Born in Doha, Qatar on 10th August, 1985
- Received Bachelor of Science in Electrical and Electronics Engineering from Islamic University of Technology, Board Bazar, Gazipur-1704, Bangladesh on 30th Oct, 2007.
- Completed Master of Science in Electrical Engineering from King Fahd University of Petroleum and Minerals, Dhahran, Saudi Arabia in July, 2014.